A phagocyte-specific *Irf8* gene enhancer establishes early conventional dendritic cell commitment

DISSERTATION

zur Erlangung des akademischen Grades

doctor rerum naturalium

(Dr. rer. nat.)

im Fachbereich Molekularbiologie

eingereicht an der

Mathematisch Naturwissenschaftlichen Fakultät

der Universität Potsdam

von

Diplom-Ingenieur (FH) Jörg Schönheit

geboren am 02.05.1978 in Berlin

Potsdam, den 28.04.2011

Published online at the
Institutional Repository of the University of Potsdam:
URL http://opus.kobv.de/ubp/volltexte/2011/5548/
URN urn:nbn:de:kobv:517-opus-55482
http://nbn-resolving.de/urn:nbn:de:kobv:517-opus-55482

Table of contents

Abstract

Haematopoietic development is a complex process that is strictly hierarchically organized. Here, the phagocyte lineages are a very heterogeneous cell compartment with specialized functions in innate immunity and induction of adaptive immune responses. Their generation from a common precursor must be tightly controlled. Interference within lineage formation programs for example by mutation or change in expression levels of transcription factors (TF) is causative to leukaemia. However, the molecular mechanisms driving specification into distinct phagocytes remain poorly understood. In the present study I identify the transcription factor Interferon Regulatory Factor 8 (IRF8) as the specification factor of dendritic cell (DC) commitment in early phagocyte precursors.

Employing an IRF8 reporter mouse, I showed the distinct *Irf8* expression in haematopoietic lineage diversification and isolated a novel bone marrow resident progenitor which selectively differentiates into $CD8\alpha^+$ conventional dendritic cells (cDCs) *in vivo*. This progenitor strictly depends on *Irf8* expression to properly establish its transcriptional DC program while suppressing a lineage-inappropriate neutrophile program.

Moreover, I demonstrated that *Irf8* expression during this cDC commitment-step depends on a newly discovered myeloid-specific *cis*-enhancer which is controlled by the haematopoietic transcription factors PU.1 and RUNX1. Interference with their binding leads to abrogation of *Irf8* expression, subsequently to disturbed cell fate decisions, demonstrating the importance of these factors for proper phagocyte cell development.

Collectively, these data delineate a transcriptional program establishing cDC fate choice with IRF8 in its center.

Zusammenfassung

Die Differenzierung von hämatopoietischen Zellen ist ein komplexer Prozess, der strikt hierarchisch organisiert ist. Dabei stellen die Phagozyten eine sehr heterogene Zellpopulation dar, mit hochspezialisierten Funktionen im angeborenen Immunsystem sowie während der Initialisierung der adaptiven Immunreaktion. Ihre Entwicklung, ausgehend von einer gemeinsamen Vorläuferzelle, unterliegt einer strikten Kontrolle. Die Beeinträchtigung dieser Linienentscheidungsprogramme, z.B. durch Mutationen oder Änderungen der Expressionslevel von Transkriptionsfaktoren kann Leukämie auslösen. Die molekularen Mechanismen, welche die linienspezifische Entwicklung steuern, sind allerdings noch nicht im Detail bekannt.

In dieser Arbeit zeige ich den maßgeblichen Einfluss des Transkriptionsfaktors Interferon Regulierender Faktor 8 (IRF8) auf die Entwicklung von dendritischen Zellen (DC) innerhalb der Phagozyten. Mittels einer IRF8-Reporter Maus stellte ich die sehr differenziellen Expressionsmuster von *Irf8* in der hämatopoietischen Entwicklung dar. Dabei konnte ich eine neue, im Knochenmark lokalisierte, Vorläuferpopulation isolieren, die *in vivo* spezifisch Differenzierung in $CD8\alpha^+$ konventionelle dendritische Zellen (cDC) steuert. Dieser Vorläufer ist dabei absolut von der Expression von *Irf8* abhängig und etabliert auf transkriptioneller Ebene die dendritische Zellentwicklung, während gleichzeitig die Entwicklung neutrophiler Zellen unterdrückt wird.

Darüber hinaus zeigte ich, dass *Irf8* Expression während der cDC Entwicklung von einem neu charakterisierten *cis*-regulatorischen Enhancer abhängt, der spezifisch in myeloiden Zellen agiert. Ich konnte zeigen, dass die hämatopoietischen Transkriptionfaktoren PU.1 und RUNX1 mittels dieses Enhancers die *Irf8* Expression steuern. Können diese beiden Faktoren nicht mit dem Enhancer interagieren, führt das zu stark verminderter *Irf8* Expression, damit zu Veränderungen in den Differnzierungsprogrammen der Zellen, was die Bedeutung dieses regulatorischen Mechanismus unterstreicht.

Zusammengefasst beschreiben diese Daten die Etablierung der frühen cDC Entwicklung, in der IRF8 die zentrale Rolle spielt.

1 Introduction

Genome wide comparative analysis of multiple lower and higher organisms revealed that not the number of genes is causative for the complexity of an organism (Levine et al. 2003). Rather the potential of increased regulatory capabilities within the genome allows for development of higher organisms. Therefore, unravelling the mechanisms which orchestrate gene regulation is mandatory for the understanding of the development of higher organisms. How does gene encoded information get processed in a cell type specific manner?

Transcription factors (TF) are key players in gene regulation due to their ability to bind to proteins as well as to DNA, thus affecting gene expression. Here they act in a complex network in a temporally and spatially defined manner, that way determining which genes are expressed and subsequently what fate a cell will undergo. Impaired expression of a single TF within this tightly controlled network can be causative to severe developmental disorders or result in the pathogenesis of malignancies. Even though the expression patterns of many TFs are known, the mechanisms defining these patterns are poorly understood. Therefore, it is necessary to learn more about TF function and the mechanisms which define their specificity. The present study focuses on the role of the haematopoietic transcription factor Interferon Regulatory Factor 8 (IRF8) in phagocyte lineage development.

1.1 Gene regulation

Even though cells of a multi-cellular organism share the same genetic instruction sets, a great diversity of cell types with very different terminal phenotypes is generated from the originally totipotent cell. In order to establish different gene expression programs these organisms harbour a multitude of regulatory mechanisms which control gene expression. These can be grouped into three subsets. (I) Posttranslational control modifies function and stability of proteins, for example by phosphorylation (Hunter et al. 2000) or ubiquitination (Hershko et al. 1998). An important feature of posttranslational control is the covalent modification of histone tails (discussed in 1.1.3) (Shilatifard 2006). (II) Posttranscriptional mechanisms regulate and process transport and translation of mRNA. (III) Transcriptional control is the most basal mechanism of gene expression. Hence, it is involved in most regulational processes. Initiation of gene expression is mainly controlled by transcription factors and regulatory *cis*-elements. The numerical increase of these is evidence for increased complexity of higher organisms (Luscombe et al. 2004). While only two percent of the human genome makes up for protein coding sequence approximately a third of the human genome accounts for *cis*-elements (Levine et al. 2003).

1.1.1 Transcription factors (TF)

Next to epigenetic regulation such as DNA methylation or histone tail modification (discussed in 1.1.3) there is regulation directly on the genetic level. Here, transcription factors are the major driving force for gene expression and their activity determines how cells function and respond to the environment. Thus, they are involved in many biological processes such as metabolism (Accili et al. 2004), cell cycle (Simon et al. 2001), development (Bain et al. 1994; Bain et al. 1997) and differentiation (Yoshida et al. 2006; Rosenbauer et al. 2007; Decker et al. 2009). Mostly TFs are interacting with other TFs or other cofactors in comprehensive regulatory networks (Wilson et al. 2011). Approximately 10 percent of the entire human gene pool encodes for TFs (Brivanlou et al. 2002) underlining the significance of this regulatory mechanism.

Not surprisingly, TFs are overrepresented among cancer associated genes (Furney et al. 2006) and it was shown that not less than 164 TFs were directly responsible for 277 diseases or syndromes (Vaquerizas et al. 2009). However, since these factors are highly dynamic and interactive little is known about their regulation.

1.1.2 *cis*-regulatory elements

Eukaryotic expression of protein-coding genes in principle is regulated by two distinct groups of regulatory elements. (I) Proximal sequences consist of a core-promoter element (discussed in 1.1.2.1) and its accompanying regulatory elements which are flanking the transcription start site (TSS). (II) Distal regulatory elements on the other hand can be found several 100kb away from their respective promoter sequences and can be categorized into enhancers, silencers and insulators (discussed in 1.1.2.2 to 1.1.2.4).

1.1.2.1 Promoter

The promoter of a gene consists of two subsets. The core-promoter includes the TATA box, defines the TSS and indicates the direction of transcription (Smale et al. 2003). Here, the basal transcription machinery, consisting of TF-II family transcription factors, binds and recruits RNA-polymerase II which initiates transcription (Orphanides et al. 1996). The proximal promoter is directly adjacent to the core promoter and can contain multiple TF binding motifs as depicted in Figure 2. That way TFs can directly bind to a promoter sequence in order to regulate gene expression. These proximal promoter sequences vary in length and can comprise several 100bp of DNA. Their function is comparable to the function of enhancers.

1.1.2.2 Enhancer

Enhancers are regulatory *cis*-elements which activate gene expression in a temporally and spatially defined manner (Steinman et al. 1973; Moreau et al. 1981; Atchison 1988). Since enhancers differ in respect to the distance to their promoters they can act independent of distance or orientation. Enhancers can be found upstream, downstream or even within a gene itself. They contain binding motifs for multiple TFs. This accounts for their ability to interact with promoters in a cell type specific manner. For example the enhancer of the *cFMS* gene which encodes the macrophage colony stimulating factor (M-CSFR) is only active in macrophages (Follows et al. 2003; Bonifer et al. 2008). A similar cell type specific regulation was found for the *Sfpi1* gene (encoding PU.1) regulating a cluster of enhancers (Rosenbauer et al. 2004; Leddin et al. 2011). However, enhancers differ to proximal promoters solely by their distance to the promoter. They interact with their respective promoters directly and for that have to be in close proximity. That is achieved by folding of the DNA into a loop-like structure mediated by enhancer binding proteins as depicted in Figure 1 (Vilar et al. 2005). Only then they can drive expression of the gene. Interference of the crosstalk between enhancer and promoter leads to abolishment of the gene activity or result in the pathogenesis of malignancies (Rosenbauer et al. 2004).

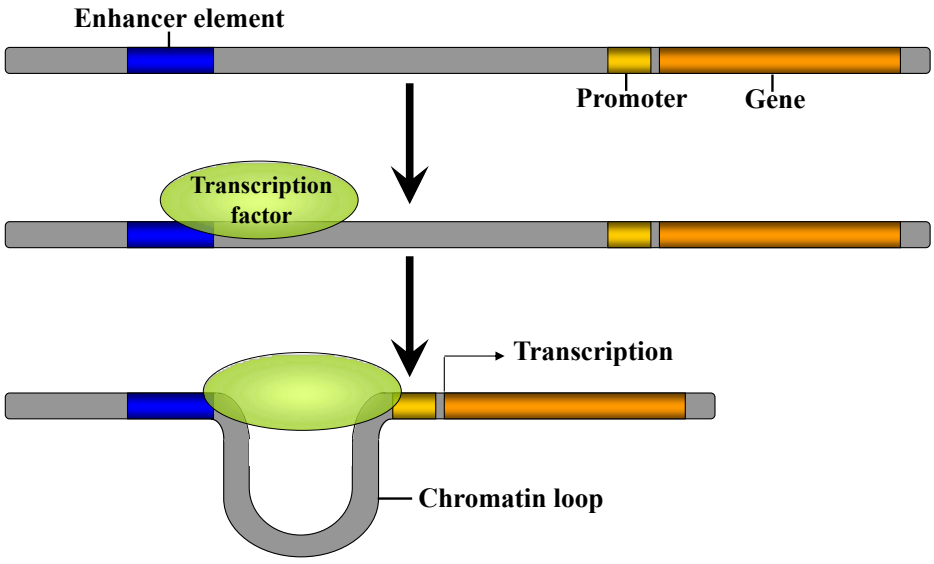

Figure 1: Changes in chromatin structure during enhancer mediated gene transcription. Transcription factors are recruited to enhancer elements. Via the formation of a chromatin loop the enhancer and the promoter are linked in a transcriptional complex. Only then, transcription is initiated. Re-drawn from (Ohlsson 2010).

1.1.2.3 Silencer

Silencers on the other hand repress the transcription of their respective gene. They share many features with enhancers for example their independency of orientation or distance from the

promoter (Ogbourne et al. 1998). However, when transcription factors bind to them, expression of the gene they control is repressed.

1.1.2.4 Insulator

Enhancers and silencers can act on multiple genes but in certain cases these interactions might be unwanted. Here, *cis*-acting regulatory DNA sequence regions termed insulators can block such interactions. Insulators are located between the enhancer(s) and promoter or silencer(s) and promoter of adjacent genes. Their function is to prevent a gene from being influenced by the activation (or repression) of its neighbours (Riethoven 2010).

Two distinct types of insulators have been discovered: enhancer-blocking insulators and barrier insulators (Gaszner et al. 2006). The enhancer-blocking insulators protect against gene activation by enhancers and interfere with the enhancer–promoter interaction only if the insulator is located between the enhancer and the promoter. Barrier insulators shield against the spread of heterochromatin, and thus of chromatin-mediated silencing (Recillas-Targa et al. 2004). In contrast to enhancers and silencers the insulators are strictly dependent on orientation and position (Maston et al. 2006). Furthermore, these elements seem to be restricted to DNA regions of high density of regulatory elements (Fourel et al. 2004).

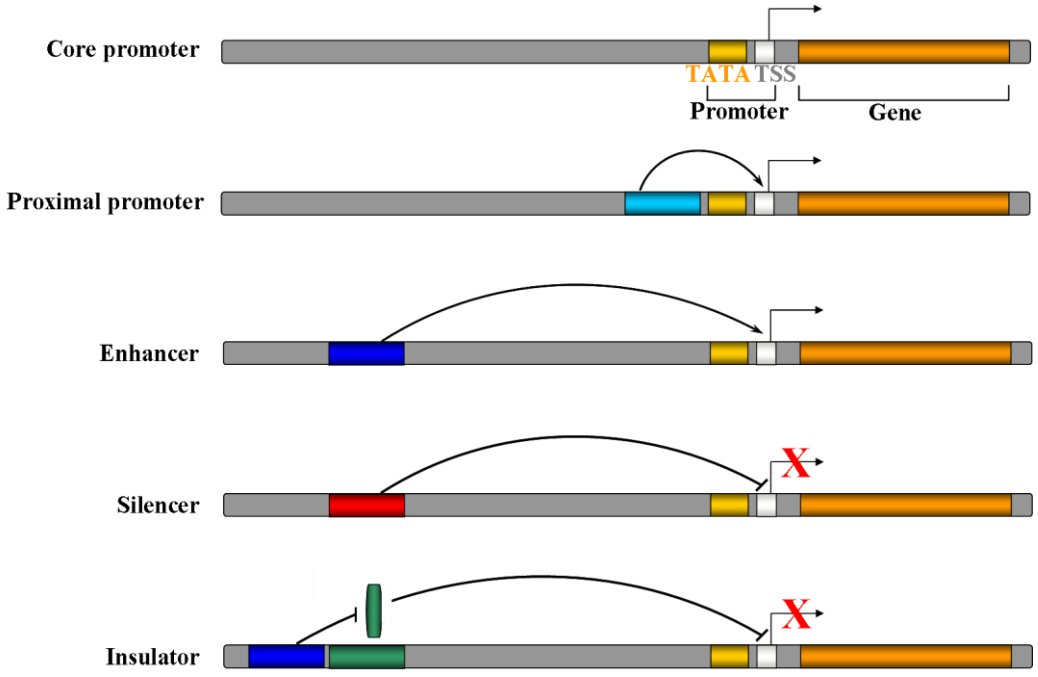

Figure 2: Overview about transcriptional regulatory elements. Core promoters consist of a TATA box (yellow) which defines the transcription start site (TSS; light gray). Different transcriptional regulatory elements can act on promoter activity to influence gene expression. Proximal promoters (light blue) and enhancers (dark blue) can positively stimulate expression, while silencers (red) repress gene expression. Insulators (green) can shield the promoter from stimuli of enhancers by blocking enhancer activity. Re-drawn from (Maston et al. 2006).

1.1.3 Histone modification

Even though the genome is the ultimate template of our hereditary, today's understanding is that the knowledge of the primary DNA sequence itself is just the foundation for understanding how the genetic program is read and implemented. Next to gene regulation mediated by transcription factors epigenetic processes were found to play major role (Lee et al. 2010; Bannister et al. 2011). At large, epigenetic modifications fall in two main categories: DNA methylation and histone tail modifications.

Depending on the nature of those modifications the overall structure of the chromatin can change. This on the other hand determines the accessibility to the underlying DNA, consequently regulating transcriptional activity. At the heart of chromatin structure conserved histone proteins act as building blocks for packaging DNA into nucleosomal repeats. N-terminal tails sticking out of these compact structures can be differently modified at specific positions. The sum of all histone modifications is thought to be deciphered as a histone code installing an epigenetic state which determines the actual readout of the genetic information of a certain locus through activation or silencing (Bannister et al. 2011). Acetylation of histone H3 lysine 9 (H3K9) is generally related to transcriptional activity at this particular site (Delabesse et al. 2005; Clayton et al. 2006). Methylation on the other hand displays more complicated patterns. While methylation of histone H3 lysine 4 (H3K4) is generally associated with transcribed chromatin, methylation of H3K9 or H3K27 usually correlates with repression (Bernstein et al. 2007).

1.2 Haematopoiesis

The haematopoietic system is a complex system consisting of various blood cell types and is strictly hierarchically organized. In the last decades it developed into a prototype experimental model system due to several advantages. (I) Haematopoietic cells are found in several organs, like in bone marrow, spleen, lymph nodes, thymus, the peritoneal cavity and the peripheral blood. (II) These cells can relatively easily be isolated, processed to single cell suspensions and used for experimental purposes. (III) The development of fluorescence activated cell sorting (FACS) in conjunction with the constantly increasing number of fluorochrome-conjugated antibodies against cellular surface antigens allowed a very precise characterization of haematopoietic cells. Furthermore, this technique allows to separate distinct cell populations on the basis of their surface marker composition. Moreover, differentiation processes of these cells can be followed both *in vitro*, by providing specific differentiation conditions like cytokines or feeder cells, or *in viv*o, by transplantation of cells.

Here, sorted cell populations can be transferred by intravenous injection into recipient animals providing a precious tool to follow up cell fates within a chosen environment or experimental setting.

1.2.1 Haematopoietic hierarchy

Haematopoiesis is the formation and development of blood cells. As most blood borne cells only have a limited lifespan that ranges from merely some hours (granulocytes) up to several months (red blood cells), replenishment of this cell pool is required. This is a continuous process throughout the entire lifespan of the organism. In humans proximately 1*E12 new cells are generated every single day (Ogawa 1993). Here, haematopoietic stem cells (HSC) that possess self renewal capacity give rise to all committed effector cells via the generation of intermediate progenitor stages as displayed in Figure 3. Of particular interest are white blood cells due to their function in the immune system. As displayed in Figure 3, classically the lymphoid- and the myeloid branch can be distinguished (Akashi et al. 2000; Traver et al. 2004). Common myeloid progenitors (CMP) generate red blood cells (RBC) and platelets which are responsible for oxygen transport and blood clotting, respectively. Moreover, the CMP also gives rise to cells of the innate immune system that is encompassing mast cells, granulocytes (or neutrophiles) and monocytes/macrophages (discussed in detail in 1.2.2.1). These heterogeneous cell populations are forming the myeloid branch of white blood cells. On the other hand, common lymphoid progenitors (CLP) give rise to B-cells, T-cells and natural killer cells. This lymphoid cell branch is known to compose the adaptive immune system.

Another heterogeneous cell population called dendritic cells (DC) are at the junction between myeloid and lymphoid cells as well as between innate and adaptive immune system, respectively. DCs are involved in both types of the immune responses and it has been shown that they originate from early myeloid as well as early lymphoid progenitors (Traver et al. 2000; Ardavin 2003) (discussed in detail in 1.2.2.2).

Collectively, HSCs give rise to progeny that gradually loses multipotency and the capacity to self renew while becoming restricted to one cell lineage via multiple intermediate progenitor stages (Metcalf 1999). At the end of lineage commitment fully differentiated cells arise either as members of the lymphoid or of the myeloid branch. The complexity of this system clearly demands tight regulation of cell fate choices during differentiation into the mature effector cells.

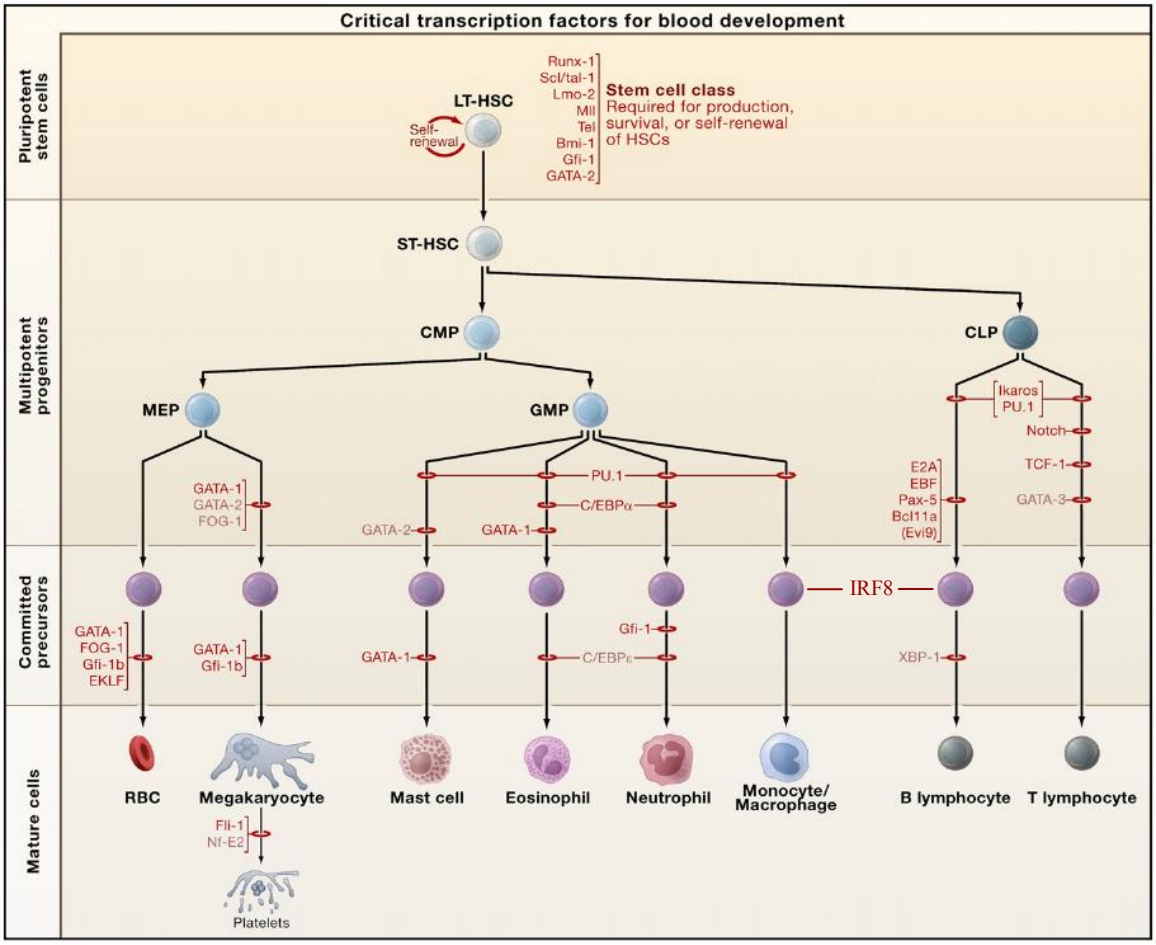

Figure 3: Scheme of haematopoietic system. The stages at which haematopoietic development is blocked in the absence of a given transcription factor, as determined through conventional gene knockouts, are indicated by red bars. The factors depicted in black have been associated with oncogenesis. Those factors in light font have not yet been found translocated or mutated in human/mouse haematologic malignancies. Abbreviations: LT-HSC, long-term haematopoietic stem cell; ST-HSC, short-term haematopoietic stem cell; CMP, common myeloid progenitor; CLP, common lymphoid progenitor; MEP, megakaryocyte/erythroid progenitor; GMP, granulocyte/macrophage progenitor; RBCs, red blood cells. Figure and legend taken from (Orkin et al. 2008) with permission of Cell.

1.2.2 The phagocyte classification

The phagocyte system was defined by van Furth in the 1980s as a cell family originating from myeloid precursors in the bone marrow (van Furth 1980). These differentiate to form circulating blood monocytes which eventually enter tissues to become tissue macrophages, found in every organ in the body. Phagocytes are capable of engulfing and digesting pathogens and cellular debris, moreover, their signalling capacity triggers the adaptive immune system. Thus they are placed at the frontier of immune responses to fight off infections and to clear off dead cells (Geissmann et al. 2010a) Today, dendritic cells are also placed into this classification due to overlapping marker expression and similar functionality of this cell moiety (Hume 2006; Chang 2009).

1.2.2.1 Monocytes/macrophages

Monocytes/macrophages are the outposts of the immune system in detecting invading pathogens or foreign antigens. In mice, roughly six percent of all blood borne leucocytes are monocytes (Sunderkotter et al. 2004). They also function as control switches for immune system balance between pro- and anti-inflammatory reactions. Hereditary, all monocytes develop of a morrow resident myeloid precursor which eventually migrates to the bloodstream to patrol there (Gordon et al. 2005). Their maturation is strongly influenced by expression of TFs like PU.1 and IRF8 (Rosenbauer et al. 2007). Monocytes/macrophages have been extensively characterised for expression of surface markers (Geissmann et al. 2003; Yona et al. 2010). Ly6C expression in combination with the macrophage-colony stimulating factor receptor (M-CSFR) is mainly used to distinguish monocytes ($Ly6C^+$; $M\text{-}CSFR^+$) from granulocytes ($Ly6C^+$; $M\text{-}CSFR^-$) (Hume 2006). Monocytes can be attracted to inflammatory sites (Swirski et al. 2009) and mature into macrophages which colonize all organs of the body with selected properties as for example Kupffer cells in the liver, osteoclasts in the bone or microglia in neuronal tissues. Hence, they form a heterogeneous cell compartment and were also described to give rise to certain DC subsets demonstrating the low borders between the two cell types (Varol et al. 2007). Functionally they are involved in inflammation, wound repair, tissue remodelling, bacterial clearance and production of inflammatory cytokines (Woollard et al. 2010).

1.2.2.2 Dendritic cells (DCs)

$CD11c^+$ dendritic cells are the second compartment of the mononuclear phagocytes. Although the original definition did not include DCs, recent findings placed DCs among the mononuclear phagocytes (Yona et al. 2010; Bar-On et al. 2011). They comprise a functionally diverse group of antigen presenting cells (APC) that include plasmacytoid DCs (pDC) and conventional DCs (cDCs). In mice lymphoid tissue cDCs mostly can be sub-grouped into $CD8\alpha^+$ DCs (Carbone et al. 1990; Aliberti et al. 2003) and $CD4^+$ DCs (Tamura et al. 2005). Their ability to cross-present antigens to T-cells makes DCs a crucial cell compartment for onset of adaptive immunity (Geissmann et al. 2010b; Steinman et al. 2010). Furthermore, non lymphoid tissue DCs, namely $CD103^+$ DCs or Langerhans cells can be found in lung, gastrointestinal tract, and skin (Schiavoni et al. 2002; Schiavoni et al. 2004; Ginhoux et al. 2009; Edelson et al. 2010). Development of this cell compartment is dependent on expression of transcription factors such as IRF8, PU.1, Id2 and Batf3 (Hacker et al. 2003; Heinz et al. 2006; Ginhoux et al. 2009).

Recently, much effort has been invested in revealing the processes of progenitor cells to differentiate into the diverse subgroups of effector cells as displayed in Figure 4. It was believed that DCs origin from the myeloid as well as from the lymphoid branch (Traver et al. 2000; Ardavin 2003). However, the earliest dendritic progenitor still has the potential to give rise to macrophages and dendritic cells. Hence, it was named macrophage-dendritic progenitor (MDP) (Fogg et al. 2006; Waskow et al. 2008). Within this progenitor lies another more specified precursor. This common dendritic cell progenitor (CDP) (Onai et al. 2007) *in vivo* exclusively gives rise to different subgroups of dendritic cells.

Only then, a more differentiated progenitor was described, which had lost the potential to mature into pDCs but mainly gave rise to cDCs. Thus, it was termed the pre-cDC (Liu et al. 2009). This progenitor was found in the marrow as well as in the periphery, allowing for speculations about just another bone marrow resident but more immature progenitor.

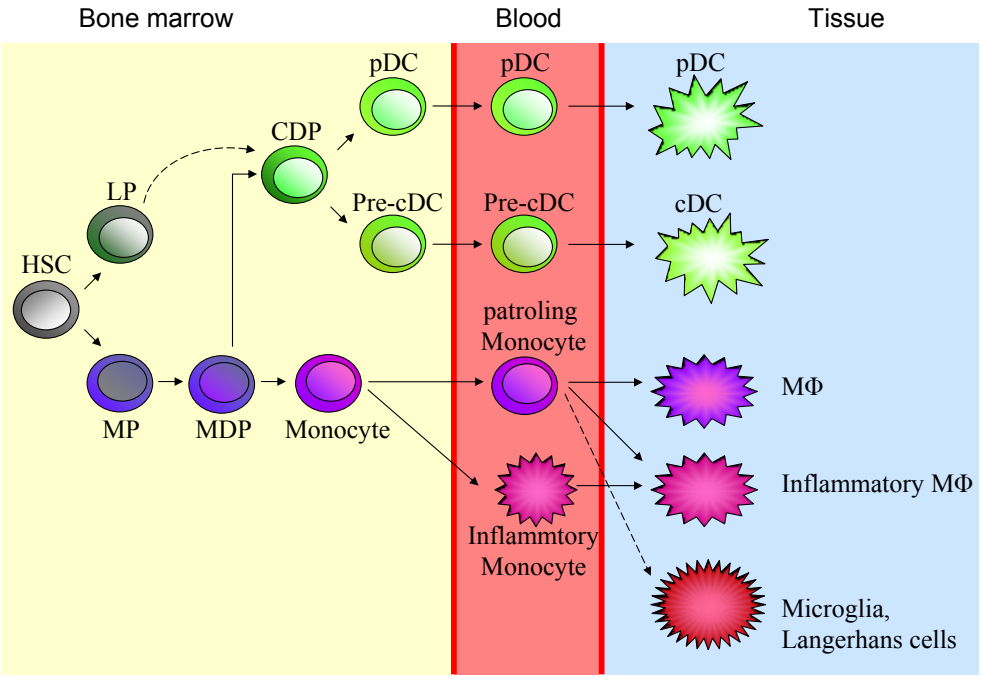

Figure 4: The mononuclear phagocyte development. In the bone marrow (BM) of vertebrates, haematopoietic stem cells (HSC) give rise to myeloid (MP) and lymphoid (LP) committed precursors. MPs further develop into bipotential monocyte/macrophage and dendritic cell (DC) precursors (MDPs). MDPs give rise to common DC precursors (CDP) and monocytes which leave the marrow to enter the bloodstream. CDPs give rise to preclassical dendritic cells (pre-cDCs) and plasmacytoid dendritic cells (pDCs). Pre-cDCs circulate in blood and enter lymphoid tissue, where they give rise to conventional DCs (cDC), while pDCs can be found in blood and in tissues. Monocytes in the blood can be divided into inflammatory monocytes which can mature into inflammatory macrophages (MΦ) when entering the tissue under inflammatory conditions. Patrolling monocytes in the blood contribute to generation of specialized phagocytes such as MΦ, microglia and Langerhans cells. Microglia and Langerhans cells can furthermore renew independently from the bone marrow. LPs also contribute to the generation of pDCs and cDCs, however, the mechanisms so far are not resolved. Revieved by (Geissmann et al. 2010b).

1.3 Transcription factors in haematopoiesis

In haematopoiesis lineage diversification is controlled by genetic regulation through TFs as well as by epigenetic processes like histone modification or DNA methylation. A multitude of TFs, each acting specifically at the required position like a gearwheel of an unbelievably complex machinery, have been identified to be involved in the pathway choice of blood cell development (Heinz et al. 2010). Factors as RUNX1 and SCL1 were found to be indispensable for early haematopoietic development (Loose et al. 2007; Friedman 2009). In more lineage committed cells other factors become important. So the Ets-factor (Sharrocks 2001) PU.1 was shown to be a master switch factor instructing myeloid differentiation (Rosenbauer et al. 2007). PU.1 null mice display a lack of distinct myeloid cell populations like granulocyte-macrophage progenitors (GMPs) and mature myeloid cells. In lymphoid cells again other factors control lineage fates, as for example Pax5 in B-cell development (Carotta et al. 2008; Decker et al. 2009). The Interferon Regulatory Factor 8 (IRF8) interestingly plays an important role in the orchestration of myeloid as well as of lymphoid cell development (discussed in 1.4).

1.4 IRF8

The Interferon regulatory factor 8 (IRF8, also termed Interferon consensus sequence binding protein (ICSBP)) is a transcription factor with expression restricted to the haematopoietic system. It is involved in the formation of myeloid cells (Holtschke et al. 1996; Tamura et al. 2000), DCs (Tsujimura et al. 2002; Tsujimura et al. 2003a; la Sala et al. 2009) and B-cells (Wang et al. 2008; Wang et al. 2009). Furthermore, it is associated with bone metabolism (Zhao et al. 2009), tumor suppressor activity (Holtschke et al. 1996) and apoptosis (Yang et al. 2007). However, the main function of this family of TFs is their involvement in antiviral defense and immune regulation (Battistini 2009).

1.4.1 Function of Interferon regulatory factor family members

As a member of the Interferon Regulating Factor family that consists of 10 members as depicted in Figure 5, IRF8 contains a DNA binding domain (DBD) as well as an IFN association domain (IAD). Even though the IRF8 protein contains a DBD it mostly acts as a heterodimer with partner proteins where the partner binds specific DNA motifs. Due to the variety of immune reactions different response pathways have evolved. Here IRF8 (or its

binding partner) can for example act through binding to the IFNγ activation site (GAS) or the IFN stimulated response element (ISRE) (Kanno et al. 2005).

Of the family members IRF4 shares the highest homology to IRF8 and both are involved in B-cell generation partially with redundant functions (Lu et al. 2003; Wang et al. 2009). In myeloid cell development IRF8 was found to interact with its family members IRF3 and IRF4, respectively (Li et al. 2011b; Marecki et al. 1999). As the family name suggests all members are involved in Interferon (IFN) mediated antiviral responses. Noteworthy to mention is IRF5 which induces inflammatory cytokines (IL6, IL12, TNF) and tumor suppressors (Krausgruber et al. 2010).

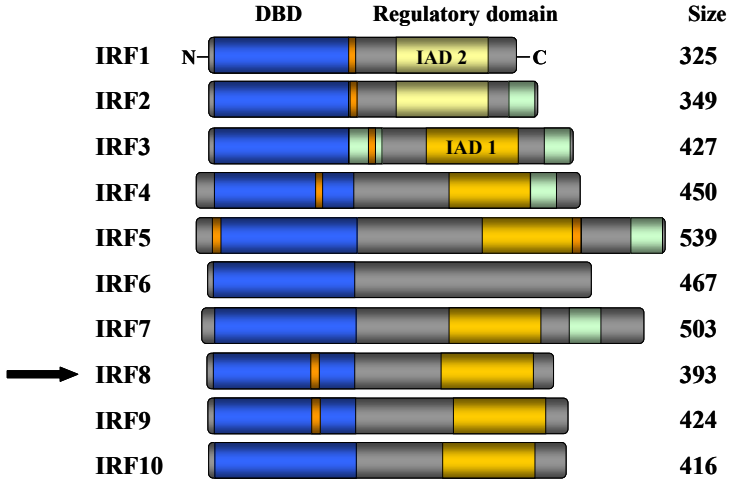

Figure 5: Structure of interferon-regulatory factors. All interferon-regulatory factors are composed of a DNA-binding domain (DBD; blue) and a regulatory domain (yellow). For all IRFs, the DBD is defined by 5 tryptophan residues that are each separated by 10–18 amino acids. Most IRFs also contain an IRF-association domain (IAD) of either type 1 (deep yellow) or type 2 (pale yellow). Some IRFs contain a repression domain(s) (mint green) and a nuclear-localization signal(s) (orange). For IRF1, -3, -5 and -7, activity depends on phosphorylation. IRF8 is indicated by filled arrow. The size of each IRF in number of amino acids is also indicated. C, carboxyl terminus; N, amino terminus. Legend taken from (Lohoff et al. 2005)**.**

The interaction of the Ets factor PU.1 with IRF8 is well known for the formation of myeloid- and B-cells (Kanno et al. 2005).

On genetic level *Irf8* expression is induced by pathogens, lipo-poly-saccharid (LPS) and Interferon gamma (IFNγ) in mouse macrophages and T-cells, which is mediated by the GAS element in the *Irf8* promoter. On the other hand, IRF8 also regulates IFNγ expression, thus establishing a feedback loop. Its role here is intensively studied (Giese et al. 1997; la Sala et al. 2009; Tailor et al. 2007).

1.4.2 Description of the *Irf8*$^{-/-}$ mouse phenotype

Targeted deletion of *Irf8* in mice (further discussed in 2.2.1.2) revealed an enhanced susceptibility to virus infections associated with an impaired production of IFNγ and a lack of

antigen presenting CD8α$^+$ DCs cells (Holtschke et al. 1996; Aliberti et al. 2003; Esashi et al. 2008). A second more unexpected phenotype was a myelo proliferative syndrome (MPS) which strongly resembled human chronic myeloid leukaemia (CML). In blood development immature myeloid progenitors are accumulating in the bone marrow which lead to an expansion of the granulocyte compartment at the expense of macrophages and DCs (Holtschke et al. 1996; Turcotte et al. 2005). This chronic phase can progress rapidly into an acute myeloid leukaemia, showing the role of IRF8 in proliferation, differentiation and as a tumor suppressor gene. Moreover, *Irf8* is often strongly down-regulated in human myeloid leukaemias demonstrating its clinical importance (Schmidt et al. 1998; Schmidt et al. 2001). Increased knowledge on this gene might contribute to a better understanding of human myeloid leukaemia.

1.5 Aims of the thesis

Irf8 is a gene with model character. Its restricted expression to cells of the immune system calls for a tight regulation of gene expression. On the functional side IRF8 is involved in many different processes, as cell proliferation, differentiation, tumor suppression or host defence. Thus, understanding of the mechanistical processes that underlie *Irf8* regulation was a driving force of the current study. Specifically the following tasks were attended to:

I) Characterization of *Irf8* expression in the haematopoietic system on single cell level.
   A reporter mouse was generated which harboured a murine *Irf8* containing PAC equipped with a VENUS (enhanced yellow fluorescent protein) reporter. Reporter expression was assessed throughout the haematopoietic system. Here, a new progenitor could be discovered and was analyzed for its lineage commitment capacity.

II) Finding of regulatory factors that are involved in the lineage specific expression patterns of *Irf8*.
   Employing computational and molecular biological tools a new phagocyte specific *cis* regulatory element to *Irf8* was discovered and analyzed for its regulational activity.

2 Materials and Methods

2.1 Materials

2.1.1 General equipment

Device	Manufacturer
Agarose gel chambers	Biostep (Jahnsdorf, Germany)
Bioruptor	Diagenode (Liége, Belgium)
CHEF Mapper XA System	Biorad (Munich, Germany)
DW2 waterbath	Julabo (Seelbach, Germany)
FACS Calibur	BD-Biosciences (Heidelberg, Germany)
FACS LSRII	BD-Biosciences
FACS Aria	BD-Biosciences
Geldoc 2000	Biorad
Hybridization oven Hybridiser HB-1D	Techne (Jahnsdorf, Germany)
Incubator	Binder (Tuttlingen, Germany)
Laminar flow hood	BDK (Sonnenbühl-Genkingen, Germany)
Luminometer Centro 960	Berthold Technologies (Berlin, Germany)
Mastercycler Gradient	Eppendorf (Wesseling-Berzdorf, Germany)
Microscope DMIL	Leica (Wetzlar, Germany)
Microscopy Immersion Oil	Merck (Darmstadt, Germany)
Multicentrifuge 3 S-R	Heraeus (Dormagen, Germany)
Nanodrop Spectrophotometer	Nanodrop (Wilmington, DE, USA)
Nylon membrane	Pall Corporation (Dreieich, Germany)
Power supply EV231	Consort (Turnhaut, Belgium)
PVDF membrane	Pall Corporation
TCS SPE confocal microscope	Leica
Sephadex G25-spin column	Roche (Penzberg, Germany)
Stratalinker 2400	Stratagene (Waldbronn, Germany)
Thermomixer compact	Eppendorf
Tri Carb 2800 TC	Perkin Elmer (Rodgau, Germany)
Unimax 1010 shaker	Heidolph (Schwabach, Germany)
Vortex Genie 2	Scientific Industries (Bohemia, NY, USA)
XAR film	Kodak (see Sigmaaldrich)
5415c benchtop centrifuge	Eppendorf
7300 Real Time PCR System	Applied Biosystems (Carlsbad, CA, USA)

2.1.2 Cell culture equipment

Cell culture dishes, sterile, different sizes	TPP or BD (Trasadingen, Swiss)
Cell strainer, sterile, different sizes	BD-Biosciences
Centrifuge tubes, sterile, different sizes	TPP or BD
Cryotubes, sterile, 1.2 ml	Nunc (Langenselbold, Germany)
Disposable scalpel for single-use, sterile	B.Braun (Melsungen, Germany)
Needles for single-use, sterile, different sizes	Dispomed (Gelnhausen, Germany)
Neubauer cell-counter chamber	Superior Marienfeld (Lauda, Germany)
Polystyrene tubes, 5 ml	BD-Biosciences
Rotilabo Filter sterile, 0.22 and 0.45 µM PVDF	Roth (Karlsruhe, Germany)
Serological pipettes	BD-Biosciences
Syringes for single-use, sterile, different sizes	B.Braun, Omnifix, BS Plastic

2.1.3 Chemicals and reagents

Agarose	Roth / Biorad
Bromphenol blue	Roth
Bovine serum albumin (BSA)	Roth
ß-Mercaptoethanol	Sigma (Munich, Germany)
Chloroform/Isoamylalcohol	Roth
dNTPs	Fermentas (St. Leon-Rot, Germany)
DTT	Fermentas
Ethanol absolute	MDC-Lager
Ethidium bromide	Roth
Ethylenediaminetetraacetate (EDTA)	Roth
Formaldehyde	Roth
Giemsa stain	Fluka (Munich, Germany)
Glacial acetic acid	Roth
Glycerol	Roth
Hepes	PAA (Pasching, Austria)
High molecular weight marker	Fermentas
Histofix	Roth
Hoechst 33342	Invitrogen (Darmstadt, Germany)
Hybri-Quick	Roth
Isopropanol	Roth
KCl	Roth
KH_2PO_4	Roth
Lambda ladder	NEB (Frankfurt/M, Germany)
LB medium	Roth
LB agar	Roth
Low molecular weight marker	Fermentas
May/Grünwald stain	Fluka
$MgCl_2$	Roth
Na_2HPO_4	Roth
NaCl	Roth
Southern blot membrane	Pall Corporation
Phenol	Roth
poly(I:C)	Invivogen (Toulouse, France)
Propidium iodide (PI)	Sigma
Proteinase K (reconstituted to 10 mg/mL in water)	Invitrogen
Protease Inhibitor cocktail	Sigma
RNase free water	Qiagen (Hilden, Germany)
Sodium citrate	Roth
Sodium dodecyl sulfate (SDS)	Roth
Trichlormethan (Chloroform)	Roth
Tris base	Roth
Tris-Cl	Roth
Triton X100	Roth
Trizol	PeqLab (Erlangen, Germany)
Trypan blue solution	Sigma
Xylene	Roth
Xylene cyanol	Roth
[α-^{32}P]dCTP	Amersham (Freiburg, Germany)
[γ-^{32}P]dATP	Amersham

2.1.4 Cell culture media and reagents

Accutase, 1 x Concentrate	PAA
Dulbecco's modified Eagle's Medium (DMEM), high Glucose (4.5 g/l)	PAA
Dulbecco's PBS 1 x, without Ca & Mg	PAA
Fetal Calf Serum (FCS)	Biochrom (Berlin, Germany)
Iscove's modified DMEM (IMDM)	PAA
MethoCult® M3234	Stem Cell Technologies (Sirocco, France)
MethoCult® M3630	Stem Cell Technologies
Penicillin/Streptomycin, 100 x Concentrate	PAA
Stable Glutamine, 200 mM Concentrate	PAA
Trypsin EDTA (1:250), 1 x Concentrate	PAA
N,N-dimethylsulfoxide (DMSO)	Roth

2.1.5 Buffers

ACK (red blood cells lysis buffer)	0.15 M NH_4Cl, 10 mM $KHCO_3$, 0.1 mM EDTA, pH 7.3 in water
ChIP cell lysis buffer	10 mM Tris pH 8.0, 10 mM NaCl, 0.2 % NP40, protease inhibitors
ChIP nuclei lysis buffer	50 mM Tris pH 8.1, 10 mM EDTA, 1 % SDS, protease inhibitors
ChIP IP dilution buffer	20 mM Tris pH 8.1, 2 mM EDTA, 150 mM NaCl, 1 % Triton X-100, 0.01 % SDS, protease inhibitors
ChIP IP wash buffer 1	20 mM Tris pH 8.1, 2 mM EDTA, 50 mM NaCl, 1 % Triton X-100, 0.1 % SDS, protease inhibitors
ChIP IP wash buffer 2	10 mM Tris pH 8.1, 1 mM EDTA, 0.25 M LiCl, 1 % NP40, 1 % deoxycholic acid, protease inhibitors
ChIP elution buffer	100 mM $NaHCO_3$, 1 % SDS
DNase - Glycerol/TKN buffer	50 % glycerol, 50 mM Tris pH 8.0, 100 mM KCl, 5 mM $MgCl_2$
DNase - buffer A	100 mM NaCl, 50 mM Tris pH 8.0, 3 mM $MgCl_2$
DNase - 2x TNE buffer	10 mM Tris pH 8.0, 600 mM NaCl, 20 mM EDTA
DNase stop mix	10 mM Tris pH 8.0, 600 mM NaCl, 20 mM EDTA, 0.1 % SDS
Nuclear extract buffer A	10 mM HEPES pH 7.9, 1.5 mM $MgCl_2$, 10 mM NaCl, protease inhibitors
Nuclear extract buffer C	20 mM HEPES pH 7.9, 25 % glycerol,

	0.42 M NaCl, 1.5 mM $MgCl_2$, 0.2 mM EDTA
FACS buffer	2 % (v/v) FCS, 2 mM EDTA, in PBS
Freezing medium	50 % (v/v) medium, 40 % FCS (v/v), 10 % (v/v) DMSO
Phosphate buffered saline (PBS)	137 mM NaCl, 2.7 mM KCl, 10 mM Na_2HPO_4, 2 mM KH_2PO_4, pH 7.4 in water
Southern blot wash solution I	100 ml 20 x SSC, 10 ml 20 % SDS, in 890 ml water
Southern blot wash solution II	10 ml 20 x SSC, 10 ml 20 % SDS, in 980 ml water
Tail digestion buffer	10 mM Tris-HCl pH 8.0, 10 mM EDTA pH 8.0, 50 mM NaCl, 0.5 % (v/v) SDS, in water
TE buffer	10 mM Tris, 1 mM EDTA, pH 7.5 in water
3C cell lysis buffer	10 mM Tris pH 8.0, 10 mM NaCl, 0.2 % NP40, protease inhibitors
1x EMSA binding buffer	20 mM Hepes, pH 7.6, 10 % glycerol, 2 mM EDTA, 2 mM DTT, 10 mM $MgCl_2$, 100 mM KCl in water
1x SDS sample buffer	0.5 M Tris-HCl pH 6.8, 5 % glycerol, 2 % SDS and 100 mM DTT
1x TAE	40 mM Tris acetate, 2 mM EDTA, pH 8.5 in water
1x TBE	10.8 g Tris base, 5.5 g boric acid, 0.93 g EDTA add 1000 ml water
1x TBS	50 mM Tris acetate, pH 7.4, 150 mM NaCl
1x transfer buffer	3.4 g Tris-base, 14.4 g glycine, 200 ml methanol, add 1000 ml water
1x western running buffer	3.4 g Tris-base, 14.4 g glycine, 5 ml 20 % SDS, add 1000 ml water
4x Tris/SDS pH 6.8	18.6 g Tris-base, 6 ml 20 % SDS, pH 6.8 with HCl, add 300 ml water
4x Tris/SDS pH 8.8	91 g Tris base, 10 ml 20 % SDS, pH 8.8 with HCl, add 500 ml water
6x Loading buffer for agarose gel electrophoresis	0.25 % (w/v) bromphenol blue, 0.26 % xylene cyanol (w/v), 30 % glycerol (v/v), in water

20x SSC	3.0 M NaCl, 0.3 M sodium citrate, 1 mM EDTA

2.1.6 General enzymes

DNaseI	Fermentas
Klenow Fragment	New England Biolabs
Opti-Taq DNA polymerase	Roboklon
PFU DNA polymerase	Fermentas
Power SYBR® Green PCR Master Mix	Applied Biosystems
Protease inhibitor cocktail	Sigma
Ribo Lock RNase Inhibitor	Fermentas
Shrimp alkaline Phosphatase (SAP)	Fermentas
Superscript II	Fermentas
T4 DNA-Ligase	New England Biolabs
T4 DNA Polymerase	Fermentas
T4 Polynucleotide kinase	Fermentas
TaqMan® Universal PCR Master Mix	Applied Biosystems

2.1.7 Restriction enzymes

*Apo*I	New England Biolabs
*Bam*HI	Fermentas
*Bgl*I	Fermentas
*Bgl*II	Fermentas
*Cla*I	Fermentas
*Dpn*I	Fermentas
*Eco*RI	Fermentas
*Eco*RV	Fermentas
*Hin*dIII	Fermentas
*Kpn*I	Fermentas
*Nco*I	Fermentas / New England Biolabs
*Nde*I	Fermentas
*Nhe*I	Fermentas
*Not*I	Fermentas
*Pfo*I	Fermentas
*Pst*I	Fermentas
*Pvu*II	Fermentas
*Sac*I	Fermentas
*Sac*II	Fermentas
*Sal*I	Fermentas
*Sca*I	Fermentas
*Sfi*I	Fermentas
*Sma*I	Fermentas
*Spe*I	Fermentas
Xba	Fermentas
Xho	Fermentas

2.1.8 Mouse dissection equipment

Dissecting board and pins (sterilized)	
Scissors and forceps (sterilized)	
Scalpels (sterile)	Brand
EDTA-treated canula	Brand

2.1.9 Kits

Dual-Luciferase® Reporter Assay System	Promega (Mannheim, Germany)
Invisorb Spin DNA extraction-Kit	Invitek (Berlin, Germany)
Invisorb Spin plasmid MINI-II-Kit	Invitek
Genomic DNA Invisorb Kit III	Invitek
Nucleobond 100 kit	Marchery Nagel (Düren, Germany)
pGMTeasy vector kit	Promega
Purelink Plasmid Midi Kit	Invitrogen
Rediprime II DNA Labelling System	Amersham
RNeasy Mini or RNeasy Micro-elute Kit	Qiagen
Rapace Kit	Invitek

2.1.10 Antibodies and microbeads

Dynalbeads® Sheep anti–Rat	Invitrogen
Compensation Beads Rat IgG, κ	BD-Bioscience

2.1.11 ChIP, gelshift, Western blot antibodies

Surface receptor	Application	Supplier
acetyl histone H3	ChIP	Millipore (Schwalbach, Germany)
ß-TUBULIN	western	Sigma
GFP	western	Santa Cruz Biotech (Heidelberg, Germany)
IRF8 (C19)	western / ChIP	Santa Cruz Biotech
Pol II (N20)	ChIP	Santa Cruz Biotech
PU.1 (T-21X)	ChIP / EMSA	Santa Cruz Biotech
Rabbit IgG	ChIP / EMSA	Millipore
RUNX1	ChIP	Cell signalling (Danvers, MA, USA)

2.1.12 FACS antibodies

Surface receptor	Clone	Conjugate	Supplier
B220 / CD45.R	RA3-6B2	PE-Cy5, APC, Alexa780	Invitrogen / Biolegend (Uithoorn, Netherlends)
CD3ε	145-2C11	PE-Cy5, PE	BD-Bioscience
CD4	GK1.5	PE-Cy5, PE	BD-Bioscience
CD45.1	A20	Pacific	Biolegend
CD45.2	104	Alexa700	eBioscience (Frankfurt/M, Germany)
CD8α	53-6.7	PE-Cy5, PE, Alexa780	Biolegend
CD11b / Mac1	M1/70	PE-Cy5, APC, Alexa700	BD-Bioscience / Biolegend
CD11c	N418	PE-Cy5, APC, Pacific	Biolegend
CD19	1D3	PE-Cy5, PE	eBioscience
CD34	RAM34	APC	BD-Bioscience
CD115 / M-CSFR	AFS98	PE, APC	eBioscience

CD117 / c-Kit	2B8	APC, APC-C7, PE-Cy7	BD-Bioscience / eBioscience
CD127 / IL-7Rα	SB/199	PE-Cy5, APC	eBioscience
FcγRII/III	2.4G2	APC-Cy7, unconjugated	BD-Bioscience
Flt3	A2F10.1	PE, APC	Biolegend
IgM	R6-60.2	APC, FITC	BD-Bioscience
Ly6C	HK1.4	APC, APC-Cy7	Biolegend
MHC II	M5/114.15	PE, Alexa780	eBioscience
NK1.1	PK136	PE-Cy5	Biolegend
Sca1	E13-161-7	PE-Cy5, Pacific	eBioscience / Biolegend
Ter119	TER-119	PE-Cy5, PE	eBioscience / Biolegend

2.1.13 Immunofluorescence antibodies

Surface Receptor	Clone	Conjugate	Supplier
CD11c	N418		Abcam (Cambridge, UK)
GFP	rabbit polyclonal		Invitrogen
MARCO	ED31		Serotec (Düsseldorf, Germany)
CD169	MOMA-1		Serotec
SIGNR1	ER-TR9		Abcam
anti donkey		Alexa488, Alexa568	Invitrogen
anti-armenian hamster		DyLight 594	Jackson Immunoresearch (Suffolk, UK)

2.1.14 Cytokines

murine EPO
murine Flt3L
murine G-CSF
murine GM-CSF
murine IL3
murine IL6
murine IL11
murine M-CSF
murine SCF
Cytokines were purchased at Tebu Bio or Pepro Tech Inc. (Offenbach and Hamburg, Germany)

2.1.15 Oligonucleotides

Genotyping	**Primer sequence (5'-sequence-3')**	**Reference**
Irf8		
Irf8-1	CAT GGC ACT GGT CCA GAT GTC TTC C	Holtschke, 1996
Irf8-2	CTT CCA GGG GAT ACG GAA CAT GGT	
Irf8-3	CGA AGG AGC AAA GCT GCT ATT GGC C	
Runx1		
m*AML1* P5	TAG GGA GTG CTG CTT GCT CT	Putz, 2006
m*AML1* P6	GCC GGG TGC AAT ATT AAG TC	
m*AML1* P7	CTC TGG GAA ACC AGG GAG TG	
Mx1-Cre sense	CAA TTT ACT GAC CGT ACA C	
Mx1-Cre anti	TAA TCG CCA TCT TCC AGC AG	

CX3CR1		
CX3CR1-1	TTC ACG TTC GGT CTG GTG GG	Jung, 2000
CX3CR1-2	GGT TCC TAG TGG AGC TAG GG	
CX3CR1-3	GAT CAC TCT CGG CAT GGA CG	
PU.1 URE		
URE-1	CGG GAT CCC TGG TCA GTT TTC TCA C	Tenen lab, Boston, MA, USA
URE-2	ATT TGC GGC CGC TTG CAA TGA GGG ACA AAC AA	
URE-3	GCC AAC TCA GCA CTC AGG CA	
-50kb element		
m*Irf8 lox*P1-FRT sense	GGG ATC AAG ACA GGA GGT ATT TAT T	
m*Irf8 lox*P1-FRT anti	CGT GGT TGT GCT TTA TAT GTA GGT C	
m*Irf8 lox*P2 sense	AAC TGC AAC CTC TGT CTT GTG TCT	
m*Irf8 lox*P2 anti	AAT TCT AAC TGG GAC TCA GCC AAC	
***Irf8*-VENUS PAC**		
m*Irf8*-LA-sense-A	CAG TCC TAA GAC CCA GTG AAA AGC	
m*Irf8*-IRES-anti-B	ATA ACA TAT AGA CAA ACG CAC ACC	
CMV-Cre sense	CGC CAT CCA CGC TGT TTT GAC C	Su, 2002
CMV-Cre anti	CAG CCC GGA CCG ACG ATG AAG	

Molecular cloning	**Primer sequence (5'-sequence-3')**	**Reference**
***Irf8*-VENUS PAC cloning**		
Exon9-left arm-sense	AGA CGA ATC GAT CCG CGG CTG TGT GCT GAG GTC TTT CG	
Exon9-left arm-anti	AGA CGA ATC GAT ATG AGC CCA GAG CAC AGT TT	
Exon9-right arm-sense	AGG CGG CCG CCA GTG CCC ACC CAC GTA	
Exon9-right arm-anti	AGA CGA CCG CGG CCC AGC ACC TTC ACA CAG TA	
*lox*P-Pfo1-sense	AGA CGA TCC AGG AGG AAC TTC ATC AGT CAG GTA CA	
*lox*P-Pfo1-anti	AGA CGA TCC TGG AGC ATG CGG CCG CTC TAG AAC TAG TGG A	
m*Irf8*-LA-sense	CAG TCC TAA GAC CCA GTG AAA AGC	
m*Irf8*-IRES-anti	ATA ACA TAT AGA CAA ACG CAC ACC	
m*Irf8*-IRES-2-anti	CAT ATT ATC ATC GTG TTT TTC AAA GG	
m*Irf8*-VENUS-anti	GCT CTC TTA CTT GTA CAG CTC GTC	
m*Irf8*-VENUS-sense	GAG TAC AAC TAC AAC AGC CAC AAC	
m*Irf8*-VENUS-2-sense	TGG ACG AGC TGT ACA AGT AAG AGA G	
m*Irf8*-Exon9-anti	AGG AAG ATT GCA ATG AGT TCA AAG	
m*Irf8*-Exon9-sense	TAAGAGAATTCCGAAAGGATGTG	
m*Irf8*-ZEO-anti	CGA TAT ACT ATG CCG ATG ATT AAT TG	
m*Irf8lox*P1-FRT-sense	GGG ATC AAG ACA GGA GGT ATT TAT T	
m*Irf8lox*P1-FRT-anti	CGT GGT TGT GCT TTA TAT GTA GGT C	
m*Irf8lox*P2-sense	AAC TGC AAC CTC TGT CTT GTG TCT	
m*Irf8lox*P2-anti	AAT TCT AAC TGG GAC TCA GCC AAC	
sh-RNA cloning		
sh-RNA-mPu.1-sense	ACC TCG AAG CTC ACC TAC CAG TTC TCA AGA GGA ACT GGT AGG TGA GCT TCT T	Lausen, 2006
sh-RNA-mPu.1-anti	CAA AAA GAA GCT CAC CTA CCA GTT CCT CTT GAG AAC TGG TAG GTG AGC TTC G	
sh-RNA-mRunx1-sense	ACC TCC CCC GAA GAC ATC GGC AGA AAT CAA GAG TTT CTG CCG ATG TCT TCG GGG TT	Lausen, 2006
sh-RNA-mRunx1-anti	CAA AAA CCC CGA AGA CAT CGG CAG AAA CTC TTG ATT TCT GCC GAT GTC TTC GGG GG	

Luciferase vector cloning	**(mutated bases are underlined)**
-50kb Pu.1site-mutated-A-sense	AAA AGC AGA AGA GCG CAA GAG GAA AAA CAT
-50kb Pu.1site-mutated-A-anti	ATG TTT TTC CTC TTG CGC TCT TCT GCT TTT
-50kb Pu.1site-mutated-B-sense	AAA AGC AGA AGA GGA AAA GAG CGC AAA CAT
-50kb Pu.1site-mutated-B-anti	ATG TTT GCG CTC TTT TCC TCT TCT GCT TTT
Runx1-A sense	GATC GCC CCG GGG CGT ACA CGC AGC AGG
Runx1-A anti	GATC CCT GCT GCG TGT ACG CCC CGG GGC
Runx1-B sense	GATC GGC TGA GGC AAG TAC AAG CCA TGG
Runx1-B anti	GATC CCA TGG CTT GTA CTT GCC TCA GCC

3C	**Recognition site**	**Primer sequence (5'-sequence-3')**	**Reference**
3C GapDH prom anti	GapDH promoter	TGC ACC ATA TCA AGG GTG CCC GT	Spilianakis, 2004
3C GapDH enh anti	GapDH enhancer	TAG ACC AGC CCC CAT TAT TGA ATG	
3C -50kb sense PCR1	-50kb	TTC ATA GGC TGT TTA GCA ACC CCG	
3C -50kb sense PCR2	-50kb	AAA AGC AAT CAG GGA CAT GGA AAC	
3C -38kb sense PCR1	-38kb	GGA GAA GAT GGA AAT TGG CTT TA	
3C -38kb sense PCR2	-38kb	TGG GGT AGG GGT AGT GAT GGG A	
3C -16kb sense PCR1	-16kb	TTA CCA TCT GTG CCC TTT GCG T	
3C -16kb sense PCR2	-16kb	GTT TTC TAG TTA GTG GTT TGA	
3C -11kb sense PCR1	-11kb	TCT ACG TTT TCA GTA AAT TGA	
3C -11kb sense PCR2	-11kb	TAT CTC TTG GCA ATA GTT CCC A	
3C IRF8 prom sense	IRF8 promoter	AGA AGA GGC TGG GTT AGA GAA TTT	
3C IRF8 prom anti	IRF8 promoter	CGA AGT GTT CTA GAG AGT CCA TCA	

ChIP	**Primer sequence (5'-sequence-3')**	**Reference**
-50kb ChIP sense	GGG GAG GGA AAA GCA ATC	
50kb ChIP anti	CTT TTC CCA GGC TGA GTC C	
38kb ChIP sense	GAA ATC AGC CAC AGG AAG GA	
38kb ChIP anti	AAG GGC CTG AGC TGA GAG T	
16kb ChIP sense	GCT GCC TCT TGC CGA TAG	
16kb ChIP anti	TCT GGT TTT CGC TTG GAG	
11kb ChIP sense	AAG AAG ACA CTC GGG GGA AG	
11kb ChIP anti	GGA GAT CAT GGC TGT GTG TG	
Irf8 prom ChIP sense	CAG AGA AGG CGG ATT TGG	
Irf8 prom ChIP anti	GCG CGC CTG CTT TTA TAG	
Irf8 Intron 2 3 sense	GCT TCA GCA AAG CAG GAG TC	
Irf8 Intron 2 3 anti	AGA GCG ACT GCG TAA CCA AC	
+28kb ChIP sense	CAG ATG ATG GCT CAA AGC AA	
+28kb ChIP anti	GAC ATG ATT TCC TGT GCT TTT T	
+53kb ChIP sense	AAT GTT TGC AGC CCT GTT ATG	
+53kb ChIP anti	GCA TGC AGA GCA ATG TGT TG	
+61kb ChIP sense	CAG GGA CCT TCC TTC TGT CC	
+61kb ChIP anti	ACA CCT GTT GCC TCC TTC AG	
ßActin prom sense	TTT CAA AAG GAG GGG AGA GG	Leddin, 2011
ßActin prom anti	CTC GAG CCA TAA AAG GCA AC	
MyoD1 sense	CAT ACC CGT ACC TTG GGA TG	Sawado, 2001
MyoD1 anti	CGG AGC TTT GTA GCA AAA GG	

EMSA	Primer sequence (5' sequence 3')	Reference
50kb Pu.1 wt sense	AAA AGC AGA AGA GGA AAA GAG GAA AAA CAT	
50kb Pu.1 wt anti	ATG TTT TTC CTC TTT TCC TCT TCT GCT TTT	
50kb Pu.1 mutated sense	AAA AGC AGA AGA GCG CAA GAG CGC AAA CAT	
50kb Pu.1 mutated anti	ATG TTT GCG CTC TTG CGC TCT TCT GCT TTT	
50kb Pu.1 a mutated sense	AAA AGC AGA AGA GCG CAA GAG GAA AAA CAT	
50kb Pu.1 a mutated anti	ATG TTT TTC CTC TTG CGC TCT TCT GCT TTT	
50kb Pu.1 b mutated sense	AAA AGC AGA AGA GGA AAA GAG CGC AAA CAT	
50kb Pu.1 b mutated anti	ATG TTT GCG CTC TTT TCC TCT TCT GCT TTT	
12kb perfect Pu.1 sense	GATC TCC CCA TGG CTT CCT CTT TCC TTC C	Leddin, 2011
12kb perfect Pu.1 anti	GATC GGA AGG AAA GAG GAA GCC ATG GGG A	
	(mutated bases are underlined)	

Gene expression analysis	Primer sequence (5' sequence 3')	Reference
m*GapDH* sense	AAG GGC TCA TGA CCA CAG TC	
m*GapDH* anti	CAC ATT GGG GGT AGG AAC AC	
m*ßactin* sense	TGA CAT C CG TAA AGA CCT CTA	
m*ßactin* anti	CAG GAG GAG CAA TGA TCT TGA	
m*Irf8* sense	GCT GAT CAA GGA ACC TTG TG	
m*Irf8* anti	CAG GCC TGC ACT GGG CTG	
m*Foxf1a* sense	GCA GAA CTG CAA GGC ATC C	
m*Foxf1a* anti	GTA AGA TCC TCC GCC TGT TG	
m*Cox4i1* sense	TTC AGT TGT ACC GCA TCC AG	
m*Cox4i1* anti	TGG GGC CAT ACA CAT AGC TC	
taqman expression probes / assays		
m*Irf8* taqman sense	CAG GCC TGC CAC TGG TG	
m*Irf8* taqman anti	CCA CTG GGA GAA AGC TGA ATG	
m*Irf8* taqman probe	CCG GAT ATG CCG CCT ATG ACA CAC A - FAM	
m*Pu.1* taqman sense	AGA AGC TGA TGG CTT GGA GC	
m*Pu.1* taqman sense	GCG AAT CTT TTT CTT GCT GCC	
m*Pu.1* Taqman probe	TGG GCC AGG TCT TCT GCA CGG - FAM	
ßactin endogenous control	4352341E	ABI
m*Runx1* taqman assay	Mm01213405_m1	ABI

2.1.16 Software

Software	Application	Supplier
Vector NTI	plasmid sequence analysis software	Invitrogen
CellQuest Pro	flow cytometry analyzing software	BD Bioscience
FACSDiva	flow cytometry analyzing software	BD Bioscience
FlowJo	flow cytometry analyzing software	Treestar
7300 System SDS	real time RT PCR analyzing software	Applied Biosystems
Vista	comparative sequence analysis tool (http://genome.lbl.gov/vista/index.shtml as on Dec 06.2010)	

Blast	sequence alignment tool (http://blast.ncbi.nlm.nih.gov/Blast.cgi as on Dec 06.2010)
Primer3	primer design software (http://frodo.wi.mit.edu/primer3/ as on Dec 06.2010)
Ensembl	genome database (http://www.ensembl.org/index.html as on Dec 06.2010)
UCSB browser	genome wide sequencing analyzing software (http://genome.ucsc.edu/ as on Dec 06.2010)

2.2 Mice

General mouse work such as daily animal care, breeding and offspring separation was carried out in collaboration with the animal core facility of the Max-Delbrück-Center for Molecular Medicine, Berlin, Germany. All mice were housed and bred in specific pathogen-free animal facilities. All animal experiments were approved by the local authorities according to the German Federal Animal Protection Act.

2.2.1 Description of the used mouse strains

2.2.1.1 C57/Bl6 wt

Wildtype C57/Bl6 mice were purchased from Charles River (Charles River Laboratories, Sulzfeld, Germany) and crossed to *Irf8*-VENUS PAC and -50kbΔ*Irf8*-VENUS PAC reporter mice.

2.2.1.2 *Irf8*$^{-/-}$ mice

Interferon Regulatory Factor 8 (*Irf8* or Interferon Consensus Sequence Binding Protein, *ICSBP*) deficient mice were described before (Holtschke et al. 1996). In these mice exon two was replaced with a Neomycin cassette leading to a truncated, non functional IRF8 protein. Phenotypically, the mice display an myelo proliferative syndrome (MPS) resembling a chronic myeloid leukaemia phenotype (CML) observed in human, a block in B-cell maturation (Wang et al. 2008) and an expansion of the granulocytic compartment to the expense of macrophages an DCs (Turcotte et al. 2005).

2.2.1.3 *Irf8*-VENUS PAC & -50kbΔ*Irf8*-VENUS PAC reporter mice

Irf8-VENUS PAC and -50kbΔ*Irf8*-VENUS PAC mice were generated as described in this study. Briefly, a murine *Irf8* gene locus carrying phage artificial chromosome (PAC) was modified. A reporter cassette consisting of an internal ribosomal entry site (IRES) and a VENUS fluorescent reporter gene were integrated in the untranslated region of the PAC *Irf8* exon 9. VENUS is a GFP derivative equivalent to an enhanced YFP, thus emitting yellow light

(Nagai et al. 2002). This allowed tracing of *Irf8* expression in mice based on the VENUS signal. Furthermore, this PAC harboured a *lox*P site flanked newly discovered regulatory *cis*-element 50kb upstream of the *Irf8* transcription start site (TSS). *Irf8*-VENUS PAC reporter mice were generated by pronuclear injection of the modified murine *Irf8*-PAC into fertilized oocytes of C57Bl/6 wild type (wt) mice. The injection was done at the Max Planck Institute of Molecular Cell Biology and Genetics (MPI, Dresden, Germany). PAC positive animals were detected by PCR and FACs analysis. Three PAC reporter strains were maintained in parallel, showing similar reporter expression. Two out of three reporter strains were bred to Cre deleter mice. Cre mediated recombination under the ubiquitously active cytomegalovirus (CMV) promoter excised the *lox*P site flanked region, resulting in a complete deletion of the *cis*-element within all cells of these mice. Those strains were named -50kbΔ*Irf8*-VENUS PAC. Furthermore, these mice were bred into the *Irf8* deficient background. This lead to two homozygous deficient endogenous *Irf8* alleles and one functional PAC based *Irf8* locus, with or without the *cis*-element, respectively.

2.2.1.4 CMV-Cre deleter mice

Mice carrying the Cre recombinase under the control of the CMV promoter have been generated as described (Su et al. 2002). This promoter confers constitutive strong expression in mammalian cells, thus, allows for Cre recombinase activity in all cell types. This strain was used to excise *lox*P site flanked regions, consequently resulting in complete deletion of the target sequence. Mice were kindly provided by the group of Thomas Blankenstein, MDC-Berlin.

2.2.1.5 URE$^{-/-}$ mice

URE knockout mice were generated as described (Rosenbauer et al. 2004; 2006) and got provided by the Tenen lab, Boston, MA, USA. These mice carry a neomycin insertion in the Pu.1 regulatory element, called upstream regulatory element (URE) (Li et al. 2001; Okuno et al. 2005), which reduces *Pu*.1 expression to 20 % of wt levels. Phenotypically, the mice are deficient in generating normal numbers of macrophages and B-cells, develop acute myeloid leukaemia (AML) and T-cell lymphomas.

2.2.1.6 Conditional *Runx1*$^{-/-}$ mice

Conditional *Runx1*$^{-/-}$ mice were generated as described (Putz et al. 2006) and got provided by the Buchholz lab, Dresden, Germany. Here, exon 5 of *Runx1* is flanked by *lox*P sites and a

neomycin cassette. In order to achieve a deletion, the mice also carry the Cre recombinase under control of the IFN-inducible *Mx1* promoter (Kuhn et al. 1995). The *Mx1* promoter was induced to high levels of transcription by administration of synthetic double-stranded RNA, PolyIPolyC (poly (I:C)). Expression of the Cre recombinase causes the *lox*P site flanked sequence to be removed. To induce excision of floxed *Runx1* exon 5, mice received 300 µg poly (I:C) in PBS per intra-peritoneal injection every other day for a total of five injections. Phenotypically, these mice develop a myelo displastic syndrome (MDS) and splenomegaly with an expansion of the myeloid compartment.

2.2.1.7 *CX_3CR1*-GFP mice

The Fractalkine receptor (*CX_3CR1*) reporter mice were generated as described (Jung et al. 2000) and got provided by the Jung laboratory, Rehovot, Israel. *CX_3CR1* is expressed in monocytes and their progenitors (Geissmann et al. 2003; Fogg et al. 2006). A GFP knockin replaced the *CX_3CR1* locus and allowed tracing of GFP expression under the control of the *CX_3CR1* promoter. Those mice were bred to the *Irf8*-VENUS PAC reporter mice. Expression of *CX_3CR1* and *Irf8* was traced based on GFP and VENUS fluorescent signals, respectively.

2.2.2 Mousework

2.2.2.1 Genotyping

Mice offspring were tagged according to standard protocols. Genotyping was done either by locus-specific polymerase chain reaction (PCR) on genomic DNA extracted from tail tissue, or by means of flow cytometry on fluorescent markers.

2.2.2.2 Isolation of mouse organs

Mice organs were harvested after euthanizing the mice with CO_2. Animals were pinned down on a dissecting board, the belly was facing up. Subsequently the animals were opened with scissors and forceps, upper and lower legs as well as upper arms were removed, when necessary other organs as spleen were removed, too. All organs were kept in cold PBS until preparation. Single cell suspensions were generated by cutting the organ into small pieces and subsequently filtering it through a cell strainer (Becton Dickens). Bone marrow was isolated by flushing the bones with phosphate buffered saline (PBS). Peripheral blood of living mice or sacrificed mice was taken from the tail vein or from the heart, respectively, using EDTA treated canula.

2.2.2.3 Transplantation experiments

For *in vivo* differentiation assays, young CD45.1$^+$ congenic recipient mice (3-4 weeks of age) were irradiated with a sub-lethal dose of 6 Gy total body irradiation with the 18-MeV photon beam of a linear electron accelerator with a dose rate of 0.18 Gy/min. These mice were then reconstituted with freshly isolated BM cells of CD45.2$^+$ donor mice within 24 h after irradiation. Therefore, a cell suspension with the desired cell number per 200 µl in sterile PBS was prepared and injected intravenously in the tail vein of the fixed recipient animal. Animals were sacrificed and analyzed 11 days after transplantation.

2.2.2.4 Immunofluorescence staining and confocal microscopy

For immunofluorescence studies, the spleens were sliced and fixed in PBS containing 4 % paraformaldehyde (45 min, 4°C), followed by cryoprotection in 30 % sucrose-containing PBS for 24h. Frozen spleen tissue was cut into 12 µm thick sections with a cryostat and mounted onto object slides. For staining, sections were incubated with 20 % normal donkey/ normal goat serum (NDS/NGS) and 0.3 % Triton-X100 in TBS for 1 hour. Afterwards, sections were incubated overnight at 4°C in 1 % NDS/NGS, 0.3 % Triton-X100 containing TBS with antibodies against following markers: CD11c (clone N418, Abcam), GFP (rabbit polyclonal, Invitrogen), MARCO (clone ED31, Serotec), CD169 (clone MOMA-1, Serotec) or SIGNR1 (clone ER-TR9, Abcam). After thorough washing in TBS, sections were incubated overnight at 4°C with the appropriate Alexa 488 or Alexa 568-conjugated secondary donkey antibodies (Invitrogen) or DyLight 594-conjugated anti-armenian hamster goat antibody (Jackson Immunoresearch) diluted in 1 % NDS/NGS, 0.3 % Triton-X100-containing TBS. Finally, sections were washed in TBS and coverslipped. A Leica TCS SPE confocal microscope was used to obtain images of the stained sections, which represent single confocal planes of the spleen tissue.

2.3 Cell culture

2.3.1 Cultivation and cryo-preservation of primary cells and cell lines

All cell lines described here were grown in indicated media supplemented with fetal calf serum (FCS) and antibiotics (Penicillin/Streptomycin) in an incubator at 37°C and 5 % CO_2. Further media complements are stated in the individual chapter. For passaging of adherent cells, medium was aspired, cells were washed once with PBS and incubated with 0.05 % trypsin-EDTA (~5 min, 37°C) (4 ml trypsin per 10cm dish). Once detached, cells were resuspended in an appropriate amount of medium, centrifuged (1200 rpm (Eppendorf 5415c centrifuge, rotor

FA 24-24-11, or stated otherwise), 5 min, room temperature (RT)), and the cell suspension was transferred in different dilutions to new tissue culture dishes. Alternatively, adherent cells were carefully dislodged using a cell scraper and appropriate aliquots were distributed to new culture vessels. Suspension cells were passaged and supplied with fresh medium twice a week. For cryo-preservation, medium was removed, cells were taken up in cryomedium (50 % (v/v) DMEM, 40 % (v/v) FCS and 10 % (v/v) DMSO) and finally transferred into cryo-tubes. For 24 h, cryo-tubes were stored in Styrofoam boxes at -80°C, after which they were placed in liquid nitrogen.

2.3.2 Cell lines

RAW 264.7 cells (ATCC: TIB-71) are murine macrophage like cells derived of an Abelson murine leukaemia virus induced tumor of a BALB/c mouse. Cells were grown adherent in DMEM with 10 % (v/v) FCS and were sub-cultivated twice per week.

NIH3T3 cells (ATCC: CRL-1655) are murine embryo derived fibroblasts. They were grown adherent in DMEM with 10 % (v/v) FCS and were sub-cultured three times per week.

The growth-factor independent cell line 416B is a primitive myeloid cell line, which was isolated from a long-term culture of mouse bone marrow cells infected with Friend leukaemia virus. They were maintained in suspension and upon M-CSF stimulation they could be differentiated into monocytes (Dexter et al. 1979).

2.3.3 Thawing of cells

Cells were thawed quickly at 37°C and transferred drop wise to 10 ml medium. After centrifugation (1200 rpm, 5 min, RT), supernatant was discarded and pellet was resuspended in 1 ml medium. Cells were plated in an appropriate cell number on culture dishes.

2.3.4 Assessment of cell number and cell viability

Cells were harvested, centrifuged (1200 rpm, 5 min, RT), the resulting cell pellet was resuspended in PBS. A small aliquot was removed and mixed in a ratio of 1:9 with trypan blue solution. The mix was incubated for 1 min, an aliquot was transferred to the Neubauer chamber and checked for equal distribution of the cells in all four big quadrants. If more samples were counted, the trypan blue solution was added shortly before counting and cells were placed on ice. Dead cells stained blue, viable cells remained white.

2.3.5 Stable and transient transfection of cells

For stable transfection assays, cells were needed in logarithmic growth phase. Hence, cell lines were propagated at low cell density. DMEM without supplements was used to resuspend the cells to a final cell concentration of 1*E07/ml. For transfection 20 µg linearized plasmid and 2 µg antibiotic resistance cassette carrying vector were mixed to 500 µl cell suspension and incubated for 5 min at RT. The cell/DNA mix was transferred to a 0.4 ml electroporation cuvette (Biorad) and electroporated in a Biorad electroporation device (Genepulser Xcell, Biorad), following standard electroporation protocols. Positively transfected cells were identified by antibiotic resistance and propagated for downstream application.

Transient transfections were conducted employing chemical transfection reagents. Briefly, cells were grown in logarithmic phase at a low cell density on 6-well culture vessels. Usually 5.0 µg plasmid was transfected using 12 µl Fugene 6 (Roche) following the instructions of the manufacturer. Transfected cells were FACs purified based on GFP marker expression and subsequently analyzed 24-48 h post transfection.

2.3.6 Generation of stable reporter gene cell lines

Stable transfection by electroporation was required for downstream reporter assays. Cells were prepared as described in 2.3.5. After electroporation, cells were counted again and distributed in different cell densities to culture vessels for 48 hours. Antibiotic selection started then depending on the cell line used for two to four weeks with frequent change of antibiotic containing medium. After selection of antibiotic resistant colonies, single cell clones were picked from the adherent cell colonies and further propagated. Bulk cultures were maintained as well for downstream reporter assays.

2.3.7 Methylcellulose differentiation assays

In order to test the proliferation and differentiation capacity of stem- and progenitor cells methylcellulose assays were conducted. Therefore, BM cells were harvested, haematopoietic stem- and progenitor cells, *Irf8*-VENUS positive and *Irf8*-VENUS negative myeloid progenitor cells were FACS sorted. An appropriate cell number (usually 0.25 to 1.0*E03 cells) was mixed with the semi-solid Methocult medium supplemented with different cytokines promoting cell specific differentiation conditions (Methylcellulose (MC), Stem Cell technologies). Cells were seeded in 1 ml of this suspension in triplicates and were plated onto 35 mm cell culture dishes. All dishes were put into a 150 mm cell culture vessel together with an open dish filled with water to prevent drying of the semi-solid media. Five to seven days after plating the resulting

colonies were scored with an inverted light microscope (Leica DMEL, Leica) (Kaiho et al. 1985), phenotyped based on colony morphology and subsequently isolated for FACS analysis (fluorescence activated cell sorting) or cell morphology assessment.

For evaluating mononuclear phagocyte potential the following cytokine cocktails were administered:

Table 1: Methylcellulose (MC) cytokine complements supporting mononuclear phagocyte cell differentiation potential

	MC	IL3	IL6	SCF	M-CSF	GM-CSF	Flt3L
Monocyte potential	3234	10 ng/ml	10 ng/ml	50 ng/ml	10 ng/ml	-	-
Dendritic potential	3234	10 ng/ml	10 ng/ml	50 ng/ml	-	10 ng/ml	-
Dendritic potential	3234	10 ng/ml	10 ng/ml	50 ng/ml	-	-	100 ng/ml

Evaluation of combined myeloid, erythroid and megakaryocytic potential was tested using following cytokines:

Table 2: Methylcellulose (MC) cytokine complements supporting myelo-erythroid differentiation potential

	MC	IL3	IL6	SCF	EPO
Myelo-erythroid potential	3234	10 ng/ml	10 ng/ml	50 ng/ml	3 U/ml

2.3.8 Liquid culture differentiation assays

To study the proliferation and differentiation capacity of stem and progenitor cells in respect to cell morphology, liquid culture differentiation assays were conducted. Haematopoietic stem- and progenitor cells, *Irf8*-VENUS positive and *Irf8*-VENUS negative myeloid progenitor cells were FACS sorted. 0.2 to 1.2*E04 FACS purified cells (described in 2.6) were seeded in 24-well cell culture dishes, which were coated with sterile glass slides allowing attachment of adherent cells. IMDM supplemented with the cytokine mixes indicated in Table 1 and Table 2 induced differentiation of the cells. After five days of differentiation the glass slides were removed, washed once in PBS to remove not adherent cells. After air-drying the slides were fixed in Methanol and stained with May-Grünwald and Giemsa stain. Alternatively, adherent cells were phenotyped based on morphology, using an inverted light microscope (Leica DMEL, Leica). Subsequently cells were washed once with PBS and detached employing Accutase (~5 min, 37°C) (0.5 ml Accutase per well). Once detached, cells were resuspended in an appropriate amount of medium, centrifuged (1200 rpm, 5 min, RT) and used for FACS analysis.

2.3.9 Cytospin and May-Grünwald / Giemsa staining

Cell morphology was assessed by spinning suspensory cells or trypsinized adherent cells in a cytospin-centrifuge (Wescor 7120 slide strainer, Logan, UT, USA) at low acceleration (800 rpm, 5 min) on a glass slide, followed by an air-drying step. Cells were fixed in Methanol for 10min and subsequently subjected to May-Grünwald staining solution for 5 min. After a brief washing step with water, a second staining with Giemsa stain for 30 min was performed. Cells were washed again with water, dried and photographed with an Axioplan2 microscope/camera system (Zeiss).

2.4 Bacterial strains and plasmids

2.4.1 Bacterial strains

Bacterial strains used for plasmid and PAC expression are listed below in Table 3.

Frozen stocks of the bacterial strains in logarithmic growth phase are stored in lysogeny broth (LB) and 10 % (v/v) dimethylsulfoxide (DMSO) at –80°C.

Table 3: Bacterial strains used for plasmid or PAC expression

Bacterial strain	Relevant feature	Source
Escherichia coli DH10B	PAC expression	Invitrogen
Escherichia coli GT115	plasmid expression	Invivogen

2.4.2 Plasmid and PAC expression

2.4.2.1 Mini- and maxiprep

Plasmid DNA (pDNA) was extracted using Mini preparation (Invisorb® Spin Plasmid Mini Two kit, Ivitek) for low amounts and Maxi preparation (PureLink™ HiPure Plasmid Maxiprep kit, Invitrogen) for larger amounts of pDNA. For both applications LB medium was inoculated with either one colony from the LB agar plate or with bacterial pre-culture. The culture was incubated at 37° C for 4-8 h at 200 rpm on a shaker. Then, the suspension was transferred into centrifuge tubes and centrifuged (Mini: 13.000 rpm, 5 min, RT; Maxi: 6000 rpm, 15 min, 4°C). The clarified supernatant was removed and the bacterial pellet was resuspended in 250 µl buffer A (Mini) or buffer R3 10 ml (Maxi), then lysed by adding 250 µl buffer B (Mini) or 10 ml buffer L7 (Maxi) for 5 min at RT. Subsequently, lysis was stopped with 250 µl buffer C (Mini) or 10 ml buffer N3 (Maxi) and the mixture was neutralized at 4°C for 5 min. The supernatant containing the plasmid DNA was clarified by centrifuging at 4°C for 5-10 min at 13000 rpm (Mini) or 4500 rpm (Maxi) before it was transferred onto the respective column. After loading the column, it was washed twice with wash buffer (Mini: 750 µl; Maxi: 20 ml)

and pDNA was eluted with 30 µl Tris/EDTA buffer (TE) (Mini) or 5 ml elution buffer (Maxi). At this point the eluate of the Mini preparation was used in downstream applications or stored at -20°C. The eluate of the Maxi preparation was precipitated using 3.7 ml isopropanol and centrifuged (1 h, 4°C, 4500 rpm). The pDNA pellet was washed with 70 % ethanol (EtOH), air-dried and finally resuspended in TE buffer.

2.4.2.2 PAC DNA preparation

The PAC DNA was isolated using an anion exchanger column purification system (NucleoBond® BAC 100 kit, Marcherey Nagel). The protocol essentially follows Maxi preparation conditions and was conducted following the recommendations of the manufacturer. After precipitation, PAC DNA was carefully resuspended in 100 µl TE buffer using a pipette tip of which the tip was cut. That way sheering forces were reduced and PAC DNA integrity was maintained. DNA concentration was determined using the Nanodrop (see 2.5.4) and appropriate amounts of DNA were linearized for subsequent injection in fertilized oocytes. PCA DNA was stored at 4°C up to two weeks.

2.4.3 Plasmid cloning

2.4.3.1 Restriction digest of DNA

For analytical purposes, plasmids from mini preparations (see 2.4.2.1) were digested with appropriate restriction enzymes to identify positive clones with the respective insert. 500 ng plasmid DNA was digested in a mixture of 1 x restriction buffer and 10 U of each restriction enzyme (1 h, 37°C). The fragment pattern was visualized by agarose gel electrophoresis. Positive plasmids were sent to sequencing.

For preparative purposes, plasmid DNA and PCR products were digested with appropriate restriction enzymes to obtain compatible sticky or blunt ends. The fragment pattern was visualized by agarose gel electrophoresis of which target DNA was extracted (see 2.4.3.2).

2.4.3.2 Gel purification / extraction

Appropriately sized DNA fragments were isolated from agarose gels using a scalpel and purified using the Gel extraction kit (Invitek) according to the manufacturer's instructions. Obtained fragments or linearized target vector were further used in downstream applications. DNA was eluted with 20 µl TE buffer and was stored at -20°C.

2.4.3.3 Blunting of restriction site overhangs

To allow for restriction site independent cloning as well as for merging of a sticky restriction digest overhang to a blunt overhang, blunting reactions were carried out. Therefore the sticky overhang containing DNA fragment was incubated with T4 DNA Polymerase (Fermentas) (37°C, 30 min) and subsequently heat inactivated (15 min, 65°C). The blunted fragment was purified as described (2.4.3.5) and then used for ligation.

2.4.3.4 Dephosphorylation of vector

The target plasmid vector was dephosphorylated prior to the ligation reaction to prevent the backbone from spontaneous religation. 1 Unit (U) Shrimp alkaline phosphatase (SAP; Fermentas) and up to 2 µg linearized pDNA per 20 µl mix were combined. Dephosphorylation reaction was carried out at 37°C for 30 min, heat inactivated for 15 min at 65°C and subsequently purified as described (2.4.3.5).

2.4.3.5 DNA cleanup

After dephosphorylation of the vector (2.4.3.4) or blunting of restriction site overhangs (2.4.3.3), pDNA was purified from the reaction mixture by using the PCRapace kit (Invitek) according to the manufacturer's instructions. DNA was eluted with 20 µl TE buffer and stored at -20°C.

2.4.3.6 Ligation

Typically 5-fold excess of insert over the plasmid backbone was used in a ligation reaction mix containing backbone, insert and 400 U T4 DNA ligase (NEB) in 1 x ligation buffer. The ligation reaction was carried out overnight at 16°C.

2.4.3.7 Transformation of chemically competent *E. coli*

10 µl ligation mixture was transformed into GT115 chemically competent *E. coli* cells. Bacteria were incubated with the plasmid solution on ice for 20 min, heat-shocked at 42°C for 90 sec and incubated on ice for 2 more minutes. 1 ml pre-warmed LB medium was added to the bacteria-DNA mixture, followed by incubation (1 h, while shaking). Subsequently, bacteria were spread onto LB-agar plates containing the selective antibiotic and incubated at 37° C overnight to allow colony growth.

2.4.4 Generation of PAC-reporter constructs

2.4.4.1 Cloning of PAC recombination target plasmids

For the modification of the murine *Irf8*-VENUS PAC a target construct was assembled in a plasmid vector harbouring the IRES-VENUS reporter cassette and an antibiotic selection cassette. These sequences were flanked by two homology arms, allowing for precise incorporation of the reporter during homologous recombination. The homology arms were generated by PCR amplification using the indicated primers (see 2.1.14), employing *PFU* Polymerase that exhibits proofreading capacity. This resulted in a 490bp left homology arm (5'-site of *Irf8* Exon9) and a 524 bp right homology arm (3'-site of *Irf8* Exon9), respectively. These fragments were cloned into the pGMTeasy vector (Stratagene) following standard protocols. Positive clones were identified by blue/white selection. Plasmid DNA was extracted by Miniprep (see 2.4.2.1). Accuracy of the DNA fragment was assessed using restriction enzyme digestion followed by electrophoretic separation. The homology arms were then transferred into the pBluescript Vector (Invitrogen) that contained a zeocin antibiotic marker under the control of the EM7 prokaryotic promoter, allowing for selection of positively transfected plasmids in bacterial hosts. Here, the left homology arm was transferred by *Not*I/*Sac*II restriction digest, followed by the transfer of the right homology arm by *Cla*I restriction digest. Finally, the IRES-VENUS cassette was cloned into the pBluescript as a *Bam*HI fragment. The resulting vector contained the proximal left homology arm, followed by the zeocin selection cassette, followed by the IRES-VENUS cassette and the distal right homology arm. The vector was verified by sequencing and by PCR. Finally it was linearized for subsequent homologous recombination (2.4.4.2). A schematic draft is displayed in Figure 6.
In a second modification step, the newly discovered -50kb regulatory element was flanked with *lox*P sites. Therefore, a second targeting vector was assembled. The *lox*P sites were generated by PCR amplification using the indicated primers (see 2.1.14), employing PFU Polymerase as described. *Pfo*I restriction site overhangs were incorporated into the primers. This allowed targeted integration of the *lox*P fragment into the unique *Pfo*I restriction site of the target vector which already contained the -50kb Element (Figure **7**A). In a second step the same *lox*P fragment was blunted and cloned into the *Sma*I site of the already described zeocin cassette containing vector (B). In the next step this enlarged fragment containing zeocin cassette and *lox*P site was removed via *Eco*RV/*Sac*II restriction, blunted and relegated into the blunted *Sfi*I site of the targeting vector (C). That way parts of the original -50kb element containing fragment became separated from the -50kb core region by the *lox*P sites and served as

homology arms. The vector was verified by sequencing as well as by PCR and was linearized for subsequent homologous recombination. A schematic draft is displayed in Figure 7

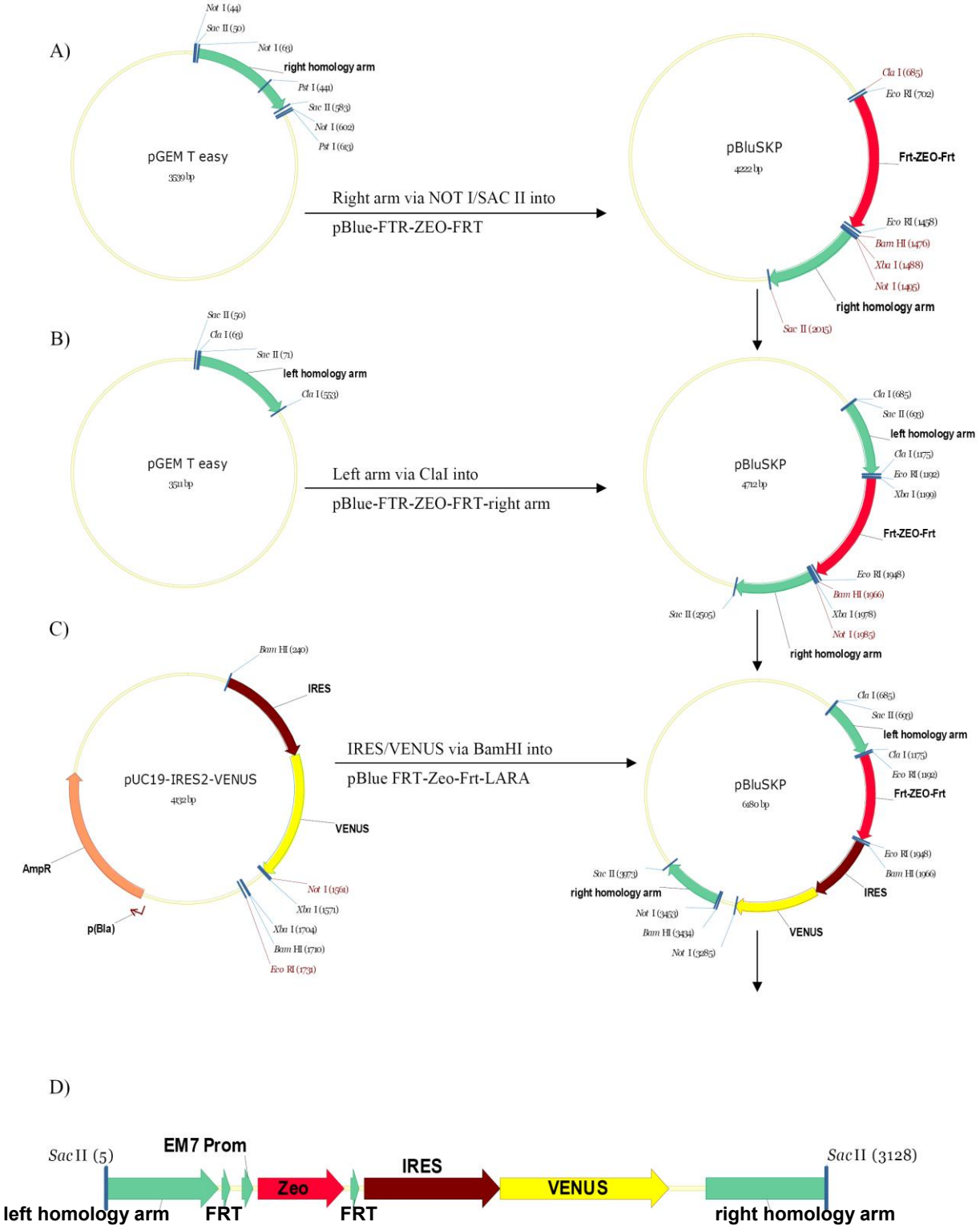

Figure 6: Cloning strategy for *Irf8* PAC VENUS reporter cassette. Homology arms were PCR amplified and sub-cloned into the pGMTeasy vector. **A)** The 3' located homology arm (right arm) was transferred by *Not*I/*Sac*II restriction, **B)** the 5' located homology arm (left arm) was transferred using *Cla*I into the pBluescript vetor containing the zeocin selection cassette. **C)** The IRES-VENUS reporter cassette was integrated between the homology arms, next to zeocin cassette via cloning with *Bam*HI. All intermediate steps were verified either by sequencing or by restriction enzyme digestion. **D)** The final construct was linearized by *Sac*II digestion and used for electroporation.

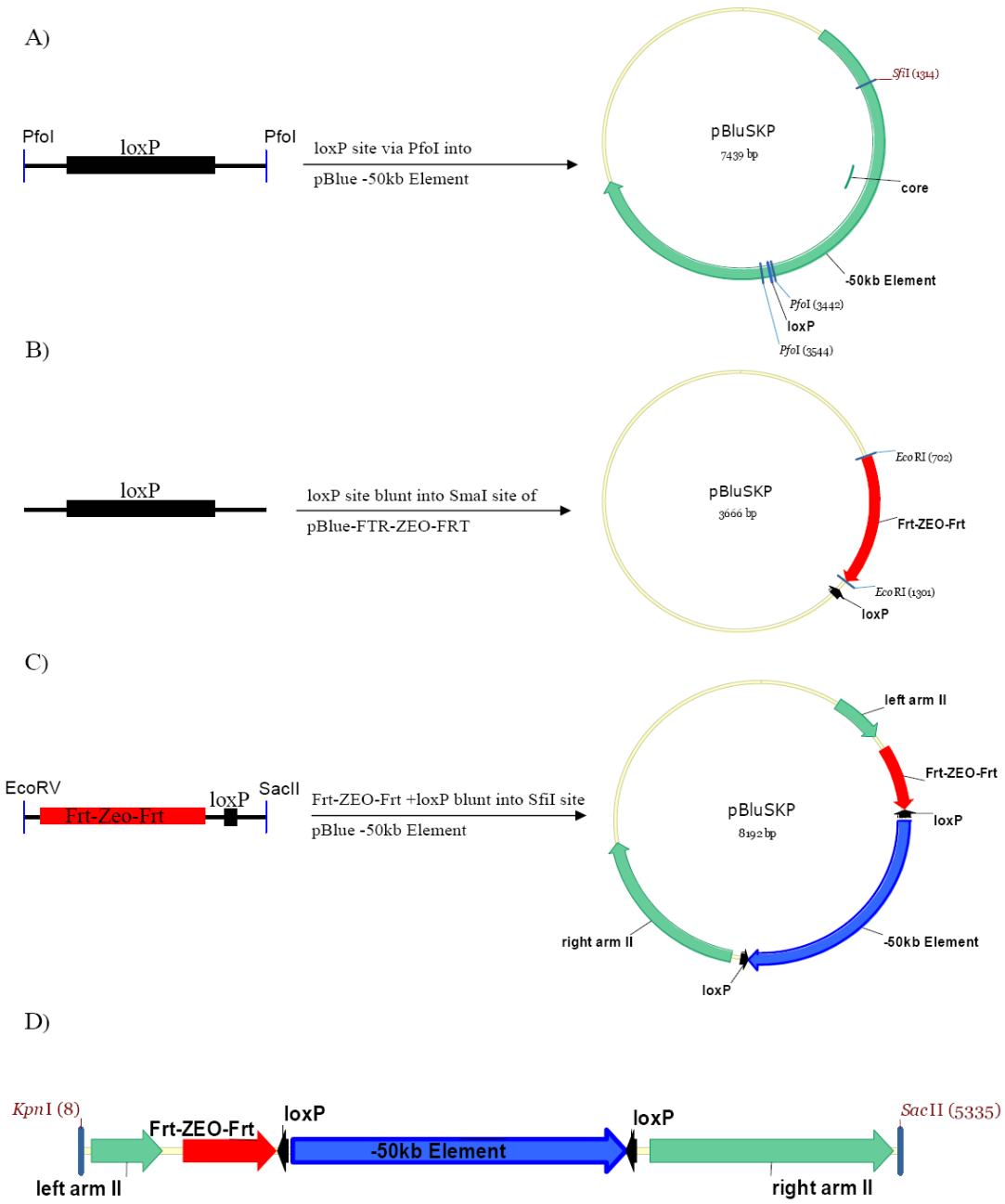

Figure 7: Cloning strategy for *lox*P site flanked -50kb element. A) *lox*P sites were PCR amplified and cloned into the *Pfo*I site of a pBluescript vector that contained the -50kb element *Bam*HI fragment taken from the IRF8-PAC. **B)** The *lox*P site fragment was blunted and inserted into the *Sma*I site of the pBluescript vetor containing the zeocin selection cassette. **C)** The zeocin selection cassette together with the *lox*P site was removed via *Eco*RV/*Sac*II restriction and cloned blunt into the *Sfi*I site of the targeting vector. All intermediate steps were verified either by sequencing or by restriction enzyme digestion. **D)** The final construct was linearized by *Kpn*I/*Sac*II digestion and used for electroporation.

2.4.4.2 Homologous recombination of the PAC in bacteria

A λ-phage carrying the recombinase gene (Liu et al. 2003) under a temperature sensitive promoter was transfected by electroporation to the *E. coli* DH10B that harboured the unmodified *Irf8*-PAC construct. PAC and phage double positive cells were selected using the appropriate antibiotics, namely kanamycin (Kan) resistance for selection of the PAC and

tetracyclin (Tet) for the phage. Single colonies of those cells were made electrocompetent following standard protocols.

The linearized reporter construct was electroporated into the PAC and phage containing *E. coli* DH10B. Recombination was induced by heat shock (2.4.3.7) and clones were selected employing a double antibiotic selection strategy for a recombined PAC construct, using Kan and Zeo, respectively. PAC DNA of antibiotic resistant clones was further verified for successful recombination by PCR and sequencing. Since most of the successfully recombined clones also contained additional not recombined PAC copies, as detected by PCR, the PAC was isolated by Maxiprep and was re-electroporated. This way also the λ-phage was excluded to avoid further unspecific recombineering events.

The zeocin resistance cassette of the modified PAC was deleted by introduction and subsequent activation of an Flp-recombinase carrying plasmid. This was achieved by electroporation of the Flp-plasmid into the modified PAC carrying bacteria as described before. Flp activation under the arabinose sensitive promoter was done as described (Liu et al. 2003). Bacteria that had lost the Zeo resistance were selected and again validated by PCR and sequencing. A schematic draft states the individual steps as shown in the Figure 8 below.

A)

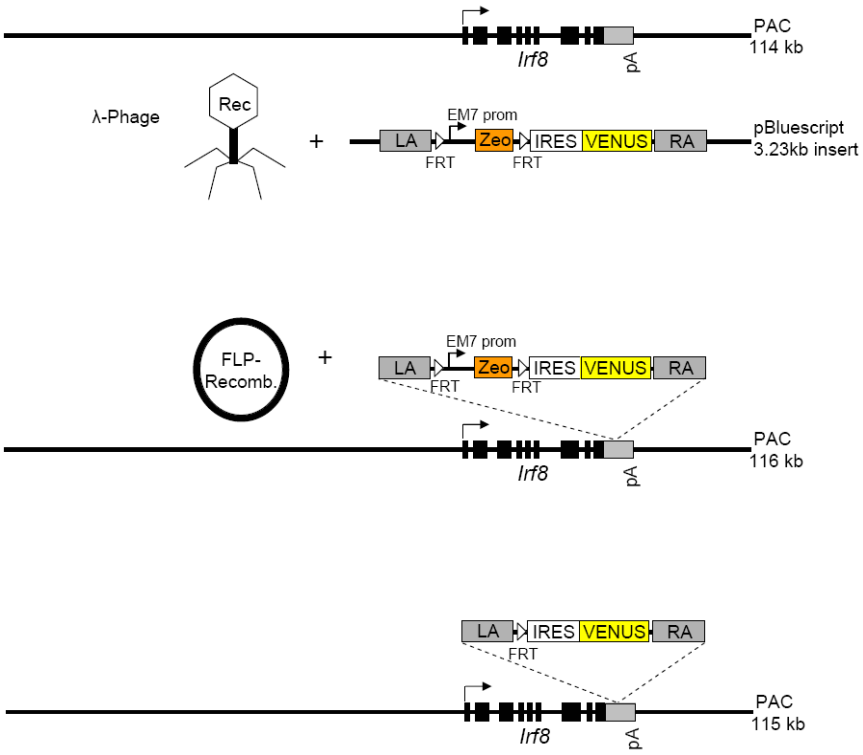

B)

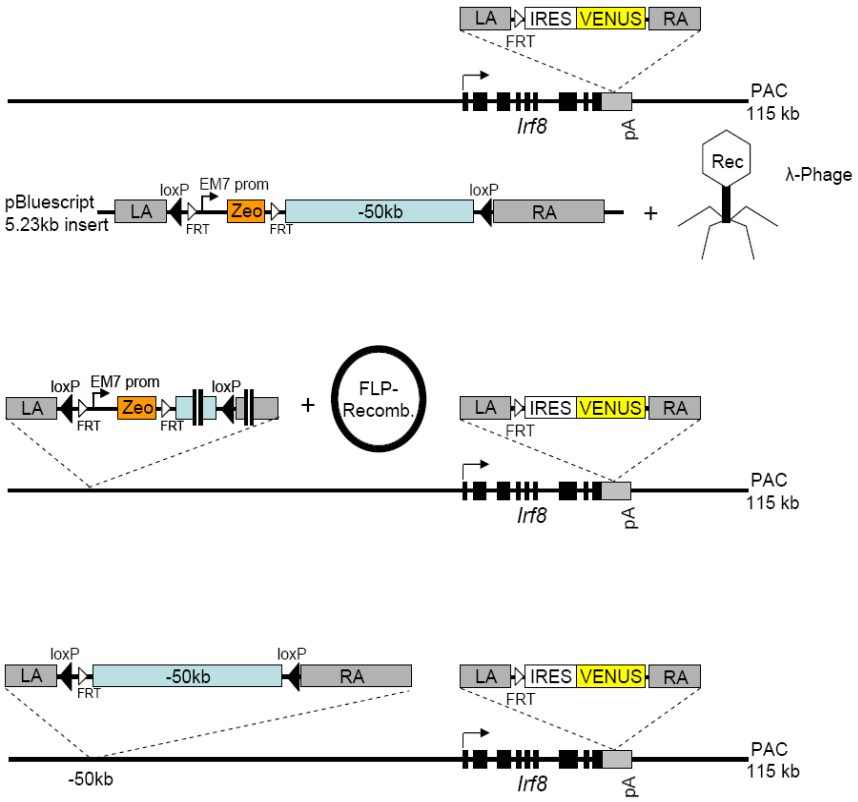

Figure 8: Homologous recombination of *Irf8*-VENUS PAC in bacteria. A) Schematic draft of homologous recombination strategy. PAC containing bacteria are equipped with the recombinase carrying λ-phage and the Venus-recombination plasmid by electroporation. After antibiotic induced selection of the recombined PAC the FLP recombinase carrying plasmid was introduced by electroporation. FLP-recombinase mediated excision of the Zeo selection cassette resulted in the final reporter cassette carrying PAC. **B)** Introduction of the λ-phage and the -50kb recombination plasmid by electroporation followed by selection produced a double modified PAC which was selected with the appropriate antibiotics. Activation of FLP-recombinase deleted the Zeo selection cassette. This yielded in the final transgenic *Irf8*-VENUS PAC construct.

2.4.5 Cloning of luciferase reporter constructs

The pXP2 luciferase reporter vector (ATCC: 37577) backbone was equipped with a 1.9 kb *Irf8*-promoter sequence fragment in the unique *Xba* site. This basic promoter vector was further complemented with different regulatory element containing fragments of varying sizes into the *Bam*HI site. The regulatory element containing fragments originated from the *Bam*HI digested murine *Irf8*-PAC, while the promoter fragment was provided by Marina Scheller, MDC. All plasmids were verified by PCR and sequencing.

2.4.6 Cloning of sh-RNA constructs

Sh-RNA hairpin sequences were taken from Lausen et al. (Lausen et al. 2006) and cloned into psi-RNA h7SK-GFPzeo vector (Invivogen) as described by the manufacturer. Sequencing confirmed accuracy of the hairpin structure. Downregulation of target genes (*Runx1*, *Pu.1*) was assessed by real-time-RT PCR (2.5.6) and by Western blotting (2.5.12 and 2.5.13).

2.5 General molecular biology

2.5.1 Preparation of genomic DNA

Genomic DNA (gDNA) was extracted following standard protocols. In brief, cells or tissue was digested with tail digestion buffer supplemented with 10 µg/ml proteinase K at 56°C for 5-12 h. gDNA was purified by addition of a phenol/chloroform mixture and subsequent centrifugation (13000 * g, 5 min, 4°C). The upper fraction, containing the gDNA, was transferred into a new tube and precipitated with isopropanol. After centrifugation (13000 * g, 20 min, 4°C) supernatant was removed and the remaining DNA pellet was washed with 70 % ethanol. After another centrifugation step (13000 * g, 5 min, 4°C) supernatant was discarded and the DNA pellet was air-dried until ethanol was completely evaporated. DNA was dissolved in TE buffer.

2.5.2 DNA free RNA preparation

Total RNA was extracted from primary cells or cell culture cultivated cells using the RNeasy® Mini Kit or RNeasy® Micro elute Kit (both: Qiagen), when extracting 10*E04 cells or less. RNA was extracted following the manufacturer's recommendations including on column DNA digestion using RNase free DNase (Qiagen).

Alternatively, cells were directly resuspended in Trizol (PeqLab) and homogenized by vortexing (for cell numbers up to 5*E05) or by passing the mixture through a 16 gauche needle several times. After incubation (5 min, RT) chloroform was added to separate RNA from DNA and proteins. Suspension was vortexed for 15 sec and incubated (5 min, RT). After centrifugation (13000 * g, 15 min, 4°C), RNA that remained in the colourless aqueous phase was transferred to a new tube. To precipitate RNA, isopropanol was added to the samples, incubated (10 min, on ice) and centrifuged (13000 * g, 10 min, 4°C). Supernatant was removed and pellet was washed with 70 % ethanol. After centrifugation (13000 * g, 10 min, 4°C) supernatant was discarded and pellet was air-dried until ethanol was completely evaporated. RNA was re-dissolved in RNase free water and incubated (10 min, 55°C). In general, RNA was stored at -80°C. All buffers, solutions, tips and other equipment were RNase free.

2.5.3 cDNA synthesis

Total RNA up to 1 µg was used for cDNA synthesis, where at first DNaseI treatment was performed to deplete gDNA traces. Therefore, 5.0 µl RNA were incubated with 1 µl DNaseI (10 U/µl), 0.8 µl 10 x DNaseI buffer and 1 µl RNase out (15 min, RT). DNaseI was inactivated by incubation with 1 µl EDTA (25 µM) (65°C, 10 min).

For cDNA synthesis Revert Aid First Strand cDNA Synthesis kit (Fermentas) was used following the manufacturer's recommendations. Briefly, genomic DNA free total RNA was incubated with 1µl random hexamer primers (100 µM stock), 4 µl 5 x reaction buffer, RiboLock™ RNase Inhibitor (20 U/µl), 2 µl dNTPs (10 µM stock) and 1 µl of RevertAid™ M-MuLV Reverse Transcriptase (200 U/µl stock) in a final volume of 20 µl for 60 min at 42°C. The reaction was stopped by heating (70°C, 15 min). cDNA was stored at -20°C. As a control, no RT samples (RNA samples which undergone DNase treatment but no reverse transcription) were generated exemplarily and used as a negative control in real time RT PCR analysis (2.5.6).

2.5.4 Quantification and quality control of RNA and dsDNA

Concentration and purity of total RNA and double stranded (ds) DNA were determined by measuring the absorbance of nucleic acids at A_{260} and A_{280} with a Nanodrop 1000 UV-spectrophotometer (Nanodrop, Wilmington, DE, USA).

Concentration [µg/ml]	=	40 * A_{260} * dilution → (A_{260} of 1=40µg/ml RNA) 50 * A_{260} * dilution → (A_{260} of 1=50µg/ml dsDNA)
Total yield [µg]	=	concentration [µg/ml] * volume of sample [ml]
Purity A_{260}/A_{280}	=	RNA 1.9 – 2.1; DNA 1.8; proteins ≤ 1.5

Quality control of total RNA was performed employing the Agilent 2100 bioanalyzer (Agilent Technologies, Palo Alto, CA, USA) using the eukaryotic RNA pico Chip. Electropherograms and Agilent-algorithm based RIN-values stated quality levels of the respective RNA samples. Only RNA with RIN-values of 8.9 and higher was used for subsequent applications.

2.5.5 Polymerase chain reaction (PCR)

PCR was performed in an Eppendorf Mastercycler (Eppendorf, Hamburg, Germany), using Opti-*Taq* Polymerase (Roboklon, Berlin, Germany).

The protocols in this study were essentially as described by the manufacturer. Primer concentration was set to 0.5 µM each primer. Concentration of dNTPs was 200µM each nucleotide. Mainly the following protocol was used:

Table 4: Basic PCR protocol

Cycles	Step	Temperature	Time
1	Polymerase activation	95°C	2 min
	Denaturation	95°C	15 sec
30-40	Annealing	57°C	15 sec
	Elongation	72°C	30 sec
1	Final elongation	72°C	2 min

2.5.6 Real-time RT-PCR

Quantitative Real-time PCR allows monitoring of DNA amplification at each cycle by measuring the amount of PCR product created during the exponential phase of amplification either due to the incorporation of the fluorescent dye SYBRgreen into the minor groove of the DNA helix, or, due to increased amounts of sequence specific TaqMan probes, which emit fluorescence upon binding to their respective complementary target site. Thus, quantification of starting material is accomplished. This principle was first put forth in 1993 when Higuchi et al. published the simultaneous amplification and detection of PCR products (Higuchi et al. 1995). Real-time PCR was performed in an ABI Prism 7300 (ABI), using the QuantiTect SYBRgreen RT-PCR one step kit® (ABI), when working with SYBRgreen, or the TaqMan Universal PCR Mastermix (ABI), when using probes. Reactions were carried out in 96 well plates in a 20 µl volume.

Table 5: Real-time-PCR protocol

Cycles	**Step**	**Temperature**	**Time**
1	Polymerase activation	95°C	15 min
	Denaturation	94°C	15 sec
35-40	Annealing / elongation	60°C	60 sec
1	Melting curve (optional with SYBRgreen)	72°C	10 min

A fluorescence reading step was performed at every elongation to detect the amount of amplification products. When SYBRgreen was used, after the last cycle a melting curve analysis was carried out, starting a gradient at 45°C increasing to 95°C (read every 1.0°C, hold for 2 sec between reads) in order to check for amplification of non-specific products.

2.5.7 Agarose gel electrophoresis

PCR products were analysed by standard agarose gel electrophoresis using 1.0 % or 2.0 % (w/v) agarose in Tris-acetate-EDTA buffer (TAE). PCR products were visualized by ethidium-

bromide staining [250 ng/ml per gel] under UV light (302 – 365 nm). Results were documented using a gel documentation system (Geldoc 2000, Biorad).

2.5.8 Pulsed field electrophoresis

Pulsed field gel electrophoresis (PFGE) was used to separate very large PAC-DNA molecules upon digestion with restriction endonucleases.

Irf8-PAC DNA was digested using *Pvu*I (over night, 37°C). DNA-molds were made by filling the digestion mix with 2 % agarose (Biorad). One DNA-mold contained 5 µg DNA was washed in Tris-borate-EDTA buffer (TBE) (1 h, 37°C). Subsequently the mold was plugged into a pocket of a 1.0 % agarose gel (Biorad) in 0.5 % TBE. PFGE was carried out for 24 h with an initial pulse of 2.8 sec, and final pulse of 13 sec. Size was analyzed by comparing the fragments to the Lambda ladder (NEB).

2.5.9 Preparation of nuclear cell extracts and whole cell lysates

Nuclear extracts were made by harvesting 1.0-3.0*E07 cells. The cells were washed twice in ice cold PBS (14000 rpm, 2 min, 4°C) and incubated in 400 µl ice-cold buffer A (15 min, 4°C, shaking) in the presence of protease inhibitors (Sigma). Twentyfive µl 10 % NP 40 were added and mixed thoroughly. After centrifugation (14000 rpm, 30 sec, 4°C) the pellet was resuspended in 50-100 µl buffer C and incubated (15 min, 4°C, shaking). After centrifugation the supernatant was flash-frozen in liquid nitrogen and stored at -80°C.

Whole cell lysates were done employing the TCA (1,1,1-trichloroethane) method. Briefly, cells were washed twice in ice cold PBS (14000 rpm, 2 min, 4°C), resuspended in 500 µl PBS and mixed with 10 % (v/v) TCA (15-30 min, 4°C). The lysate was centrifuged (14000 rpm, 2 min, 4°C) and resuspended in 1 x SDS sample buffer and stored at -20°C.

2.5.10 Electrophoretic mobility shift assay

The electrophoretic mobility shift assay (EMSA) determines the interaction between DNA and DNA-binding proteins, such as the interaction of transcription factors with their corresponding regulatory regions. It bases on different migration abilities through a non-denaturizing polyacrylamide gel of protein-DNA complexes and DNA alone. Protein-DNA complexes migrate more slowly due to their increased size than unbound, double-stranded oligonucleotides. By adding specific antibodies to the reaction prior to the gel run, complexes are further increased in size and thus further retarded, allowing identification of the bound proteins.

Oligonucleotide strands (sense and antisense) were annealed using a PCR gradient of 10 min steps each (94°C, 58°C, 37°C, 24°C, 4°C) in an Eppendorf Mastercycler Gradient. Protein extracts were made as described (see 2.5.9).

200ng of annealed oligonucleotides were end-labelled with [γ-^{32}P]dATP and T4 polynucleotide kinase (Fermentas) (30 min, 37°C). Non-incorporated oligonucleotides were removed by gel-purification using a Sephadex G25-spin column (Roche).

The binding assay was performed in a 20 µl reaction volume containing 1x EMSA binding buffer, 2 µg poly(dI/dC) and 2 µg nuclear protein extract. The mixture was incubated at 20°C, 5 min. Then, 1 µl of 5'end labelled, double-stranded oligonucleotide probe was added and incubated (30 min, 20°C). Afterwards, for supershift analysis, 2 µg of the indicated antibody were added and the mixture was additionally incubated (1 h, 4°C). Finally, protein-DNA complexes were resolved in a 5.5 % non-denaturizing polyacrylamide/1 x TBE-gel which was subsequently dried on a Whatmann 3MM filter paper and exposed to X-ray films at -80°C for hours to days depending on the intensity of the signal.

2.5.11 Southern blot analysis

For PAC copy number analysis, PAC Integrity determination, DNaseI hypersensitive assay and PAC library cloning, DNA was digested with excess amounts of restriction enzyme of choice, purified by phenol/chloroform extraction and precipitated with ethanol. After quantification of each sample, specified amounts of samples were run on a 0.7 % agarose gel. DNA in the gel was fragmentized by 0.2 M hydrochloric acid (HCl) treatment, subsequently capillary-blotted onto a nylon membrane (Biodyne B, PALL) employing 0.4 M sodium hydroxide (NaOH). Blotted DNA was cross-linked to the membrane by UV light using a quantitative cross-linker. A probe for the detection of the desired DNA fragment was prepared by random-labelling with [α-^{32}P]dCTP using the Rediprime labelling kit (Amersham). Not incorporated [α-^{32}P]dCTP was removed by employing the Rapace kit (Invitek). The labelled probe was measured for its activity with a liquid scintillation analyzer (Tri Carb 2800 TC, Perkin Elmer). Only highly active probes (>100.000 counts per minute (cpm)) were hybridized onto the pre-incubated membrane. Hybridization was carried out for 8-12 h in Roti-Hybri-Quick (Roth) at 60°C, filters were washed twice in 2 x SSC (saline-sodium citrate buffer), 0.1 % SDS and twice in 1 x SSC, 1 % SDS at 60°C for 10 min each. Washed filters were exposed to Kodak XAR film.

2.5.12 SDS-PAGE electrophoresis

Applying SDS-polyacrylamide-gel electrophoresis (SDS-PAGE), proteins were separated according to their size. This system is based on a discontinuous SDS-polyacrylamide-gel with a low-percentage stacking gel and a high-percentage running gel. The stacking gel concentrates the samples whereas they are separated in the running gel. Negatively charged SDS in loading buffer and gels attaches to hydrophobic regions of proteins in a constant weight ratio, thereby over-neutralizing positive charges, denaturing and solubilizing proteins. The scaffold of the gels, the polyacrylamide, serves as a molecular filter separating proteins only according to their size, while they are migrating towards the anode. Resolution depends on the concentration of polyacrylamide. For analysis, 12-15 µg of nuclear- or whole cell protein extracts were mixed with 1 x SDS loading buffer and incubated at 99°C, 3 min. Immediately afterwards, samples were cooled on ice for 5 min, centrifuged and loaded onto the wells of a 13 % acrylamide gel. In order to determine the size of the proteins of interest, a prestained protein ladder (Fermentas) was used as a size control marker. Gels were first run at 15 mA/gel and then at 30 mA/gel when proteins reached the separation gel. Electrophoresis was stopped when bromophenol blue exited the gel.

2.5.13 Western blot analysis

Total cell lysates were extracted as described (see 2.5.9). Proteins were resolved by SDS-PAGE (see 2.5.12) and electrotransferred to a PVDF membrane (Biotrace PVDF, PALL). Polyclonal rabbit antibodies to IRF8, PU.1 and GFP (all Santa Cruz) and RUNX1 (Covence) were used. TUBULIN (Sigma) served as control. Immunoreactive proteins were detected using horseradish peroxidase–conjugated antibodies to rabbit or mouse immunoglobulins (Santa Cruz) and the ECL system (Invitrogen).

2.5.14 Luciferase reporter assay

In reporter assays the *Firefly*-luciferase derived from firefly *Photinus pyralis* was applied as reporter gene to analyze functional implications of the *Irf8* promoter coupled to different *cis*-elements in stably transfected cell lines. The system benefits from the absence of human equivalents, the short half-life time of mRNAs and proteins and the high sensitivity (de Wet et al. 1987). The luciferase enzyme catalyzes the oxidation of the substrate, which is accompanied by light emission. Light intensity is directly proportional to the amount of luciferase. Therefore, the number of impulses indirectly allows quantification of the proteins and conclusions about

the biological activity of tested promoter – *cis*-element combinations. Luciferase activity was assessed in pools of different stably transfected cell lines or individually picked single clones.

2.5.15 ChIP analysis

Chromatin Immuno Precipitation (ChIP) is an essential tool to determine protein – DNA interactions as well as chromatin histone modifications.

Here the protocol of Forsberg et al. (Forsberg et al. 2000) was followed. Briefly, cells were grown on cell culture dishes to 80-90 % confluency, with an additional plate reserved to count cells using a haemocytometer. Typically, 4*E06 cells were used for each ChIP condition. Cells were placed on a rocker (Unimax 1010, Heidolph) and fixed with 4 % formaldehyde solution (5 min, RT), before fixation was quenched by glycine at 0.1 M final concentration (5 min, RT, shaking). The crosslinked material was scraped off the culture dish and transferred into a 15ml Falcon tube and centrifuged (220 * g, 5 min, 4°C). Then, supernatant was discarded and the cell pellet was washed with ice-cold PBS. Cells were centrifuged again and supernatant was removed completely. Cells lysis was performed by swelling the pellet in ice cold cell lysis buffer (10 min, 4°C, shaking), followed by centrifugation (5 min, 220 * g, 4°C). After removal of supernatant, the pelleted nuclei were lysed with ice cold nuclei lysis buffer (10 min, 4°C), with the nuclei pellet disrupted by occasional pipetting action.

A 10 µl aliquot of chromatin was removed and kept on ice for later. Chromatin sample was sonicated using a Bioruptor (Bioruptor, Diagenode). Here, the sample was rotating in a chilled waterbath (4°C), which conferred the sonication pulses to the sample. The following settings were applied for sonication: 14 minutes sonication time on high power (30 sec on, 30 sec off, 0.5 sec pulse rate). Following sonication another 10 µl aliquot was removed to assess sonication efficiency by agarose gel electrophoresis determining the size range of chromatin fragments produced by sonication. An 1.0 % agarose gel was used to resolve the DNA fragments. An appropriate size marker (100bp ladder, Fermentas) allowed for evaluation of fragment sizes. Only sheared chromatin between 400 bp and 800 bp average size was used in downstream immunoprecipitations.

After confirmation of the size of sonicated chromatin fragments, samples were pre-cleared. The samples were diluted in a 1.5 ml Eppendorf tube with IP Dilution Buffer to a final volume of 0.6 ml and incubated with 50 µl (1 mg/ml) IgG (from rabbit serum) (1 h, 4°C, constant rotation). 100 µl Protein A/G Agarose beads were mixed to the chromatin/IgG solution. Samples were incubated over night (4°C, constant rotation). Next day, chromatin was centrifuged (5150 * g, 2 min, 4°C), then supernatant was transferred to a new tube.

Pre-cleared chromatin was aliquoted in 200 µl fraction per immunoprecipitation condition. The following conditions were used: No antibody, Pol II antibody, PU.1 antibody (both Santa Cruz), RUNX1 antibody (Covance), anti-acetyl-Histone H3K9 antibody, IgG antibody (both Upstate/Millipore). A no chromatin control was included in which IP dilution buffer was used in place of chromatin, while a chromatin sample representative for the starting material was delegated 10 % input. The input sample was left at 4°C on ice until the reversal of protein-DNA-crosslinks. For chromatin immunoprecipitation the desired quantity of antibody (5.0 µg Pol II, 5.0 µg PU.1, 5.0 µl Runx1, 5.0 µl H3K14ac, 5.0 µg IgG) was incubated with the appropriate chromatin sample (2 h, 4°C, constant rotation). DNA-protein-antibody complexes were precipitated with 30 µl 50 % protein A/G agarose beads. After 2 h at 4°C on rotation, the chromatin/antibody/bead solution was centrifuged (5150 * g, 2 min, 4°C). Having removed the supernatant a series of washes followed. First, 500 µl IP wash I was added, vortexed briefly, centrifuged (5150 * g, 2 min, 4°C), then supernatant was removed. One more time 500 µl IP wash I added, mixed, then transferred to a new 1.5 ml tube and centrifuged as described. Beads were next washed with 500 µl IP wash II, centrifuged as previous and supernatant removed. A subsequent two washes of the beads with 500 µl TE Buffer, centrifuged as before, then removal of supernatant, completed the washes. To elute chromatin, 150 µl elution buffer was added to the beads, vortexed briefly, centrifuged (5150 * g, 2 min, RT). Supernatant was collected before a second elution again with 150 µl elution buffer was conducted in the same way, with the two elutes being combined at the end. Protein-DNA crosslinks of samples and 10 % input were reversed by addition of 20 µl 5 M NaCl, along with 1 µl RNase (1 mg/ml) to degrade RNA and aid purification of DNA (overnight, 65°C). Next day, 3 µl (20 mg/ml) proteinase K was added and left overnight (45°C). DNA was recovered from samples using phenol/chloroform (see 2.5.1). Sample was precipitated in the presence of 10 % (v/v) 3M sodium acetate (pH 5.2) and 5.0 µl glycogen (1 mg/ml) to allow quantitative precipitation for all samples. The precipitated DNA was resuspended in 50 µl water (5 min, 42°C). PCR analysis was performed immediately. Otherwise, DNA was stored at -20°C for later usage.

2.5.16 Chromosome conformation capture (3C)

Chromosome conformation capture (3C) (Dekker et al. 2002; Tolhuis et al. 2002) reveals new insight into structural properties and spatial organization of chromosomes and is most important for the understanding of gene regulation, more specific if promoters of genes are interacting with *cis*-regulatory elements as shown in Figure 9. When comparing chromatin conformation in different cell types it is mandatory to relate the results to a control region. It was first described for the *GapDH* locus to serve in 3C as normalization control (Spilianakis et al. 2004), and was adapted in this study.

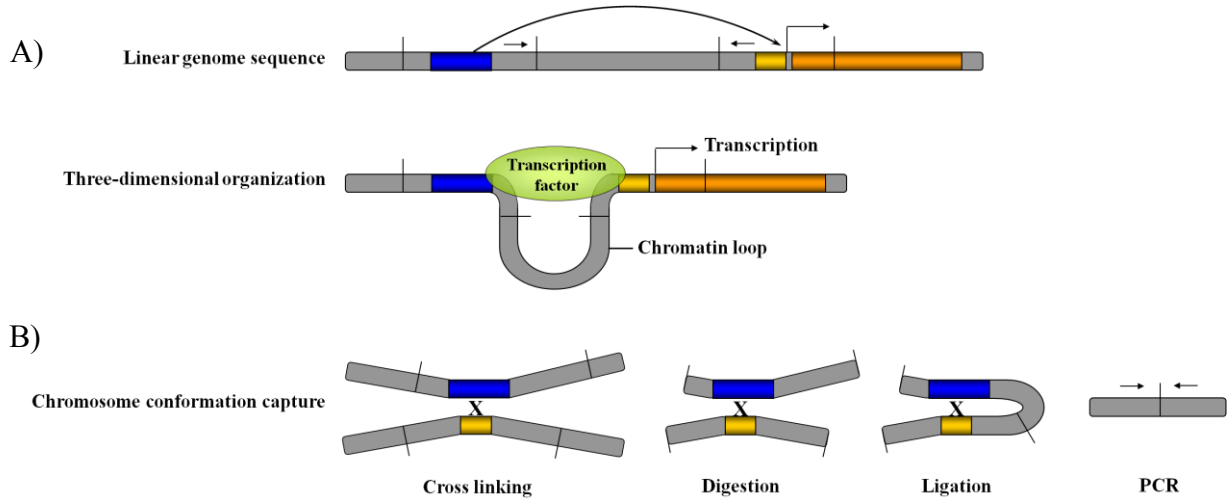

Figure 9: Interacting genetic elements can be detected by 3C. A) Promoters (yellow) and regulatory elements (blue) are linearly organized along chromosomes (top), but as a result of specific interactions between elements a complex three-dimensional organization of the genome is formed inside the cell (bottom). **B)** Schematic diagram of the 3C assay. Chromatin is cross-linked, digested with a suitable restriction enzyme (restriction sites are indicated by upright bars) and then ligated to obtain a 3C template. This template contains a collection of ligation products, each of which reflects a physical interaction between two restriction fragments. Detection is acived by restriction site spanning primers (little arrows). Legend adapted from (Dekker 2006).

Proliferating cells were crosslinked by 5.4 % formaldehyde treatment (10 min, 4°C, while shaking). The reaction was quenched by the addition of glycine to 0.1M final concentration (5 min, 4°C, while shaking). The cells were transferred in a 15 ml Falcon tube. After a centrifugation step (360 * g, 8 min, 4°C), medium was discarded and the pellet was resuspended in cold PBS and centrifuged as before. The supernatant was removed completely, before the cells were lysed in 5 ml cell lysis buffer in the presence of protease inhibitors (protease inhibitor cocktail, Sigma) (20 min, 4°C, shaking). The resulting nuclei were pelleted (600 * g, 5 min, 4°C), washed in 500 µl NEB-buffer 4 and centrifuged again. The nuclei were now lysed in the presence of 500 µl NEB-buffer 4 and 0.3 % SDS (1 h, 37°C, while shaking). This reaction was terminated by the addition of 50 µl 20 % Triton X100 (1 h, 37°C, shaking). Digestion of crosslinked chromatin with the restriction enzyme *Nco*1 (800 U) was done over night (37°C, shaking). The enzymatic reaction was stopped by the addition of 40 µl 20 % SDS

at 65°C for 20 min. Re-ligation was performed in a highly diluted manner to favour intramolecular ligation. Therefore, 80 µl of the digested material was transferred to a new 15 ml tube and incubated with 3.7 ml NEB-T4 DNA Ligase buffer supplemented with 187.5 µl 20 % Triton X100 (1h, 37°C, shaking). One ml was removed as a no-ligation control and kept for later, while the remaining 3 ml were ligated over night in the presence of 40.000 U T4 DNA ligase (NEB) at 16°C. Sample and no-ligation control were reverse crosslinked by addition of 10 µl proteinase K (10 mg/ml) (over night, 65°C). DNA was precipitated following phenol/chloroform purification. (see 2.5.1).

The sample was resuspended in 50 µl TE-buffer, DNA concentration was assessed (see 2.5.4). Typically 80ng gDNA were used in a 50µl scale semi-quantitative PCR for *GapDH* using following protocol:

Table 6: 3C nested PCR protocol

Cycles	Step	Temperature	Time
1	Polymerase activation	95°C	2 min
GapDH			
37, 40, 43	Denaturation	95°C	10 sec
Irf8	Annealing	57°C	10 sec
35 +	Elongation	72°C	10 sec
15, 20, 25			

After normalizing gDNA concentration based on *GapDH* loop formation, respective amounts of gDNA were used for a nested PCR following the indicated protocol. However, after 35 cycles of the first PCR a second PCR was started using 8 % material of the initial PCR, sampling was done after 15, 20 and 25 cycles.

2.5.17 DNaseI hypersensitive assay and genome-wide DNaseI hypersensitivity analysis

Transcriptional active chromatin elements are associated with accessible chromatin (Radomska et al. 1998). Those so called open loci are more susceptible to digestion with restriction enzymes or nucleases such as DNaseI (Li et al. 2001). Depending on their involvement in active transcriptional processes chromatin elements are more prone to digestion with DNaseI in one cell type compared to a cell type where this element is not active. DNase hypersensitive assay reveals the accessibility of a certain chromatin element at a given time, allowing for an indirect proof of active transcriptional processes at this particular site.

Proliferating cells were harvested and pelleted by centrifugation in a Multicentrifuge 3 S-R (Heraeus) (2500 rpm, 15 min, 4°C), followed by a washing step in cold PBS and one more centrifugation step. The pellet was resuspended in cold glycerol/TKN buffer, containing protease inhibitors. Subsequently, the same volume cold glycerol/TKN buffer, including 0.1 %

Saponin was added. Cell lysis was performed for 12 min with periodical pipetting. Lysis efficiency was determined by Trypan blue staining and microscopical examination. The nuclei were pelleted (4500 rpm, 20 min, 4°C) and were resuspended in 800 µl buffer A. A fraction was removed and regarded as no DNaseI control. In a time kinetic process the remaining nuclei were digested employing 30 U DNaseI (Roche) in a 35°C waterbath (DW2, Julabo), sampling every 2 min. Digestion was stopped immediately by the addition of stop-mix. All samples were subsequently digested with 5 µl proteinase K (10mg/ml) (1 h, 37°C). A fraction of every sample was run on agarose gel electrophoresis using a 0.6 % agarose gel to check for gradual DNA digestion over time of sampling. Phenol/chloroform extraction was employed (see 2.5.1). Here blue tips with cut ends were used to avoid shearing of the DNA. The DNA was resuspended in 70 µl restriction buffer (*Bam*HI buffer, Fermentas). Digestion with *Bam*HI (40 U) was performed (overnight, 37°C, constant shaking). Phenol/chloroform purification was applied as described above, DNA was quantified (see 2.5.4). Typically 15 µg digested material was separated on a 0.7 % agarose gel by gel electrophoresis. This gel was used for southern blot hybridization (see 2.5.11). A DNA probe within the putative DNaseI hypersensitive site carrying restriction fragment was labelled (Ready prime kit, Amersham) and hybridized.
Genome wide DNaseI hypersensitive analysis was done in cooperation with the Bonifer lab (C. Bonifer, Leeds, UK), Briefly, BM derived macrophages were isolated and cultured as described (Tagoh et al. 2002). Splenic $CD19^{+}IgM^{+}$ B-cells were isolated as described by (Walter et al. 2008), followed by staining with anti CD19-PE (BD Biosciences) and anti-IgM-FITC and cell sorting using a MoFlo (Beckman Coulter). DNaseI treatment was performed exactly as described in (Lefevre et al. 2005). Approximately 10 µg of isolated DNaseI treated DNA from both the macrophages and B-cells was then run on an agarose gel and fragments in the range of 100–600 bp were cut out from a sample showing similar low level DNaseI digestion as measured by real-time PCR analysis using primers amplifying an active promoter (*Tbp* locus), or an inactive region from chromosome 2, and was purified using a gel extraction kit (Qiagen). For library preparation, 10 ng of DNA fragments were processed using the Illumina sample preparation kit (Illumina) according to manufacturer's protocol. After library preparation, 200 bp fragments were isolated and analyzed by massively parallel DNA sequencing on an Illumina Genome Analyzer.

2.5.18 Site directed mutagenesis

Stratagene site directed mutagenesis kit was employed to introduce mutations of transcription factor binding motifs within reporter plasmids. Here, a PCR based method was employed,

making use of a proof-reading *PFU*-Polymerase and synthetic oligonucleotides harbouring the desired mutations. Plasmid DNA carrying the sequence of interest served as template for the reaction. Mutations within the transcription factor binding site were introduced using the indicated primers in which the mutated binding motifs are underlined.
After PCR amplification the methylation specific Endonuclease *Dpn*I was used to digest pDNA. That way only methylated parental pDNA of dam-positive bacterial origin was digested, whereas newly synthesized unmethylated DNA was not cut. Transformation in bacteria completed the protocol. The success of mutation was verified by sequencing.

2.5.19 sh-RNA mediated interference assay

In order to assess the importance of transcription factors controlling gene expression via binding to promoters or *cis*-regulatory elements of genes, sh-RNA induced interference with the respective factors was performed. sh-RNA interference constructs against Pu.1-, Runx1- and Lac-Z control were generated as described (see 2.4.6) (Lausen et al. 2006). The applied hairpins are listed with the respective binding motive underlined (see 2.1.15 sh-RNA cloning).
The psi-RNA h7SK-GFPzeo vector (Invivogen) comprising the hairpin was transfected using Fugene 6 (Roche) into stable RAW264.7 reporter cell lines (see 2.3.6). Transfected cells were FACS sorted based on GFP expression (see 2.6.1) directly into lysis buffer. Reporter activity was measured 24-48 h post transfection as described (see 2.5.14). Specificity and activity of the individual hairpins was measured by real-time RT PCR of the respective target gene as well as of additional control genes. A hairpin targeting LacZ, which is not expressed in eukaryotic cells, served as a control.

2.6 Fluorescence activated cell sorting (FACS)

2.6.1 General flow cytometry and cell sorting

For staining of cell surface antigens, about 5*E05 cells were incubated with 1 µg antibody in 100 µl PBS (20-40 min, 4°C, in the dark). Subsequently, cells were washed twice in 1 ml PBS. Non-specific binding was reduced by preincubation with unconjugated anti-FcγRII/III (2.4G2). Analysis and sorting of HSCs and intermediate progenitors was done as described (Akashi et al. 2000; Geissmann et al. 2010b). Before sorting of myeloid progenitor populations, lineage depletion of BM cells was achieved with a lineage “cocktail” of antibodies against CD3ε, CD4, CD8α, B220, CD19, CD11b, CD11c, CD127 and Gr-1. Subsequently, cells positive for these markers were depleted with immunomagnetic beads conjugated to anti-Rat. Finally, cells were resuspended in 200 µl PBS and fluorescence intensity was measured with a FORTESSA

cytometer (BD Biosciences) or the LSRII cytometer (BD Bioscience), while cell sorting was done using high-speed multicolour ARIA II and ARIA III cell sorter, always employing the FACS Diva software (BD Biosciences). Data analysis was performed with FlowJo software (Tree star). To discriminate between living and dead cells, staining with propidium iodide (PI) was accomplished by adding the substances to the cell suspension 10 min before measurement without a washing step. Before sorting, cells were filtered with a cell strainer (BD Biosciences).

2.6.2 Cell cycle analysis of fixed cells

Surface marker staining was performed as described above. Cell Fixation and permeabilization of the cell membrane was done using the BRDU-kit (BD Bioscience), according to the instructions of the manufacturer. Briefly, cells were fixed in Cytofix/Cytoperm buffer (15 min, 4°C, in the dark). Fixation was stopped by the addition of 1 ml perm/wash buffer and immediately centrifuged.

Afterwards, the cell cycle status was determined by staining at 37°C for 30 min with Hoechst 33342 in Hoechst buffer (BD Bioscience) (Cheshier et al. 1999). Cells were analyzed on a FACSAria III cell sorter (BD Bioscience), equipped with a violet laser (375 nm).

2.7 Gene expression profiling

2.7.1 Microarray procedure

Myeloid progenitors (lineage$^-$, IL7Rα$^-$, ckit$^+$, M-CSFR$^+$) were sorted from bone marrow of three independent pools of IRF8$^{+/+}$ and IRF8$^{-/-}$ mice, respectively. Every pool consisted of cells of three to four animals at the age of 8-12 weeks. Additionally, *Irf8*-VENUS$^-$ MP (lineage$^-$, IL7Rα$^-$, ckit$^+$, *Irf8*-VENUS$^-$) and *Irf8*-VENUS$^+$ MP (lineage$^-$, IL7Rα$^-$, ckit$^+$, *Irf8*-VENUS$^+$) were sorted from BM of *Irf8*-VENUS PAC positive mice (stain #88). RNA was extracted according to the RNeasy Micro Kit optimized for small amounts of RNA (see 2.5.2). One µl of RNA was used for quality control applying the Agilent 2100 bioanalyzer. High quality RNA (Rin>8.9) was used for downstream applications. For linear amplification of RNA, a strategy of two rounds of reverse transcription followed by T7 promoter-dependent *in vitro* transcription was applied according to Nugen instructions. 10 µg of amplified RNA was labelled and then hybridized to a 24-slide cartridge Affymetrix Mouse Genome 430 2.0 Array that covers ~45000 transcripts, according to Affymetrix instructions. Raw data were obtained by scanning.

2.7.2 Microarray analysis

The microarray data were analyzed using tools from the R statistical programming language (http://www.r-project.orf) downloaded from (http://bioconductor.com). The raw hybridization values of the expression set used were normalized together with the normalization function RMA from the affy library. Quality of the data was assessed with help of the arrayQualityMetrics library. The mouse4302.db library provided all probe annotation information for the analyses. To find differentially expressed genes the limma package was used. A gene was regarded as differentially expressed when the fold change was larger than 2.0 and the False Discovery Rate, resulting from applying Benjamini and Hochberg correction to the p-values, was smaller than 0.05. Density plots of the signature probe sets were generated using the sm library.

2.7.3 Gene categorization

The genes on the microarray were classified as marker into one of four categories according to their up-regulation in three mature cell types (monocytes, neutrophiles, dendritic cells). The categories considered were: genes upregulated solely in monocytes (Mono), neutrophiles (Neutroph) or dendritic cells (DC), or upregulated in both dendritic cells and monocytes (DC/Mono).

2.8 Statistical analysis

Student's t-test was carried out to determine the statistical significance of experimental results.
* $p \leq 0.05$ and ** $p \leq 0.001$.
Error bars depicted in the figures indicate standard deviation.

2.9 Collaborations and services

Results from collaborations are outlined when discussing the respective data.

Immunohistology

Staining was conducted by Francisco Fernandez Klett, Priller group, Humboldt University, Berlin, Germany.

Injection of Irf8-VENUS PAC in C57/Bl6 oocytes

Conducted by Ronald Naumann, Transgenic Core Facility (TCF), Max Planck Institute of Molecular Cell Biology and Genetics (MPI-CBG), Dresden, Germany.

DNaseI hypersensitive site - sequencing (DNaseI-seq)

Performed in cooperation with the group of Constance Bonifer, Leeds, UK.

Whole transcriptome profiling

Conducted by Thomas Stempfl, Kompetenzzentrum Fluoreszente Bioanalytik (KFB), Regensburg, Germany.

Bioinformatics of the whole transcriptome raw data

Performed in cooperation with Marie Gebhardt and Miguel A. Andrade-Navarro, Max Delbrück Center Berlin.

General mouse care and genotyping

Mice were maintained in the Rosenbauer group by Victoria Malchin, Nancy Endruhn and Christin Graubmann, Max Delbrück Center, Berlin.

3 Results

3.1 *Irf8* tracing using the *Irf8*-VENUS-PAC

Understanding of gene regulation which is e.g. mediated by transcription factors (TF) is a prerequisite of understanding the processes of cell diversification (Kaufmann et al. 2003; Yoshida et al. 2006). Acquiring more knowledge how transcription factors function throughout the process of cell differentiation allows to assemble regulatory networks which orchestrate specific cell fates (Rosenbauer et al. 2007; Wicks et al. 2011; Wilson et al. 2011). Therefore it is crucial to gain insight in transcription factor expression at single cell level for every step of cell commitment. In this study I followed expression of the haematopoietic transcription factor *Irf8* throughout phagocyte development and identified a mechanism for *Irf8* regulation in mononuclear phagocytes.

3.1.1 Generation of *Irf8*-VENUS PAC reporter

3.1.1.1 Cloning of the PAC reporter construct

In order to trace *Irf8* expression on single cell level, I employed a fluorescent reporter based approach. Therefore, a murine *Irf8* containing PAC was purchased (Deutsches Resourenzentrum für Genomforschung; RZPD), verified by sequencing and PCR, to contain the *Irf8* gene locus flanked by approximately 50kb up- and downstream sequence. This construct was equipped with a reporter cassette containing an internal ribosomal entry site (IRES) and a VENUS fluorescence marker, leading to the expression of a wildtype IRF8 protein along with the VENUS reporter from a bicistronic mRNA. This reporter cassette was introduced by homologous recombination in *E. coli* DH10B bacteria into the 3' untranslated region of *Irf8* exon 9.

In a second approach, a newly discovered *Irf8* regulatory *cis*-element, located 50kb upstream of the *Irf8* transcription start site (discussed in detail below), was flanked by *lox*P sites, again using homologous recombination in the described PAC construct. Upon Cre-recombinase activation (Sauer et al. 1989), this *lox*P site flanked region was excised from the PAC and reporter activity could now be measured in the -50kb element deficient background. A detailed schematic sketch is depicted below in Figure 10A. The cloning strategy of the transgenic construct is discussed in the Materials and Methods part in detail (see 2.4.4.1). Successful recombination was confirmed by sequencing and PCR (data not shown). Prior to injection of the prepared reporter construct a pulsed field gel electrophoresis followed by Southern blotting confirmed accurate size of the transgene PAC fragment (Figure 10B).

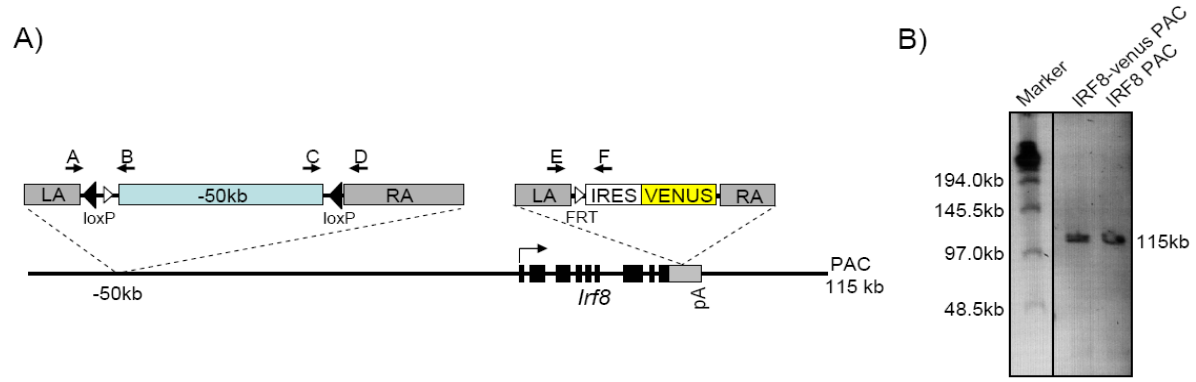

Figure 10: Schematic diagram of the *Irf8*-PAC transgenic construct. A) A murine *Irf8* gene locus carrying PAC (115kb) equipped with an IRES - VENUS fluorescent reporter cassette in the untranslated region of exon 9 of *Irf8* and *lox*P insertions flanking the newly discovered -50kb regulatory element (2.2kb) was used to generate *Irf8* reporter mice. Filled triangles determine *lox*P recombination sites, open triangles indicate FRT recombination sites, black boxes mark *Irf8* exons. Grey boxes display homology arms, where LA indicates the left homology arm and RA indicates the right homology arm. Lettered arrows indicate primer sites used for genotyping, E and F were used to genotype presence of the PAC transgen, A and D were used to determine excision of the *lox*P flanked -50kb element. pA determines the polyadenylation sequence. **B)** Pulsed field electrophoresis of *Pvu*I digested *Irf8*-PAC DNA, followed by Southern blot hybridization using the left homology arm of *Irf8* exon 9 as probe. A 115kb fragment for both, transgenic and unmodified PAC construct is shown.

3.1.1.2 Generation and validation of *Irf8*-VENUS reporter mice

Transgenic animals were generated by Ronald Naumann at the Transgenic Core Facility of the Max Planck Institute of Molecular Cell Biology and Genetics (TCF, MPI-CBG, Dresden, Germany). Stable transgenic lines from three independent founder mice (#52, #87, #88) were maintained and demonstrated complete integration of a structurally intact PAC DNA in two, three and four copies, respectively, as depicted in Figure 11 (and in data not shown). Structural integrity was determined by Southern blot analysis probing seven different regions on the *Irf8*-PAC DNA. Within the transgenic lines, no alterations or deletions were found as depicted in Figure 12.

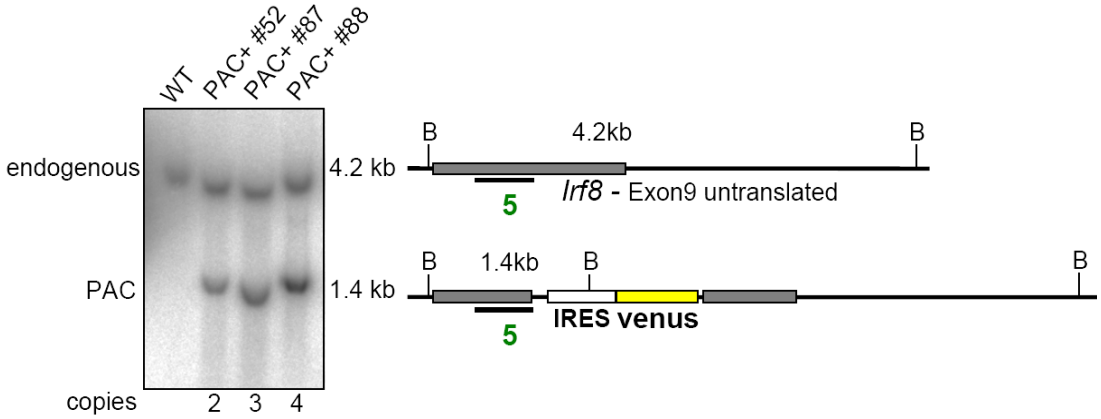

Figure 11: Copy number of PAC integrates in *Irf8*-VENUS transgenic lines. In the left panel, ratio of endogenous (4.24kb) to transgenic (1.38kb) fragments is displayed in a Southern blot. *Bgl*I (B) digested bone marrow of transgenic mice was hybridized using probe 5 (black bar). The scheme on the right depicts *Bgl*I fragments for endogenous and transgenic *Irf8* loci.

A)

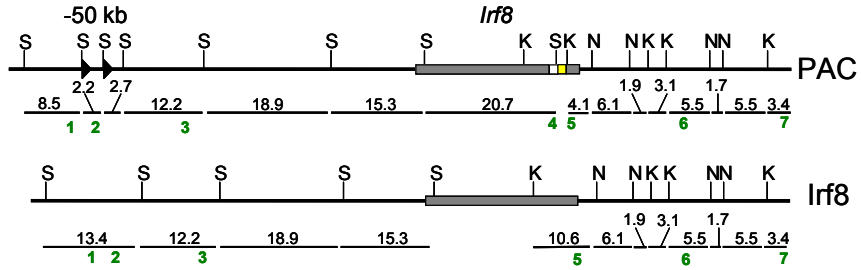

B)

Probe	1	2	3	4	5	6	7
WT	13.4	13.4	12.2	n.d.	10.6	5.5	3.4
PAC52	8.5	2.2	12.2	20.7	4.1	5.5	3.4
PAC87	8.5	2.2	12.2	20.7	4.1	5.5	3.4
PAC88	8.5	2.2	12.2	20.7	4.1	5.5	3.4

C)

Probe	1	2	3	4	5	6	7
PAC87Δ	8.5	n.d.	12.2	20.7	4.1	5.5	3.4
PAC88Δ	8.5	n.d.	12.2	20.7	4.1	5.5	3.4

Figure 12: Transgenic strains carry a structurally intact *Irf8*-VENUS PAC. A) Structural integrity of integrated *Irf8*-VENUS PAC DNA was determined by Southern hybridization using the indicated probes (green numbers). Grey boxes = the *Irf8* gene locus, white box = IRES site, yellow box = VENUS reporter; restriction enzyme motifs are indicated (S = *Spe*I; K = *Kpn*I; N = *Nhe*I). Black bars = restriction fragments, green numbers = position of the probe. **B and C)** The tables depict the sizes of the restriction fragments found (n.d. = not detected). Three to four animals per strain were tested. Southern blots can be found in the annex.

On protein level we evaluated whether the VENUS marker as expressed from the PAC transgene would accurately report *Irf8* expression. Bone marrow cells of the PAC transgenic animals were separated into VENUS$^+$ and VENUS$^-$ fractions using fluorescence activated cell sorting (FACS). IRF8 protein was analyzed by Western blotting (Figure 13A). The VENUS signal was restricted to the IRF8 positive cells, indicating that the PAC reported *Irf8* expression with high accuracy. Importantly, the additional PAC copies did not lead to enhanced *Irf8* expression over that of wildtype levels, nor did they cause any detectable phenotypic abnormalities in the transgenic animals (Figure 13B and data not shown).

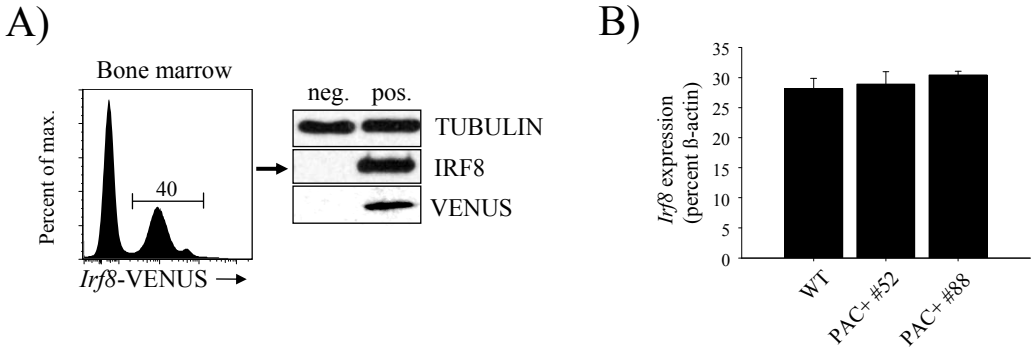

Figure 13: Correlation of VENUS reporter to endogenous IRF8. A) Flow cytometry of *Irf8*-VENUS reporter expression in total BM of *Irf8*-VENUS PAC transgenic animals (strain#88), comprising of 40 % VENUS positive cells, is displayed. VENUS positive and negative cells were FACS purified and subjected to Western blot analysis probing for IRF8, VENUS and TUBULIN. **B)** Overall amount of *Irf8* transcript appears unchanged between *Irf8*-VENUS PAC positive animals (strain #52 and strain #88) compared to C57/Bl6 wt littermate controls in splenic plasmacytoid dendritic cells (pDCs). Displayed are mean values of 2 biological replicates each comprised of 3 technical replicates analyzed for *Irf8* cDNA expression in real-time RT PCR.

3.1.2 Screening of haematopoietic cell compartments with the *Irf8*-VENUS reporter

After functionality of the VENUS reporter in transgenic animals was proven, screening of haematopoietic cell compartments by fluorocytometry was performed. *Irf8* expression in mononuclear phagocytes had been described by many groups (Scheller et al. 1999; Tamura et al. 2000; Mattei et al. 2006; Tsujimura et al. 2003a). Hence, VENUS expression patterns in myeloid and dendritic cell (DC) compartments were assessed and compared to published data and to real-time-RT PCR results obtained from FACS purified equivalent cell populations. All monocytes and DCs expressed VENUS at different levels, while granulocytes showed no expression as expected (Holtschke et al. 1996; Scheller et al. 1999; Tamura et al. 2000). B-cells served as a positive control for *Irf8* expression in lymphoid cells (Lu et al. 2003; Wang et al. 2008; Wang et al. 2009; Feng et al. 2011), whereas red blood cells were lacking expression of *Irf8*, thus serving as a negative control. In all compartments analyzed, the endogenous *Irf8* expression levels were closely paralleled by VENUS expression from the PAC as indicated by Figure 14 A and B. Consequently, the generated reporter mouse properly reported *Irf8* expression in the haematopoietic system.

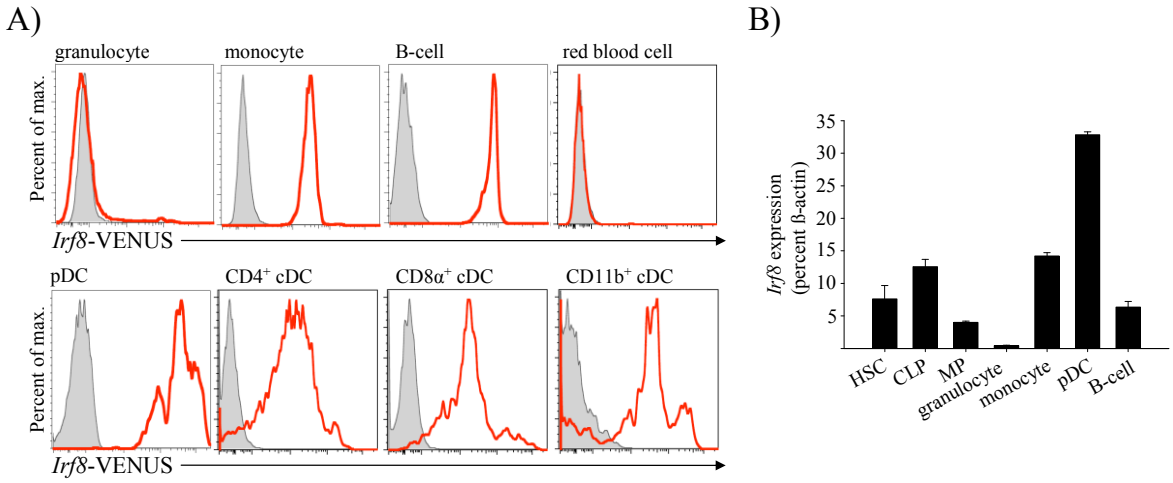

Figure 14: *Irf8* VENUS parallels endogenous *Irf8* expression patterns. A) VENUS expression of *Irf8*-VENUS PAC transgenic animal (strain #88, red) vs. C57/Bl6 littermate controls (grey area) analyzed by FACS. Peripheral blood granulocytes (CD11b$^+$, Ly6C$^+$, CD115$^-$), total monocytes (CD11b$^+$, Ly6C $^{low/high}$, CD115$^+$), B-cells (B220$^+$, IgM$^+$) and red blood cells (Ter119$^+$) are displayed. Splenic CD4$^+$, CD8α$^+$ and CD11b$^+$ cDCs are displayed. Data are representative for at least four independent experiments. **B)** Real-time RT PCR of *Irf8* expression in FACS sorted haematopoietic populations of C57/Bl6 cDNA using a mouse specific primer-probe set for *Irf8* normalized to *ß-actin*. Displayed are 2 biological replicates, each comprised of 3 technical replicates.

3.1.3 Analysis of the myeloid progenitor compartment

Next, the progenitors of the described distinct cell compartments were analyzed for VENUS activity. Haematopoietic stem cells (HSC) and multi potent progenitors (MPP) as well as the common lymphoid progenitor (CLP) showed a homogenous expression of the reporter and a distinct mRNA signal as described (Onai et al. 2007). In contrast, the myeloid progenitor

(MP) compartment was found to express the VENUS reporter only in a small subset as displayed in Figure 15 (~11 % in strain #88 and 9.5 % in strain #52 (data not shown)). These cells showed undifferentiated progenitor morphology and were restricted to the BM as depicted in Figure 15B and C. The proliferative capacity between *Irf8*$^{VENUS+}$ and *Irf8*$^{VENUS–}$ myeloid progenitors did not show a significant difference as depicted in the Hoechst33342 staining in Figure 15D. Gating on surface receptors identified progenitor (CD34) marks, myeloid (FcyR, M-CSFR) and lymphoid/dendritic (Flt3) marks for the *Irf8*$^{VENUS+}$ MP. This was indicative for a mononuclear cell fate (Scheller et al. 1999; Fogg et al. 2006; Auffray et al. 2009) as well as for a DC cell fate (Onai et al. 2007; Waskow et al. 2008).

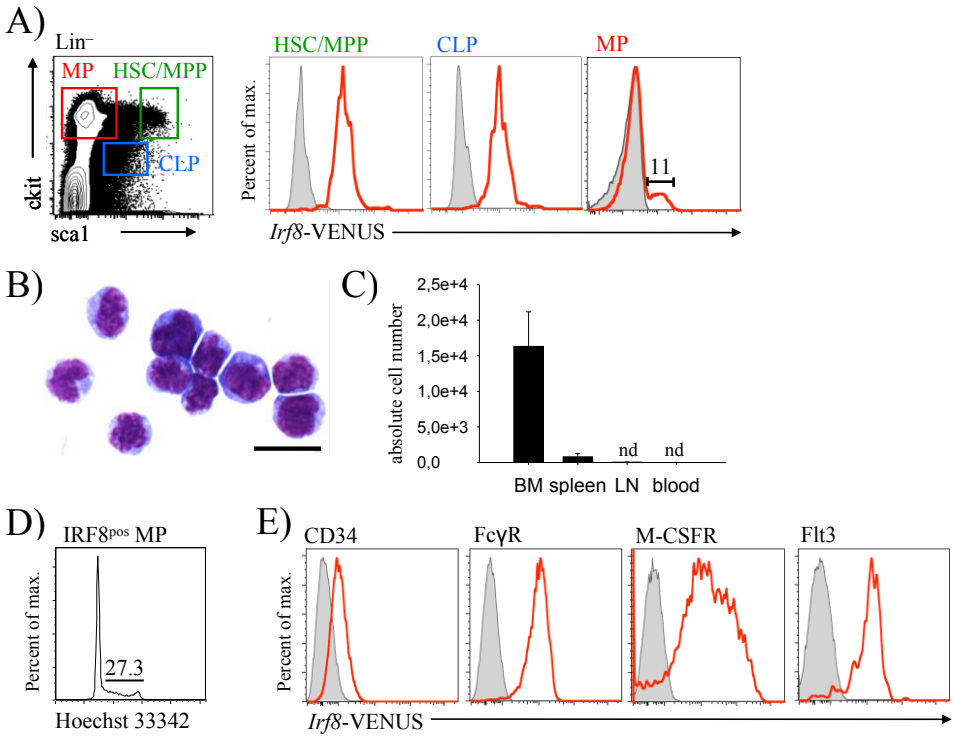

Figure 15: Characterization of *Irf8*-VENUS positive myeloid progenitor. A) FACS analysis of an *Irf8*-VENUS PAC transgenic animal (strain #88, red) vs. C57/Bl6 littermate controls (grey area) for reporter expression in stem- and early progenitor cells (lineage$^-$, ckit$^+$, sca1$^+$), common lymphoid progenitors (lineage$^-$, ckit^{intermediate}, sca1^{intermediate}, CD127$^+$) and myeloid progenitors (lineage$^-$, ckit $^{intermediate/high}$, sca1$^-$, CD127$^-$). Data are symbolic for at least four independent experiments. **B)** Representative microscopy image of cytospinned *Irf8*$^{VENUS+}$ myeloid progenitors after FACS purification, visualized by May/Gruenwald – Giemsa staining. Scale bar represents 20µm **C)** Distribution of *Irf8*$^{VENUS+}$ myeloid progenitors in haematopoietic organs and in the periphery. Absolute cell numbers of BM (femur and tibiae), whole spleen, mammary gland lymph nodes and peripheral blood are displayed. n=6 each. **D)** Cell cycle profile of *Irf8*$^{VENUS+}$ myeloid progenitors is displayed by Hoechst 33342 staining on fixed cells. Staining was done in 2 independent experiments. **E)** FACS analysis within the myeloid progenitor compartment, showing *Irf8*-VENUS expression in CD34$^+$, FcyR$^+$, CD115$^+$ and Flt3$^+$ cells of *Irf8*-VENUS PAC transgenic animal (strain #88, red) vs. C57/Bl6 littermate control (grey area).

The FACS phenotype of the *Irf8*$^{VENUS+}$ MP showed that distinct myeloid markers were expressed. For that reason classical myeloid differentiation steps were assessed for VENUS expression. Figure 16 displays the contribution of *Irf8*$^{VENUS–}$ MP and *Irf8*$^{VENUS+}$ MP to the well defined myeloid progenitors (Akashi et al. 2000). This revealed a manifestation of the

Irf8^{VENUS+} MP predominantly in the GMP (GMP = granulocyte-monocyte progenitor) compartment which had been described to promote granulocyte and monocyte cell growth (Akashi et al. 2000). However, not all GMPs expressed VENUS. The CMP (CMP = common myeloid progenitor) is a precursor of the GMP and was found to be partially VENUS positive. Clearly, there was no *Irf8*$^{VENUS+}$ MP in the MEP (MEP = megakaryocytic erythroid progenitor) compartment, which gives rise to red blood cells and the megakaryocytic branch. This suggests determination of the *Irf8*$^{VENUS+}$ MP to the myeloid pathway, but not the erythroid pathway.

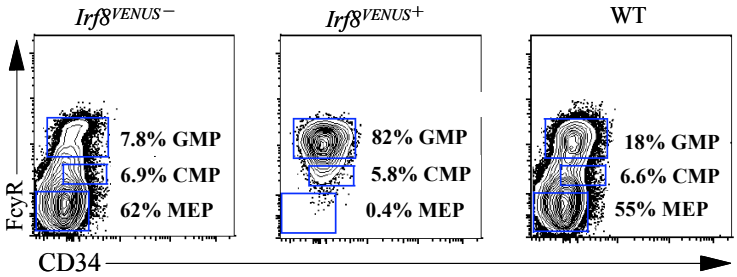

Figure 16: The *Irf8*$^{VENUS+}$ MP is a sub-fraction of classical early myeloid progenitors. FACS analysis reveals that the *Irf8*$^{VENUS+}$ MP can be placed in GMP (granulocyte-monocyte progenitor) and CMP (common myeloid progenitor), but not in MEP (megakaryocytic erythroid progenitor) compartments of early myeloid progenitors. Numbers indicate percent cells of one representative animal (n=3).

Since also markers of DC potential were expressed on the *Irf8*$^{VENUS+}$ MP, expression in known DC progenitors was analyzed. Results are shown in Figure 17. The group of Geissmann characterized the earliest multipotent progenitor that gave rise to monocytes/macrophages and DCs, terming it macrophage-dendritic cell precursor (MDP) (Fogg et al. 2006). This population expressed the chemokine receptor CX_3CR1 and ckit. Furthermore, it was defined by the expression of the M-CSFR (Waskow et al. 2008), which is a hallmark for monocyte/macrophage development (Bonifer et al. 2008). This progenitor, named MDP$^{\Delta}$, overlapped in function with the original MDP of Fogg et al. Hence, in this study both were regarded the same and named MDP (or were indicated otherwise). The *Irf8*$^{VENUS+}$ MP was found to express M-CSFR, ckit and CX_3CR1, thus overlapping with the definition of the MDP (according to Waskow et al. 2008). However, when the total cell numbers for MDP and *Irf8*$^{VENUS+}$ MP were compared, there was a 2-fold lower number for the *Irf8*$^{VENUS+}$ MP, making it a sub-population within the MDP compartment based on cell number.

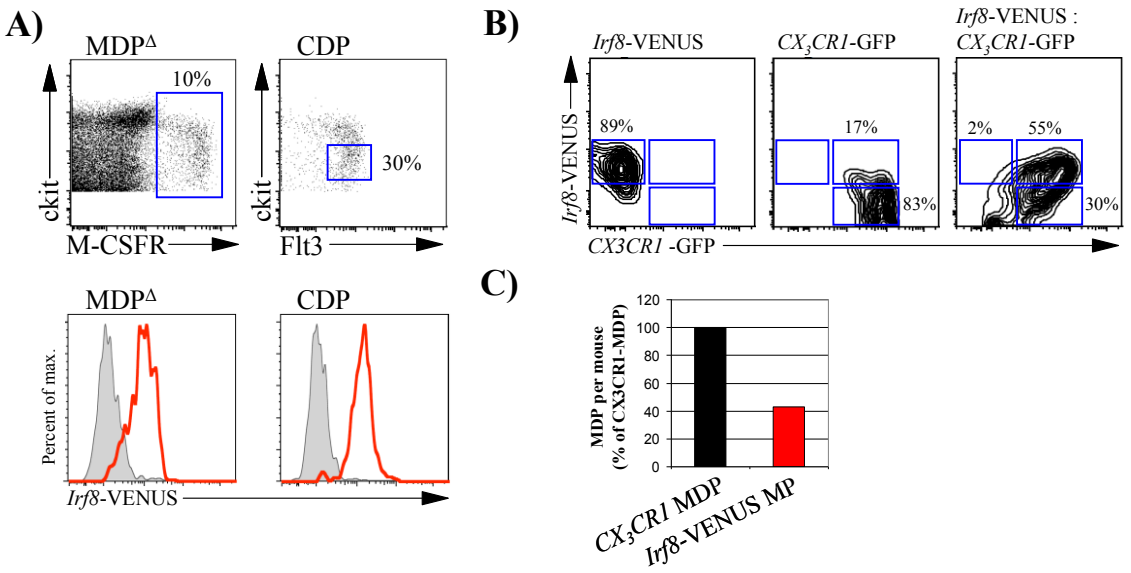

Figure 17: *Irf8*$^{VENUS+}$ MP expression in macrophage-dendritic cell progenitors (MDP) and in common dendritic cell progenitors (CDP). A) *Irf8*-VENUS expression in MDP$^{\Delta}$ (lineage^{-}, ckit $^{intermediate/high}$, sca1^{-}, CD127^{-}, M-CSFR^{+}) and CDP (lineage^{-}, ckit ^{intermediate}, sca1^{-}, CD127^{-}, M-CSFR^{+-}, FLT3^{+}). Numbers indicate percent cells of one representative animal. **B)** Contribution to the MDP compartment of *CX$_3$CR1*-GFP, *Irf8*-VENUS and *Irf8*-VENUS : *CX$_3$CR1*-GFP double transgenic mice. Numbers indicate percent cells of one representative animal of each genotype (n=3). **C)** Total cell number of *CX$_3$CR1*-GFP MDP and *Irf8*-VENUS myeloid progenitor. Displayed are average cell numbers of each genotype (n=3).

On the other hand, the common dendritic progenitor (CDP), described by Onai et al. (Onai et al. 2007) also expressed CX$_3$CR1, Flt3 as well as moderate levels of M-CSFR and ckit. The CDP was found to be located within the MDP compartment (Waskow et al. 2008), it had lost the potential to form monocytes, but retained full potential to form DCs. The *Irf8*$^{VENUS+}$ MP clearly resembled the surface marker signature of the CDP.

The conclusion at that point was that within a bipotential progenitor population, that allowed for granulocytic and monocyte cell differentiation (GMP), *Irf8* might be the lineage switch factor that drives cell fate decision toward the monocyte/macrophage cell fate, since *Irf8* was expressed in monocytes/macrophages but not in granulocytes (Tamura et al. 2000). Interestingly, in a more defined setting of myelo-erythroid progenitors that also includes DC progenitors (MDP and CDP), *Irf8* was also expressed in dendritic cell progenitors, emphasizing the *Irf8*$^{VENUS+}$ MP to be a DC progenitor as well.

In order to explore the lineage fate capacity of the *Irf8*$^{VENUS+}$ MP progenitor *in vitro* experiments under different cell fate promoting conditions, as well as *in vivo* experiments employing transplantation of FACS purified progenitors into sub-lethally irradiated recipients were conducted.

3.1.4 Functional characterization of *Irf8*$^{VENUS+}$ MP

At first, the differentiation potential of *Irf8*$^{VENUS+}$ MPs under *in vitro* conditions using methylcellulose and liquid culture assays was evaluated. In methylcellulose, myelo-erythroid growth conditions allowed a broad spectrum of cell lineages to grow. However, after seven days in culture only mononuclear phagocytes developed from the *Irf8*$^{VENUS+}$ MP cells, which also showed a profoundly reduced proliferation capacity. In comparison, the majority of colonies originating from the *Irf8*$^{VENUS–}$ MP were of granulocytic morphology accompanied by mononuclear phagocytes and some erythroid colonies. FACS analysis confirmed these findings (Figure 18 A and B and data not shown). This identified *Irf8*$^{VENUS+}$ MPs to have mononuclear cell restricted capacity *in vitro*.

In a more defined cytokine mix containing GM-CSF, promoting mononuclear cell growth, the *Irf8*$^{VENUS+}$ MP showed an increased potential for DC commitment compared to the *Irf8*$^{VENUS–}$ MP. This data was produced in liquid culture and was confirmed in methycellulose assays (Figure 18C).

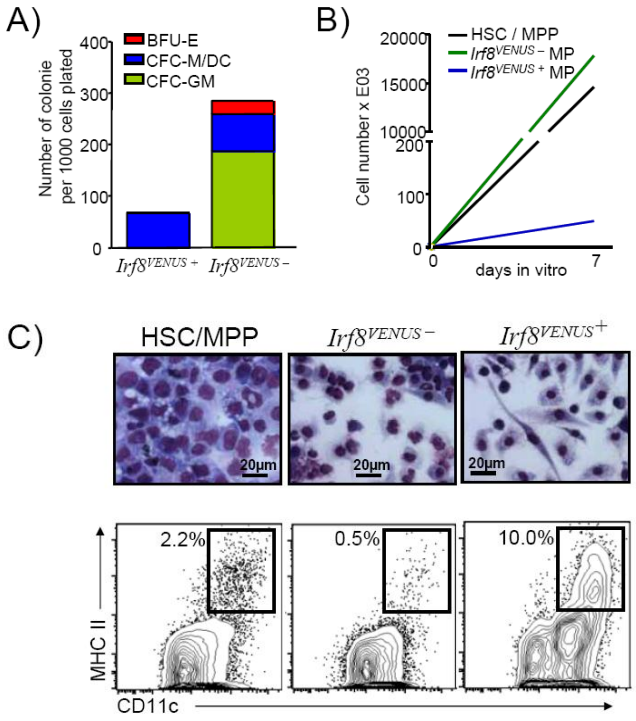

Figure 18: *Irf8*-VENUS positive myeloid progenitors have dendritic cell DC potential *in vitro*. A) Colony assay using a cytokine mix that allowed for broad haematopoietic development shows distinct colony morphology (BFU-E = erythroid colonies; CFC-M/DC = mononuclear phagocyte colonies; CFC-GM = granulocyte-monocyte colonies). **B)** Proliferation potential of plated cell populations after 7 days in methylcellulose culture. **C)** Liquid culture derived cells after 7 days in a cytokine mix promoting mononuclear phagocyte growth (rmSCF, rmIL-3, rmIL6, rmGM-CSF). HSC/MPP, *Irf8*$^{VENUS+}$ MP and *Irf8*$^{VENUS–}$ MP were FACS purified and cultured in IMDM in 12-well plates, which were covered with glass slides. Adherent cells grew on the glass surface and were stained with May/Grünwald and Giemsa. The lower FACS plots show methylcellulose derived cells originating from FACS purified HSC/MPP, *Irf8*$^{VENUS+}$ MP and *Irf8*$^{VENUS–}$ MP after 7 days using the same growth conditions. Displayed are representative FACS plots depicting DC potential (MHC II^{+}; CD11c^{+}). This experiment was performed in collaboration with Marina Scheller, Max-Delbrück-Centrum Berlin, Germany.

The capacity of the *Irf8*$^{VENUS+}$ MP to give rise to mononuclear cells was now tested under physiological conditions. Transplantation assays were applied to test the lineage commitment potential of the *Irf8*$^{VENUS+}$ MP *in vivo*. FACS purified progenitors of donor mice were transplanted via tail vein injection into sub lethally irradiated recipient mice (6 Gy). Host and graft could be distinguished based on surfacemarker expression, the host featuring the CD45.1 epitope, while the graft possessed the CD45.2 epitope (Figure 19A). LSK cells (HSCs and MPPs) served as a multipotent cell population which could generate all hematopoietic cells within the assay. After transplantation the cells were allowed to engraft and differentiate for 11days before the recipients were analyzed. Histology of splenic sections revealed a commitment of *Irf8*$^{VENUS+}$ MP exclusively towards DC formation indicated by an overlay of CD11c and VENUS signal (yellow). FACS analysis specified the finding to CD8α^{+} conventional DCs (cDCs) as depicted in figure 19B.

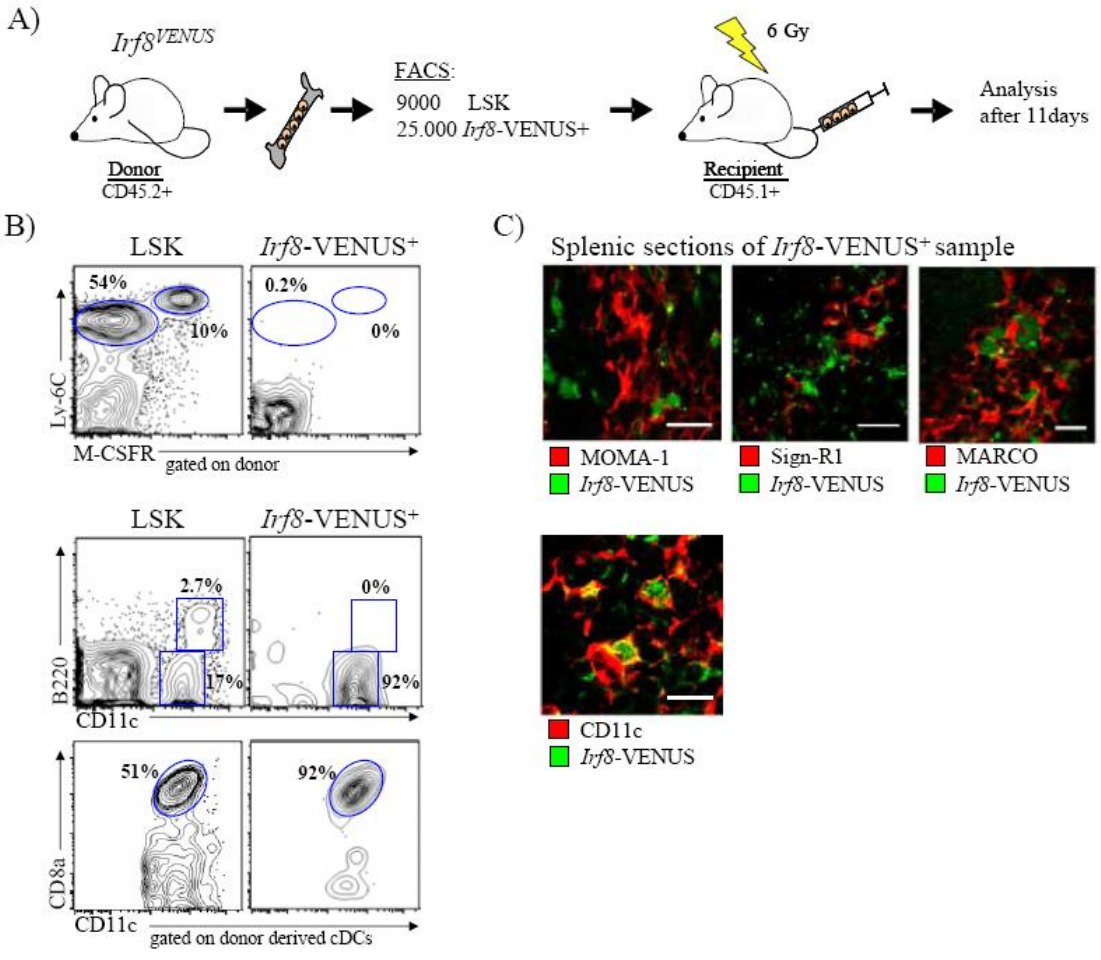

Figure 19: The *Irf8*^{VENUS} reporter marks a cDC-restricted progenitor *in vivo*. A) Schematic draft of transplantation experiment. **B)** 2.5*E04 FACS purified *Irf8*$^{VENUS+}$ cells and 9*E03 LSK cells (both: CD45.2) were transplanted into sub-lethally irradiated recipient mice (CD45.1) and were analyzed after 11 days. Displayed are representative results of 3 independent experiments. *Irf8*$^{VENUS+}$ cells exclusively matured into conventional DCs and did not give rise to monocytes, granulocytes or plasmacytoid DCs as analyzed in FACS. **C)** Histology of recipient spleen stained for the dendritic marker CD11c, confirmed presence of dendritic cells, staining for the macrophage markers MOMA-1, Sign-R1 and MARCO showed no *Irf8*-VENUS positive macrophages. Histology was conducted by F. Fernandez-Klett, Charite Berlin.

To test whether the phenotypic outcome of transplanting the *Irf8*$^{VENUS+}$ MP could be predicted already on transcriptional level, whole transcriptome micro array experiments were conducted. In *Irf8*$^{VENUS+}$ MP compared to *Irf8*$^{VENUS-}$ MP, 695 genes were at least 2-fold ($p<0.05$) up- and 693 genes were down-regulated, respectively. Figure 20 demonstrates that among the most differently regulated genes, there was a profound accumulation of mononuclear phagocyte classified genes for the *Irf8*$^{VENUS+}$ MP. This finding supported the transplantation results which led to the exclusive formation of conventional dendritic cells.

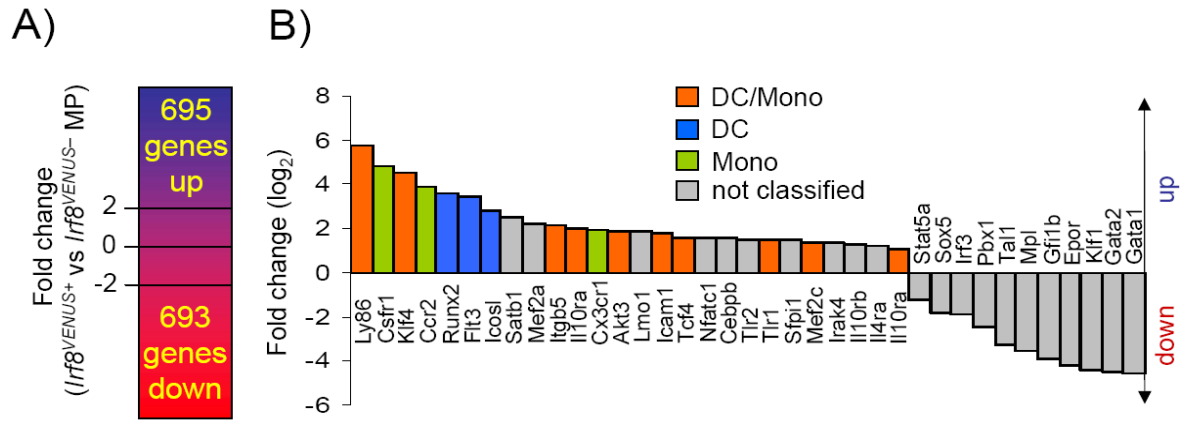

Figure 20: The *Irf8*$^{VENUS+}$ MP is transcriptionally monocytic/DC primed. A) Number of genes significantly up- and downregulated between *Irf8*$^{VENUS-}$ MP and *Irf8*$^{VENUS+}$ MP in an Affymetrix mouse whole genome 430 2.0 array. The detailed list of genes can be found in the annex. **B)** Distinct accumulation of mononuclear phagocyte classified genes among the most up-regulated genes for the *Irf8*$^{VENUS+}$ MP. Orange bars represent mixed DC/Monocyte associated genes, blue bars represent DC associated genes, green bars represent Monocyte associated genes based on separate profiles of the indicated cell types. Grey bars represent not classified genes. Results are expressed as mean value obtained from 3 different hybridizations. Bioinformatic analysis was performed in collaboration with Marie Gebhardt and M. Andrade-Navarro, Max-Delbrück-Center Berlin, Germany.

3.1.5 Aberrant myeloid progenitor in *Irf8*$^{-/-}$ mice

We postulated that the crucial checkpoint for cell fate decisions which commits progenitor cells to the mononuclear phagocyte cell fate must be located at this critical myeloid progenitor stage. We were wondering, how this important stage was controlled in the absence of the IRF8 protein. Thus, we examined the myeloid progenitor population in the *Irf8* knock out mouse. *Irf8*$^{-/-}$ mice were first described by Holtschke et al. in 1996. Phenotypically they display an expansion of neutrophile cells in the marrow and the peripheral organs. This expansion is caused by a block in cell differentiation at the myeloid progenitor level leading to a myelo proliferative disorder which often progresses to acute myeloid leukaemia (see 1.4 and 2.2.1.2). Since these mice do not contain the VENUS reporter, the population most related to the newly discovered *Irf8*$^{VENUS+}$ MP was analyzed. Indeed, applying a refined gating strategy the differentiation block was identifiable as a vast accumulation of progenitors at the MDP level (lineage$^-$, ckit$^+$, M-CSFR^{high}), forming an aberrant population, while the more

committed progenitor CDP (lineage$^-$, ckit$^+$, M-CSFR^{low}) was significantly reduced in number. At the stem cell level there was no detectable difference in cell number (Figure 21A and B), placing the block at the described myeloid progenitor cell stage.

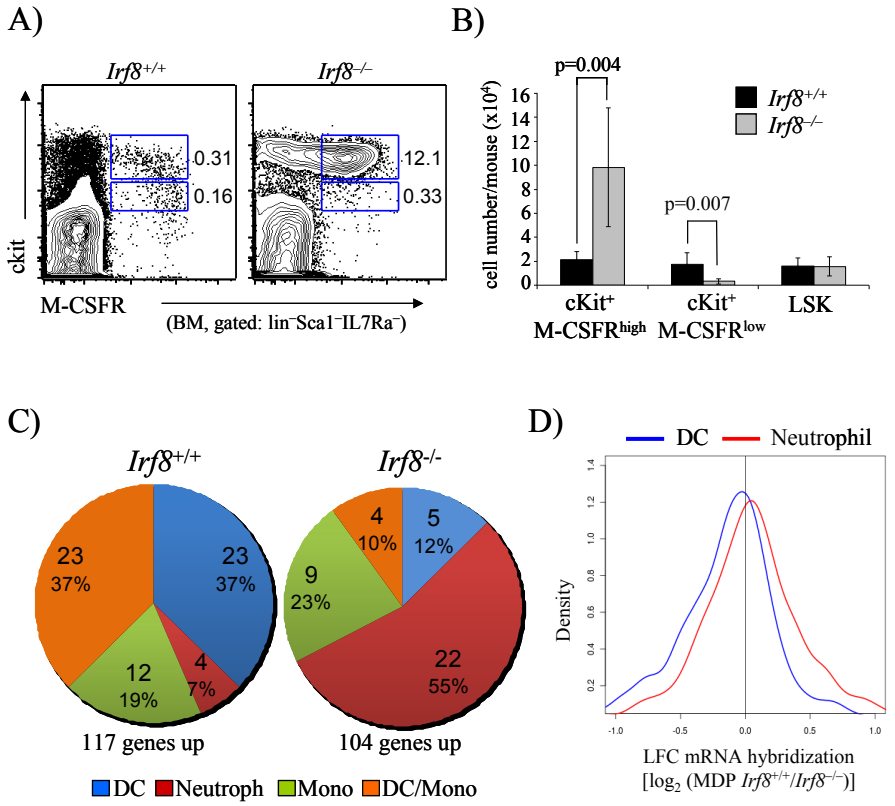

Figure 21: *Irf8*$^{-/-}$ mice show a phenotypical and genetically aberrant myeloid progenitor. A) and **B)** *Irf8* deficient animals show an accumulation of aberrant progenitor cells (ckit$^+$, M-CSFR^{high}) at the MP cell stage to the expense of more lineage restricted progenitors (ckit$^+$, M-CSFR^{low}) as displayed in FACS and in absolute numbers per mouse. **C)** Transcriptional expression at the MP stage of wildtype and *Irf8*$^{-/-}$ MP is compared, showing 107 genes up-regulated in the wildtype MP and 104 genes up-regulated in the *Irf8*$^{-/-}$ MP. Gene clusters are depicted for DC associated genes in blue, Neutrophile associated genes in red, Monocyte associated genes in green and mixed DC/Monocyte associated genes in orange. Numbers within the pie-chart represent genes being up-regulated for the particular gene cluster, percent of al classified genes are indicated for every cluster. The detailed list of genes can be found in the annex. **D)** Density plot depicting the altered gene expression signatures for the entire DC and Neutrophile associated genes in *Irf8*$^{-/-}$ and *Irf8*$^{+/+}$ animals. Blue line represents DC associated genes and red line represents Neutrophile associated genes. Bioinformatic analysis was performed in collaboration with Marie Gebhardt and M. Andrade-Navarro.

Comparing the *Irf8*$^{VENUS+}$ MP of wildtype mice to the aberrant myeloid progenitor of *Irf8*$^{-/-}$ mice, again employing whole transcriptome micro array analysis (n=3), revealed highly different expression patterns. Both data sets were compared for genes that were up-regulated between the two samples. These genes were grouped into four genetic profiles, a mixed DC/monocyte, a DC, a monocyte, and a neutrophile profile which came from whole transcriptome analysis of the respective cell type (n=3). In the wildtype *Irf8*$^{VENUS+}$ MP 117 genes in total were up-regulated compared to the *Irf8*$^{-/-}$ MP. Among these 117 up-regulated genes 23 genes (37 % of classified genes, 20 % of total) were associated with mixed

DC/monocyte profile, 23 genes (37 % of classified genes, 20 % of total) with DC, 12 genes (19 % of classified genes, 10 % of total) with monocyte, and 4 genes (7 % of classified genes, 3 % of total) with neutrophile profile.
On the other hand, the *Irf8*$^{-/-}$ MP showed a distinctly different gene expression pattern when compared to the *Irf8*$^{VENUS+}$ MP. Here, in total 104 genes were up-regulated, with 22 genes (55 % of classified genes, 22 % of total) showing a neutrophile profile, 9 genes (23 % of classified genes, 9 % of total) monocyte, 5 genes (12 % of classified genes, 5 % of total) DC, and 4 genes (10 % of classified genes, 4 % of total) a mixed DC/monocyte profile. Thus, in the absence of IRF8 the DC program was reduced, while the neutrophile program was drastically increased. The monocyte program was maintained. The log fold change of mean mRNA expression of all neutrophile associated genes (red line) and all DC associated genes (blue line) was plotted for the *Irf8*$^{-/-}$ MDP vs. the wildtype MDP (Figure 21D). The vertical line in the middle represents the mean expression of all genes. The figure clearly showed an increase of expression of the entire set of neutrophile genes in the knockout background, indicated by a shift to the right, while there was a decreased mean expression of all DC genes, indicated by a shift left to the middle.

Collectively, IRF8 showed responsible for closing the neutrophile differentiation pathway and allowing for DC commitment as emphasized by whole transcriptome analysis and *in vivo* differentiation, as well as by phenotypical analysis of the *Irf8*$^{-/-}$ animals at the myeloid progenitor stage.

3.2 *Irf8* expression is controlled by a distal *cis*-regulatory element at -50kb

3.2.1 Screening of the *Irf8* locus for regulatory active DNA elements

In order to reveal what controls *Irf8* gene expression at the myeloid progenitor cell level and how *Irf8* is regulated at that cell commitment checkpoint, *Irf8* locus configuration was assessed in detail. It is well known that gene function often is mediated cell type specifically by upstream regulatory *cis*-elements (Decker et al. 2009; Leddin et al. 2011). Hence, I screened the *Irf8* gene locus for regulatory elements. Evolutionary conservation of regulatory active DNA elements often is a prerequisite of their functionality. Mutations would be causative to changes in gene expression, mostly leading to a selective disadvantage.

3.2.1.1 Active site prediction

Four different species of mammals, plotting mouse sequence vs. human, cat and the very distantly related opossum, got compared for sequence homology. Up- and downstream of the *Irf8* locus a number of conserved areas, indicated by degrees of conservation, were found. Conservation was expressed as a peak (Figure 22). Sequences of more then 70 % conservation within a 100 bp were considered relevant. Non coding conserved DNA is marked in pink, whereas exons are marked in blue. As it is most likely that exons are conserved to mediate gene function, four upstream non coding DNA elements and three downstream non coding DNA elements showed high degrees of homology.

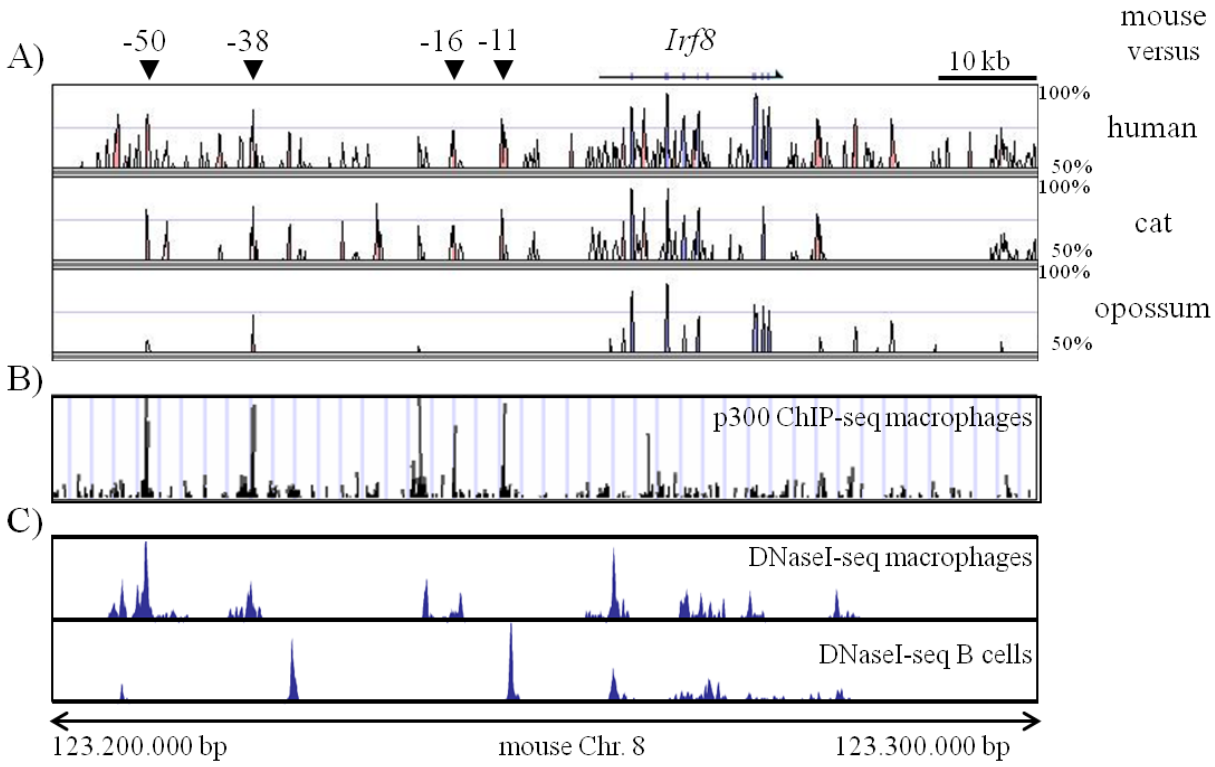

Figure 22: Putative regulatory active regions for *Irf8*. A) MVsita plot is shown for sequence conservation across ~100kb of the region of mouse chromosome 8 harbouring the *Irf8* locus. Values at the top indicate distance from the *Irf8* TSS. The conservation panels correspond to, from top to bottom, mouse/human, mouse/cat, mouse/opossum alignments. The conservation plot shows regions with at least 50 % and up to 100 % sequence conservation (y-axis). Exons are shown in blue, non-coding conserved regions are filled in pink. Positions of non-coding conservation are labelled with their distance (given in kb) upstream of the *Irf8* TSS. **B)** ChIP-sequencing using an anti-p300 AB are depicted in bone marrow derived macrophages (with permission of Immunity). **C)** An USCS genome browser derived plot for DNase I hypersensitive site sequencing profiles across the *Irf8* locus in bone marrow derived macrophages vs. splenic B-cells is shown (data set published in Blood by (Leddin et al. 2011)) with permission of Blood.

This *in silico* observation was underlined by Chromatin Immunoprecipitation (ChIP) directed against the nuclear factor complex p300 (Figure 22B) which is recruiting the basal transcriptional machinery, including RNA polymerase II, to the places of active transcription. Hence, p300 binding to a genomic sequence is indicative for transcriptional activity at this

particular site. The experiment was originally done by the group of Natoli (Ghisletti et al. 2010), while the data for p300 binding to the *Irf8* locus was analyzed and kindly provided by the group of Whei Chan (MDC). Correlation between sequence conservation and transcriptional activity based on p300 binding in macrophages can be observed.

This finding was further confirmed by DNaseI hypersensitive site screen across the locus. Sequences that are so called "open" often are transcripionally active and thus more accessible to digestion with DNaseI. This whole genome DNaseI hypersensitive site screen was recently published by our group (Leddin et al. 2011) and was applied for the *Irf8* locus. Different peak sizes denote different accessibility, as depicted in Figure 22C of the USCS browser derived plot. Bone marrow derived macrophages (BMM) showed a distinctively different DNaseI pattern compared to primary splenic B-cells. Both cell types express *Irf8* and in both cell types the *Irf8* promoter is accessible to DNaseI. However, different non coding DNA elements are DNaseI hypersensitive. These DNaseI hypersensitive sites clearly matched the evolutionary conserved DNA elements predicted by the *in silico* alignment assay.

To more rigorously test the regulatory capacity of the conserved DNA elements histone acetylation as a hallmark of transcriptional activity was assessed employing ChIP for histone H3 lysine 9/14 acetylation. Results were expressed as ratio of histone acetylation over an IgG control antibody (Delabesse et al. 2005). The ubiquitously active *ß-Actin* promoter served as a positive control, while the muscle specific *myoD1* promoter was used as negative control as described before (Sawado et al. 2001). An acetylation status comparable or higher in regard to the positive control was determined as a regulatory active sequence.

The myeloid cell line RAW264.7 expressed high levels of *Irf8*. Here, the *Irf8* locus was found to be highly acetylated. The -50kb, -16kb and -11kb located elements showed highest acetylation levels, whereas the promoter region was only moderately acetylated, suggesting that *Irf8* expression might be controlled via regulatory elements, rather then by the promoter alone. In comparison, NIH3T3 cells do not express *Irf8*, and the *Irf8* promoter as well as the conserved elements tested were not acetylated at all (Figure 23).

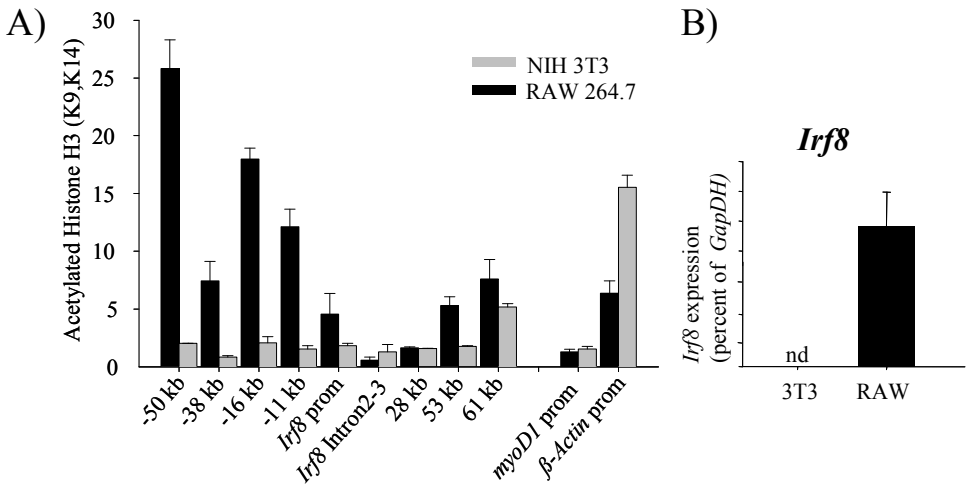

Figure 23: Regulatory active regions upstream of the *Irf8*-promoter. A) ChIP qPCR demonstrates H3K9/14 acetylation for the -50kb element, as well as for other conserved elements in RAW264.7 cells, however not in NIH 3T3 fibroblasts. Data was normalized to IgG-control antibody ChIP assay. The promoters of the muscle specific *myoD1* and the housekeeping gene *ß-Actin* served as control loci (n=3). **B)** Real-time RT PCR stating expression of *Irf8* in NIH3T3 and RAW264.7 cells (nd = not detected) (n=4).

3.2.1.2 Functionality of predicted active DNA elements

The data provided so far regarding the *Irf8* controlling elements are only correlative. Reporter assays employing the luciferase reporter-gene under the control of the *Irf8* promoter, complemented with the putative regulatory elements, were conducted. Since the *Irf8* promoter does not drive reporter expression in transient transfection assays (data not shown) the constructs were stably incorporated into the respective cell lines. These experiments proved that the *Irf8* promoter could interact with two putative regulatory elements. Displayed in Figure 24 are results of six independent pools of stably transfected cells, resulting from two independent rounds of electroporation. Individually picked clones for each construct (6 to 12) confirmed the data obtained for the pools (data not shown). In RAW264.7 cells the promoter alone gave no signal, the addition of the -50kb element or the -11kb element allowed for high reporter gene activity. NIH3T3 cells did not drive any reporter activity.

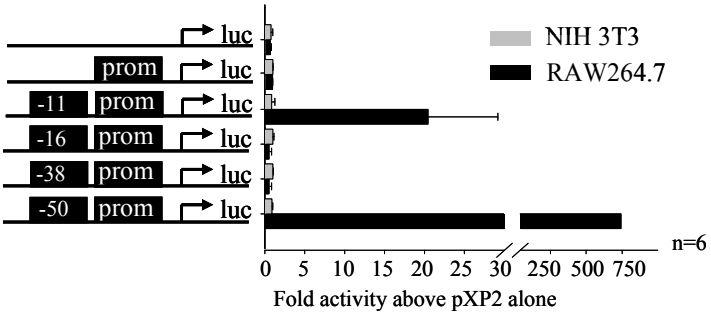

Figure 24: The -50kb element is actively driving reporter expression in myeloid cells. Schematic representation of pXP2 based luciferase (luc) reporter constructs carrying the indicated conserved sites. The -50kb element and the -11kb element drive reporter expression under the control of the *Irf8* promoter (prom) in stably transformed RAW264.7 cells, whereas in stably transformed NIH3T3 control cells no activity is detectable.

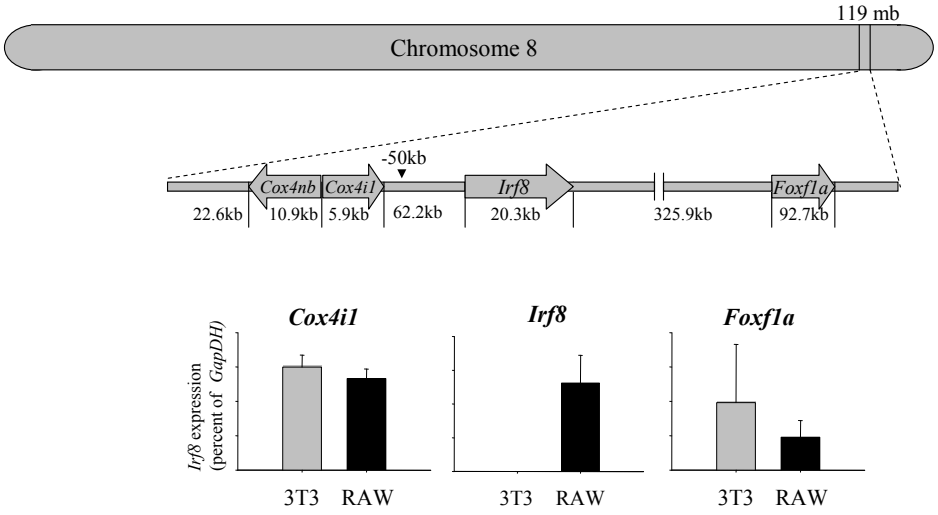

Figure 25: Expression pattern of *Irf8* and neighbouring genes. Upper panel shows location of the *Irf8* gene locus on mouse Chromosome 8, and more in detail *Irf8* neighbouring genes with distances in between the genes indicated. The real-time RT PCR results in the lower panel show different regulation of gene expression of *Irf8* compared to its neighbouring genes *Cox4i1* and *FoxF1a* in RAW 264.7 and NIH3T3 cells, respectively. (n=3)

The assays shown up to now demonstrated regulatory activity for two of the newly discovered elements. However, they only provided indirect evidence for specificity of the regulatory elements towards the *Irf8* gene. When analyzing *Irf8* neighbouring gene expression as depicted in Figure 25, it became obvious that *Irf8* neighbours are not differentially expressed in NIH3T3 and RAW264.7 cells, while *Irf8* only is expressed in RAW264.7 cells. Most likely, the reporter activity of the newly discovered enhancers is specific to the *Irf8* promoter alone.

Employing Chromatin Conformation Capture (3C) analysis (Dekker et al. 2002; Werth et al. 2010) allowed to link activity of an element to its physical proximity to a promoter which is manifested by a three-dimensional DNA loop. The *Irf8* promoter was tested for co-localization with the respective active DNA element sequences. Here, depicted in Figure 26A, the -50kb element showed a strong loop formation with the promoter in RAW264.7 cells. Artefacts were excluded by a parallel experiment omitting the ligation step. No false product formation was detected. Statistically the probability of product formation is given using the *Irf8*-PAC as a template. Every possible primer combination was tested and declared comparable (data not shown).

When testing different cell systems for loop formation, it is crucial to use an endogenous reference locus, acting comparable to a housekeeping gene in RT-PCR (Spilianakis et al. 2004). Bone marrow derived macrophages were compared to primary B-cells. Both cell types express *Irf8*, however just the BMM exerted loop formation. Hence the -50kb element was defined to be myeloid specific in this *ex vivo* assay.

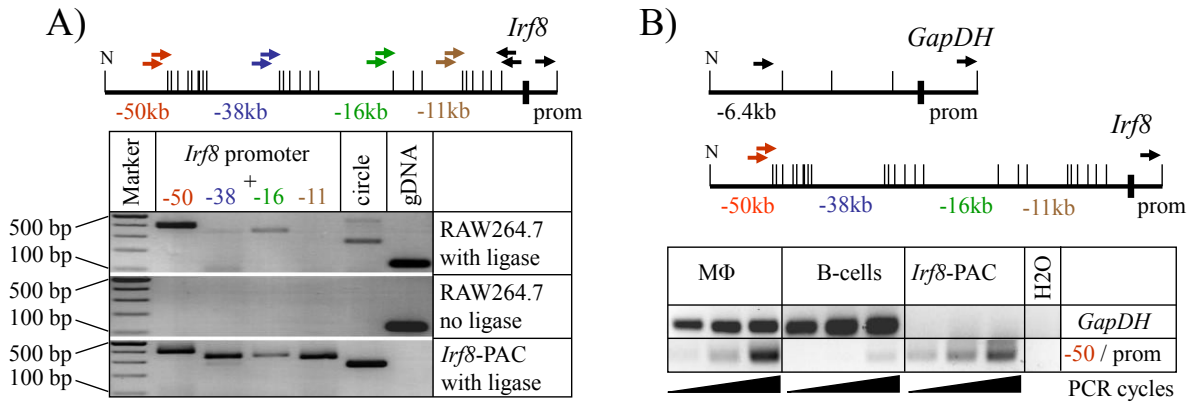

Figure 26: Chromatin conformation capture (3C) shows co-localization of the -50kb regulatory element with the *Irf8* promoter in myeloid cells. A) 3C targeting the conserved sites for physical proximity to the *Irf8* promoter in RAW264.7 cells. The no ligase control does not show artificial product formation, while the *Irf8*-PAC served as a positive control allowing product formation for all possible primer combinations. Marker: 100 bp to500 bp. **B)** Co-localization between the -50kb element and the *Irf8* promoter was assessed in BM derived macrophages and CD19+ purified primary B-cells. The DNA content was normalized to the known *GapDH* loop. The experiment was done at least 3 times, one representative nested PCR is shown. Filled triangles indicate 15, 20 and 25 PCR cycles of the second round of nested PCR.

Taken together, a number of conserved elements were found flanking the *Irf8* gene and revealed different transcriptional activity in myeloid cells. The -50kb upstream of the *Irf8* transcription start site located *cis*-element in particular was found to be an enhancer interacting with the *Irf8* promoter specifically in myeloid cells.

3.2.2 Characterization of the -50kb regulatory element

3.2.2.1 Identification of transcription factor binding motifs within the -50kb element

To test which upstream located transcription factors orchestrate *Irf8* gene function via the -50kb enhancer transcription factor binding motif analysis was applied on murine, rat, human and dog sequences. Highly conserved sites for the haematopoietic master regulators RUNX1 and PU.1 (Rosenbauer et al. 2007; Friedman 2009) were located within the homology cluster. The entire homology cluster comprises approximately 260 bp and was found to contain two RUNX1 motifs (recognition sequence: ACCACA) which are flanking two overlapping PU.1 binding motifs (recognition sequence: AAANNGGAA) as depicted in Figure 27.

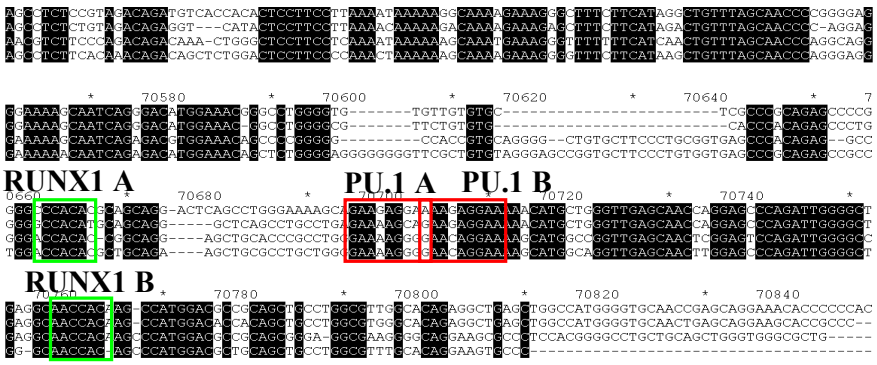

Figure 27: Identification of -50kb element transcription factor binding motifs. Sequence alignment of the -50kb element of mouse, rat, human and dog. Conserved residues in all four sequences are shown in black. The indicated PU.1 and RUNX1 binding motifs were found employing rVista software (see 2.1.16).

Binding of the identified transcription factors to their respective sites was confirmed by ChIP, assaying for RUNX1 and PU.1 binding to the -50kb element. The -38kb element, not encompassing RUNX1 or PU.1 binding motifs, served as a negative control. An IgG control antibody was included to detect any unspecific binding to the target sequence. RNA polymerase II (POL II) binding to these sequences confirmed transcriptional activity. To address possible *Irf8* auto-regulation IRF8 binding was tested for the respective DNA elements.

In the early myeloid progenitor cell line 416B there was mild transcriptional activity for the -50kb element and strong binding of RUNX1 and PU.1 protein (Figure 28A). The -38kb element, although exhibiting POL II activity, did not show RUNX1 or PU.1 binding. These results could be confirmed for PU.1 using the more differentiated RAW264.7 cells, while here transcriptional activity based on Histone H3 K9,14 acetylation was shown for the -50kb element and much less for the -38kb element as illustrated in Figure 28B.

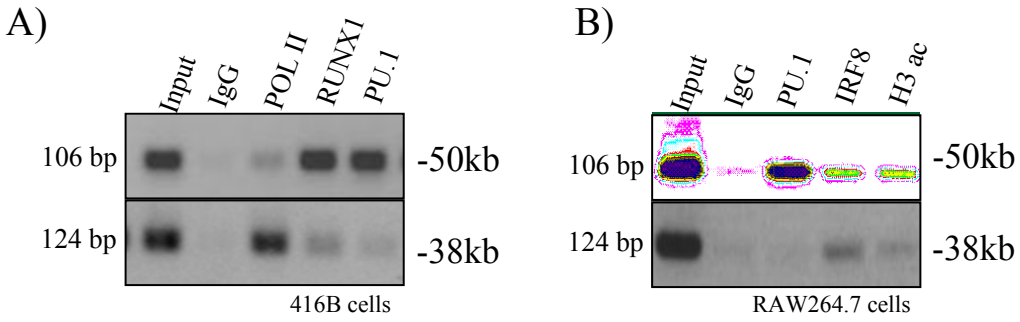

Figure 28: Transcription factor binding motif occupancy in myeloid cells. A) and **B)** ChIP PCR demonstrating binding of RUNX1 and PU.1 to the -50kb element, whereas no binding is detected for the -38kb element in 416B and RAW264.7 cells, respectively.

Primary macrophages showed an open chromatin status for the -50kb element (Figure 22C). We hypothesized the murine cell line RAW264.7 to show a similar chromatin state. NIH3T3 cells again served as a negative control. This assay confirmed the results obtained by DNaseI

– sequencing in primary macrophages. The hypersensitive site could be located in close proximity at the 3'site of the homology core region of the -50kb element. The negative control NIH3T3 cells did show no hypersensitivity to DNaseI treatment, whatsoever (Figure 29A). ChIP binding data for PU.1 was confirmed by electrophoretic mobility shift assay (EMSA) (Figure 29B). Here nuclear extracts from RAW264.7 cells showed binding of an artificial oligonucleotide containing the two overlapping PU.1 binding motifs. This binding was out-competed applying a non labelled competitor oligonucleotide bearing the same sequence as the probe, and furthermore with another oligonucleotide having a perfect PU.1 binding site (Leddin et al. 2011). When the PU.1 binding motif was mutated (ga*ggaa*gc to ga*gcgc*gc) no competition was detectable anymore. That demonstrated specificity of the used oligonucleotide. The addition of PU.1 antibody to the cell extract resulted in a supershift as indicated in the figure. An IgG control antibody did not produce a supershift, underlining the specificity of PU.1 binding to the sequence tested.

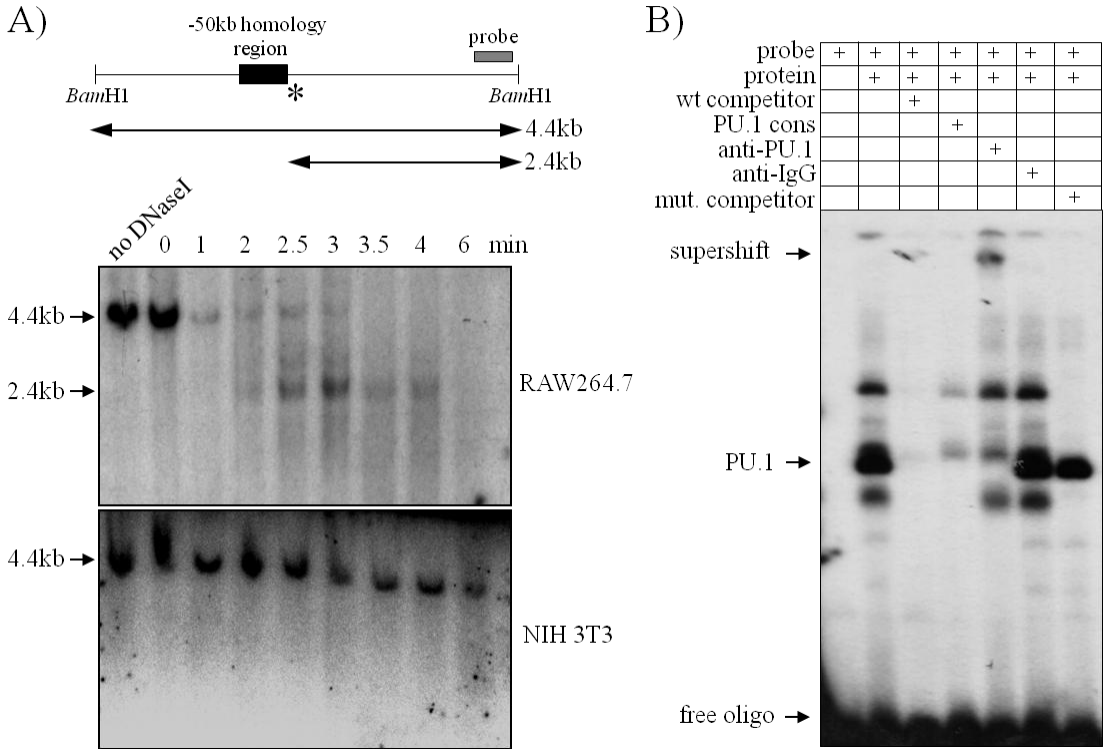

Figure 29: The -50kb locus is open in myeloid cells and allows binding of the transcription factor PU.1. A) The scheme in the upper panel indicates the 4.4kb *Bam*HI fragment detected in Southern hybridization of a DNaseI hypersensitive assay. Black box indicates the location of the -50kb conserved site. Numbers indicate time of treatment or the absence of DNaseI (no DNaseI). The grey bar shows location of the probe used and the asterisk determines the DNaseI hypersensitive site (DHS). The DHS could be detected in RAW264.7 macrophages as a 2.4kb fragment, whereas in NIH3T3 cells the chromatin is not susceptible to DNaseI treatment. **B)** Gel shift assay demonstrates PU.1 binding to the -50kb element. RAW264.7 cell nuclear extracts were incubated with α^{32}P-labeled probe containing the potential PU.1 binding motifs of the -50kb element, as well as an unlabeled competitor oligonucleotide and a PU.1 binding sequence containing control oligonucleotide, as indicated. A mutated oligonucleotide with base pair exchanges from ga*ggaa*gc to ga*gcgc*gc in the PU.1 motif was used (mut. competitor) to show specificity. At last, an antibody to PU.1 was used and shows a supershift complex, whereas an IgG control antibody does not shift. Sequences of all oligonuclotides are listed in Material and Methods.

RUNX1 and PU.1 are indispensable for -50kb element functionality

To validate the relevance of the transcription factors binding the -50kb element sh-RNA constructs against RUNX1 and PU.1 (Lausen et al. 2006) were employed. Knockdown studies in the stable RAW264.7 reporter lines containing the luciferase reporter driven by the *Irf8* promoter and enhanced by the -50kb element were performed. Here, the sh-RNA construct was transiently transfected to the stable cell lines. Transfected cells were FACS sorted based on the GFP marker of the sh-RNA carrying plasmid and subsequently analyzed. When RUNX1 and PU.1 are knocked down a highly significant down regulation of reporter activity was observed. In comparison, a control sh-RNA scramble construct (Figure 30A) showed no difference in reporter activity, demonstrating the importance of the two transcription factors controlling *Irf8* via the -50kb enhancer.

That finding was confirmed by a mutation study of the described reporter construct. Namely, binding motifs for the respective transcription factors were mutated employing site directed mutagenesis. Stable RAW264.7 cell lines were generated carrying the indicated mutations. Significantly lower reporter activity compared to the non mutated control was observed in all cases (Figure 30B).

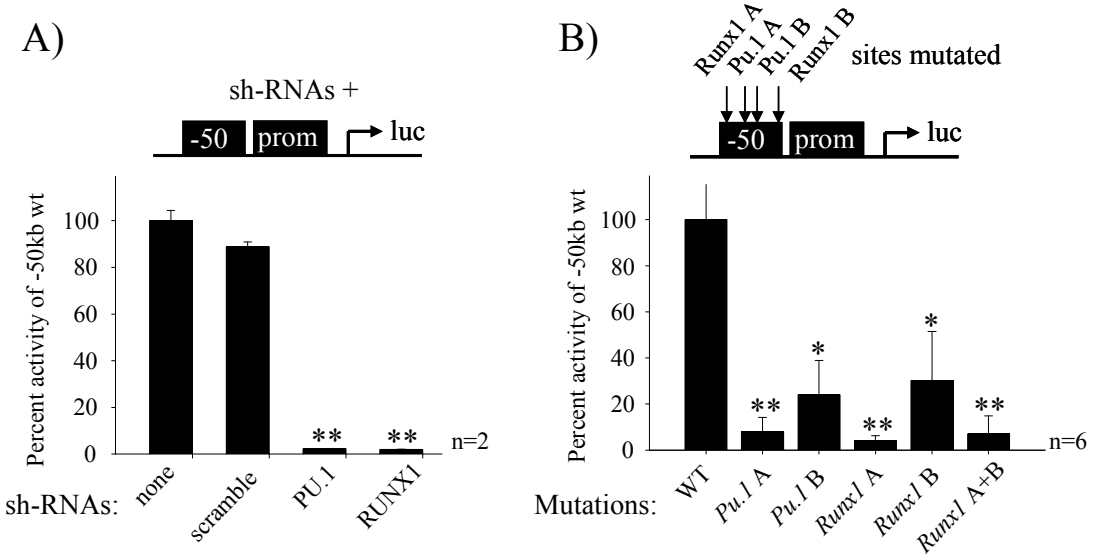

Figure 30: Reduced activity of the -50kb enhancer in the absence of upstream TFs RUNX1 and PU.1. A) Luciferase expression in -50kb reporter construct stably transformed RAW264.7 cells, transfected with sh-RNA constructs against *Pu.1*, *Runx1* and scramble control is shown. Displayed are results for 2 independent experiments with 3 technical replicates. **B)** The effect of mutation of transcription factor binding sites in luciferase reporter assays is shown. Pu.1 sites were mutated individually, whereas Runx1 sites were mutated individually and together. Stable RAW264.7 cell lines were constructed and 6 different single clones analyzed. Mutated sequences can be found in Material and Methods.

Taken together, the -50kb element is an enhancer for *Irf8* gene expression exclusively in myeloid cells. It confers its activity by two upstream located transcription factors RUNX1 and

PU.1. down regulation of the mentioned TFs leads to abrogated *Irf8* promoter activity, indicating the importance of those two factors for normal *Irf8* function in myeloid cells.

3.2.2.2 *In vivo* relevance of the binding sites for *Irf8* function

Binding of the two transcription factors RUNX1 and PU.1 to the -50kb element showed to be important for proper *Irf8* function as found by knockdown and mutation studies in stable RAW234.7 reporter cell lines. Whether this artificial setup confers *in vivo* relevance, was assessed in mice with decreased expression of PU.1 ($URE^{-/-}$ mouse) and mice deficient for RUNX1.

The $URE^{-/-}$ mice carry a deletion of an upstream enhancer to *Pu.1*. Thus, the mice only express 15 % of *Pu.1* in the progenitor compartment (Rosenbauer et al. 2004). In this compartment *Irf8* expression was decreased to almost non detectable levels (Figure 31A).

In an inducible *Runx1* knockout mouse model (Putz et al. 2006) stem cells and myeloid progenitor cells were analyzed for *Irf8* expression and found to express just 25 % or less *Irf8* compared to not excised littermate control mice (Figure 31B).

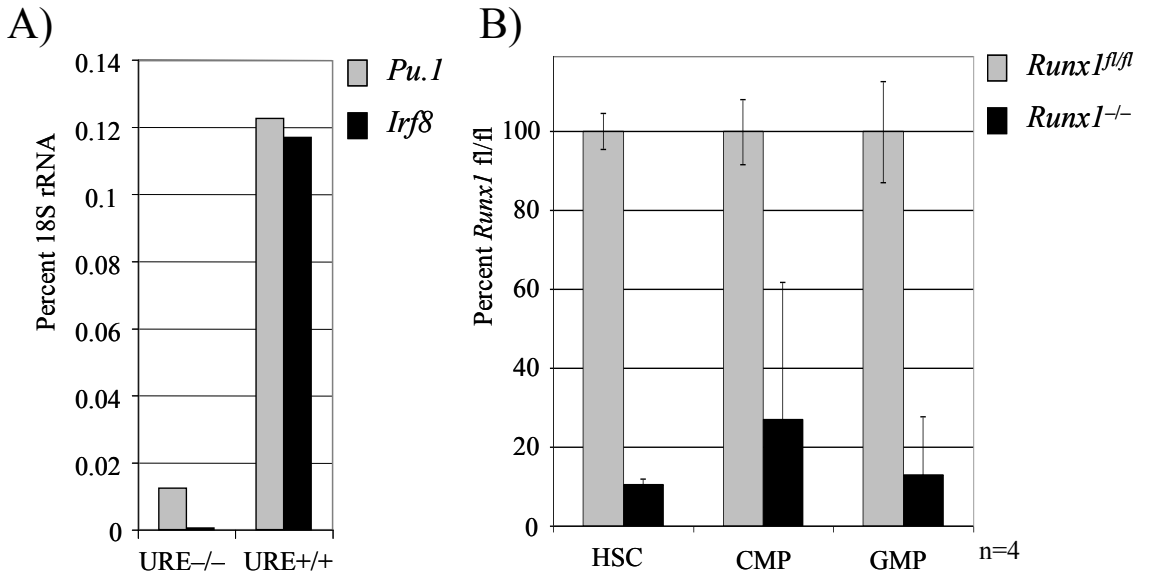

Figure 31: *In vivo* relevance of PU.1 and RUNX1 binding to the -50kb enhancer for *Irf8* function. A) Real-time RT PCR for *Irf8* and *Pu.1* expression levels in LSK cells (lineage$^-$, ckit $^{intermediate/high}$, sca1$^-$) of PU.1 enhancer element lacking mice ($URE^{-/-}$) vs. wildtype control mice is shown (n=2). **B)** *Irf8* expression levels were measured by real-time RT PCR in conditional RUNX1 deficient animals vs. non excised littermates of HSC (lineage$^-$, ckit $^{intermediate/high}$, sca1$^+$, Flt3$^-$), CMPs (common myeloid progenitors, lineage$^-$, ckit $^{intermediate/high}$, sca1$^-$, CD34$^+$, FcγRII/III^{low}), GMPs (granulocyte monocyte progenitors, lineage$^-$, ckit $^{intermediate/high}$, sca1$^-$, CD34$^+$, FcγRII/III$^+$). Values of $Runx1^{-/-}$ mice were expressed as percent of non excised littermate control mice. Results are representative for 4 animals of each genotype.

In both mouse models we found *Irf8* expression severely reduced, implying the importance of the two genes for proper *Irf8* expression *in vivo*. Both, RUNX1 and PU.1 can be put upstream of *Irf8* expression, probably regulating *Irf8* in myeloid cells via the -50kb element.

3.3 *In vivo* relevance of the -50kb regulatory element

It was demonstrated that the -50kb element is an enhancer for *Irf8* expression specifically in myeloid cells. Interference with proper -50kb function, e.g. by mutating the binding motifs for the important upstream transcription factors RUNX1 and PU.1, resulted in the loss of function of the enhancer and thus deregulation of the *Irf8* promoter. Mouse models with impaired RUNX1 or PU.1 function show severely lower *Irf8* expression.

The question arose, whether this correlation could be confirmed *in vivo* inducing a deletion of the -50kb element in our reporter mouse model.

3.3.1 Excision of the floxed -50kb element shows myeloid specific loss of *Irf8*-VENUS expression *in vivo*

The -50kb element turned out to be essential for normal *Irf8* regulation in the myeloid compartment *in vitro*. As described in 2.4.4.1 the -50kb regulatory region was floxed on the PAC construct before transgenic lines were established. Hence, the next step was to delete the enhancer from the PAC *in vivo* and subsequently to screen haematopoietic compartments for altered *Irf8* expression in the absence of the -50kb element. A simplified scheme depicts the -50kb locus in -50kb positive animals before and in -50kb element deficient animals after excision (Figure 32A).

After breeding of PAC positive animals to Cre-recombinase positive animals under the ubiquitously active CMV promoter (Su et al. 2002), the floxed -50kb element was efficiently deleted as shown in Figure 32B. This mouse line was named -50kbΔ*Irf8*-VENUS PAC. Primer flanking the two *lox*P sites (primer A and B and C and D; Figure 10) identified not excised *Irf8*-VENUS transgenic animals in PCR, while -50kb element deficient *Irf8*-VENUS transgenic animals were identified by primers spanning the whole floxed region (primer A and D, Figure 10). Copy number and integrity of not excised PAC sequence were evaluated and remained unchanged (data not shown).

Interestingly, the deletion of the -50kb element had no impact on the earliest HSCs, but all myeloid progenitor compartments up to differentiated monocytes showed a profound decrease of reporter signal (Figure 32C and D), demonstrating a high specificity of the enhancer for the myeloid compartment.

On the other hand, DC subsets reacted differently to the loss of the element. While pDCs showed only moderate decrease in activity, the $CD8\alpha^+$ cDCs diminished by almost 50 %. Reporter activity in lymphoid B-cells was only mildly affected by the deletion of the -50kb element. The bar graph of FACS mean fluorescent data (MFI) in Figure 32D underlines the findings how important the -50kb element is in myeloid cells.

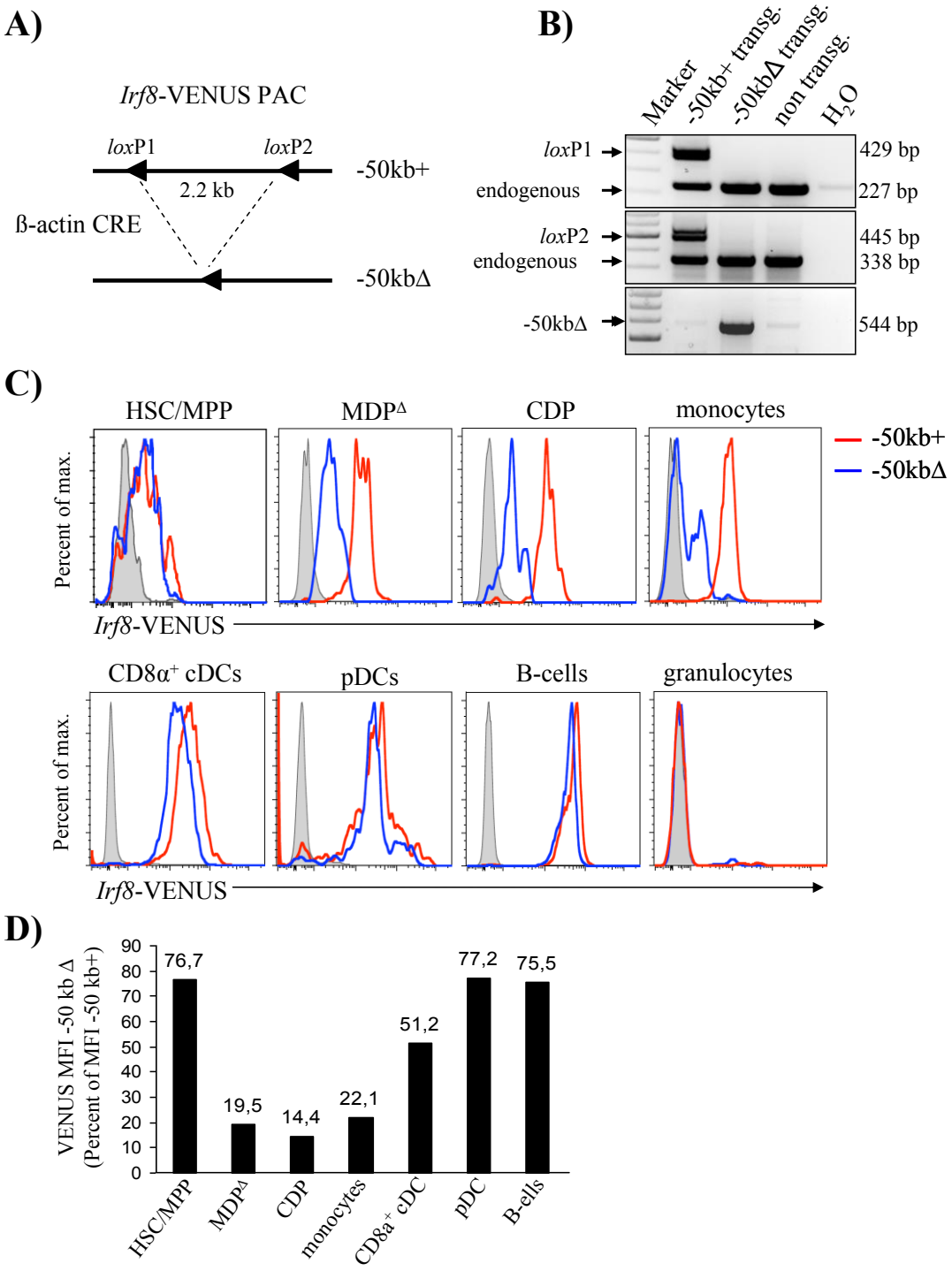

Figure 32: Excision of floxed -50kb element shows myeloid specific loss of *Irf8*-VENUS expression in wildtype background. A) Schematic draft of -50kb element carrying transgenic animals and in -50kb deficient transgenic animals after Cre-recombinase excision of a 2.2 kb DNA fragment. **B)** Genotyping for the floxed -50kb locus in not excised, excised and C57/Bl6 littermate control animals by PCR on genomic DNA. **C)** FACS analysis of *Irf8*-VENUS expression of *Irf8*- VENUS PAC transgenic animal (strain #88, red) vs. -50kbΔ*Irf8*-VENUS PAC transgenic animal (strain #88Δ, blue) vs. C57/Bl6 littermate controls (grey area). Peripheral blood granulocytes ($CD11b^+$, $Ly6C^+$, $CD115^-$), total monocytes ($CD11b^+$, $Ly6C^{low/high}$, $CD115^+$) and B-cells ($B220^+$, IgM^+) are displayed. Spleenic $CD8\alpha^+$ cDCs ($CD11c^+$) and pDCs ($CD11c^+$, $B220^+$) are displayed. BM resident HSC/MPP ($lineage^-$, $ckit^+$, $sca1^+$), MDP^{Δ} ($ckit^+$, M-$CSFR^{high}$) and CDP ($ckit^+$, M-$CSFR^{low}$) are displayed. Data are representative for at least four independent studies. Similar results were obtained with strain #87. **D)** Mean fluorescent intensity (MFI) of -50kbΔ*Irf8*- VENUS PAC is reduced compared to *Irf8*- VENUS PAC transgenic animals specifically in the myeloid compartment.

3.3.2 Incomplete rescue of *Irf8* deficiency by -50kbΔ*Irf8*-VENUS PAC

In order to test the *Irf8* chromosomal unit that is included in the murine *Irf8*-PAC for its capacity to rescue the *Irf8*$^{-/-}$ mouse phenotype, the knockout mouse was crossed to the *Irf8*-VENUS PAC- and the -50kbΔ*Irf8*-VENUS PAC transgenic mouse, respectively. This led to a mouse with two impaired endogenous alleles complemented with a functional artificial PAC construct (Figure 33A). Assuming all elements for proper *Irf8* regulation were located on the PAC, and the PAC responded independently of the integration site and furthermore normally interacted with endogenous cofactors, the *Irf8*$^{-/-}$ mouse phenotype should be rescued by the presence of the murine *Irf8*-VENUS PAC. In terms of the -50kb element deficient *Irf8*-VENUS PAC a myeloid phenotype could remain, due to the importance of the element for normal *Irf8* regulation in myelopoiesis. Therefore the myeloid progenitor and the differentiated myeloid compartment were screened in the *Irf8*$^{-/-}$:*Irf8*-VENUS-PAC, and *Irf8*$^{-/-}$:-50kbΔ*Irf8*-VENUS-PAC animals.

The BM of *Irf8*$^{-/-}$:*Irf8*-VENUS-PAC animals appeared normal after extraction out of the bone (Figure 33D), and displayed normal ratios of myeloid progenitors, however there were more ckit positive cells in total compared to wt control mice. Differentiated monocytes of the periphery were comparable to wt controls with no significant differences (Figure 33B). Re-introduction of the murine *Irf8*-PAC construct in the *Irf8* deficient background did rescue the myeloid phenotype.

When the -50kb element deficient *Irf8*-PAC was introduced into the *Irf8*$^{-/-}$ mice, only a partial rescue was observed. In BM resident progenitors there still was an accumulation of ckit positive cells that went along with a 50 % reduced number of myeloid progenitors. The differentiation block could not fully be rescued, which led to a reduced number of differentiated monocytes/macrophages in the periphery. Interestingly, in either case the spleen weight was still increased. Further studies are needed to fully explore what is causative for enlarged spleens in *Irf8*$^{-/-}$:*Irf8*-VENUS-PAC, and *Irf8*$^{-/-}$:-50kbΔ*Irf8*-VENUS-PAC animals. Regarding the myeloid system introduction of the murine IRF8-PAC is sufficient to restore proper myeloid cell development in IRF8 deficient mice.

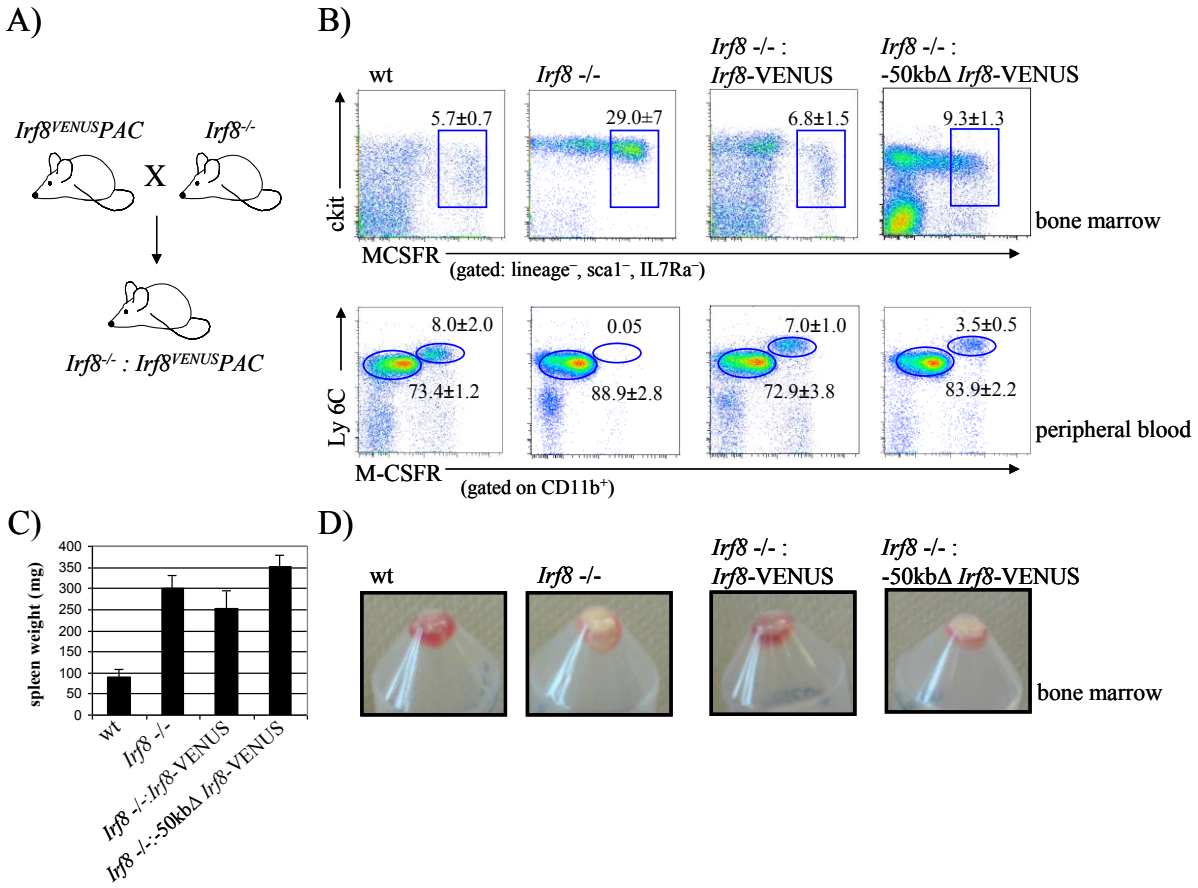

Figure 33: The murine *Irf8*^{VENUS}-PAC rescues the myeloid phenotype of *Irf8*$^{-/-}$ mice, while the -50kb element deficient *Irf8*^{VENUS}-PAC only partially rescues the phenotype. A) Crossing scheme of *Irf8*^{VENUS}-PAC mice to *Irf8*$^{-/-}$ mice. **B)** FACS analysis of myeloid progenitor (upper panel: lineage^{-}, sca1^{-}, ckit$^{low/high}$; M-CSFR^{+}) and differentiated monocyte/macrophage compartments (lower panel: Ly6C^{high}; M-CSFR^{+}) show normal numbers of cells after rescue with the complete *Irf8*-VENUS-PAC construct. The -50kb deficient -50kbΔ*Irf8*-VENUS-PAC shows only partial rescue within the indicated compartments. Displayed are representative plots of one animal of each genotype. At least 3 age matched animals of each genotype were analyzed. **C)** Spleen weight of each genotype (n=3) shows increased weight for *Irf8*$^{-/-}$ and PAC rescued animals. Displayed are average spleen weights of 3 age matched animals per genotype. **D)** Extracted BM shows increased amount of white blood cells for *Irf8*$^{-/-}$ and *Irf8*$^{-/-}$ **:** -50kbΔ*Irf8*-VENUS-PAC mice.

4 Discussion

One major concept the haematology field tries to address is how haematopoietic cell development is orchestrated. Transcription factors are among the crucial players in the organization of specific cell fates and lineage identity (Rosenbauer et al. 2007; Friedman 2009). The Interferon regulatory factor 8 is a transcription factor that is involved in interferon-γ controlled immunity and haematopoietic differentiation of myeloid cells, dendritic cells and B-cells (Wang et al. 2009). *Irf8* deficiency has severe consequences in the mouse model, leading to a syndrome reminiscent to human chronic myeloid leukaemia (Holtschke et al. 1996). Moreover, human patients with this disease have strongly down-regulated levels of *Irf8* (Schmidt et al. 1998; Schmidt et al. 2001). These findings were indicative for an important role of deregulated IRF8 in the pathology of myeloid leukaemia. However, regulation of IRF8 during haematopoietic development was essentially unknown. In this study I investigated mechanisms by which *Irf8* regulates mononuclear phagocyte development and provide new insights into the transcriptional regulation of DC cell fate decisions and DC subset formation.

4.1 Diverse expression of IRF8 in haematopoiesis

One model of haematopoietic lineage commitment proposes that not only presence but relative expression levels of transcription factors influence cell fate decisions (Orkin et al. 2002; Nutt et al. 2005; Rosenbauer et al. 2007). The low number of haematopoietic stem cells and early multipotent progenitors as well as the multitude of cell lineages and their differentiation stages made testing of that model using endogenous expression levels in primary cells complicated. In fact, it relied on of FACS purification of bulk cell populations based on surface marker expression and subsequent expression analysis of RNA or protein. Until now the general IRF8 levels and especially its involvement in the orchestration of haematopoietic cell differentiation was not examined in detail.

This is the first comprehensive study following *Irf8* gene expression patterns throughout haematopoiesis. Here, *Irf8* levels are visualized *in vivo* on single cell level. VENUS reporter signals, originating from a murine *Irf8*-VENUS PAC mouse model, were assessed in multiple haematopoietic cell compartments and showed both a resemblance of known *Irf8* expression patterns as well as remarkable heterogeneous *Irf8* expression in the myeloid progenitor compartment.

Some effort had been put into examining the role of IRF8 in B-cell commitment, where IRF8 interacts with a number of other transcription factors. Together with the transcription factor

PU.1 it was found to drive early lymphoid progenitors into B-cell differentiation, while restricting myeloid differentiation. In pre-pro B-cell transition IRF8 interacts with its family member IRF4, thus generating immature B-cells (Wang et al. 2009). Consequently, IRF8 is strongly involved in B-cell development, and VENUS expression in B-cells was used to confirm accuracy of the reporter. The other lymphoid cell compartment, comprised of T-cells, was mostly negative for VENUS reporter expression (data not shown), as only activated T-cells were described to express *Irf8* (Weisz et al. 1992). Hence, T-cells were not analyzed in detail.

The phagocyte system is the other major cell compartment known to express *Irf8*. It had been reported that IRF8 shifts the differentiation potential of bipotential precursors towards macrophage fate (Tsujimura et al. 2002). Subsequently, expression was thoroughly studied in the phagocyte system. Much of what is known about the biology of IRF8 has come from studies of mice bearing a null mutation (*Irf8*$^{-/-}$), these mice had severely decreased numbers of macrophages (Holtschke et al. 1996; Turcotte et al. 2005), and reduced IFNγ response during infection (Giese et al. 1997). Thus, IRF8 is critical for macrophage development and function. Monocytes in the BM and peripheral blood as well as macrophages of the spleen showed homogenous VENUS reporter expression, while the granulocyte compartment was negative for the reporter. This confirmed earlier findings (Tamura et al. 2000). Other macrophage associated cell compartments as for example microglia cells (Merad et al. 2009) of the brain were not analyzed in this study.

Another phagocyte compartment is the dendritic cell compartment that consists of numerous subsets, making DCs a very heterogeneous cell type (Merad et al. 2009). VENUS expression patterns in these subsets were found to be diverse. pDCs are specialized to respond to viral infections with a massive production of IFNα. On the other hand, CD8α^{+} cDCs are involved in antigen presentation to T-cells, however, both DC subsets depend on IL12 signalling, which is controlled by IRF8 (Tsujimura et al. 2003b). Therefore, IRF8 is indispensable for the generation of pDCs and CD8α^{+} cDCs. VENUS expression in these subsets was expected. Interestingly, also CD4^{+} cDCs showed distinct VENUS expression. Probably IRF8 interacts in CD4^{+} cDCs with its family member IRF4, but is not absolutely required for generation of this subset. In comparison, IRF4 null mice are deficient in giving rise to normal numbers of CD4^{+} cDCs (Tamura et al. 2005). Non lymphoid DC subsets as CD103^{+} DCs or Langerhansche cells (LC) are also known to express IRF8 (Edelson et al. 2010; Schiavoni et al. 2004) but were not analyzed in this study.

Collectively, *Irf8* is expressed at individual levels throughout all mononuclear phagocyte compartments tested, ranging from monocytes and macrophages to diverse subsets of dendritic cells.

4.2 The *Irf8*-VENUS reporter marks a new progenitor that is constraint to cDC cell growth

Much less is known about *Irf8* expression in stem and progenitor cells. Although *Irf8* has been detected at low levels in haematopoietic stem and early progenitor cells (Onai et al. 2007), its function at this early stage stays elusive. Early lymphoid progenitors had been described to be regulated by IRF8 orchestrating B-cell commitment, as discussed above. In myeloid progenitor cells, IRF8 controls lineage selection by stimulating macrophage differentiation while inhibiting the growth of granulocytes (Tamura et al. 2000; Tsujimura et al. 2002). I showed here for the myeloid progenitor compartment, according to Akashi and Weissmann (Akashi et al. 2000), the distribution of Irf8-VENUS expressing cells within the GMP compartment. Surprisingly, the IRF8 positive cells only made up for about 10-15 %. This subpopulation was named *Irf8*-VENUS$^+$ MP. In recent years, new sets of myeloid progenitors have been discovered as reviewed by Geissmann (Geissmann et al. 2010b). Based on surface receptor expression, the *Irf8*-VENUS$^+$ MP clearly fell into the MDP compartment. *In vitro* differentiation emphasised a lineage potential of *Irf8*-VENUS$^+$ MP to differentiate into macrophages (data not shown) and DCs. Interestingly, the developmental lineage relationships in transplantation studies were different, while the MDP gave rise to macrophages as well as to DCs (Fogg et al. 2006; Waskow et al. 2008), the *Irf8*-VENUS$^+$ MP cell fate commitment was CD8α^+ cDC biased. On top of that, double transgenic mice which were labelling the chemokine receptor *CX_3CR1*, that marks the MDP, as well as IRF8, revealed the *Irf8*-VENUS$^+$ MP to be a subset of the MDP (our own observation). That implied that the *Irf8*-VENUS$^+$ MP rather was a DC progenitor subset within the MDP than a myeloid progenitor.

Indeed, the *Irf8*-VENUS$^+$ MP also shared surface expression markers with the CDP, which was found to replenish cDCs as well as pDCs (Onai et al. 2007). However, the *Irf8*-VENUS$^+$ MP showed a more lineage restricted differentiation capacity. This suggests it must be placed downstream or in parallel of the CDP.

Recently another precursor for the generation of cDCs, termed pre-cDC had been described (Liu et al. 2009). This progenitor shared surface expression patterns with the *Irf8*-VENUS$^+$ MP, CDP and to some extend to the MDP. However, in contrast to these progenitors it was

not a bone marrow restricted precursor, since it was also found in the periphery and secondary haematopoietic organs.

This makes the *Irf8*-VENUS$^+$ MP a new progenitor with a distinct differentiation capacity within the mononuclear phagocyte progenitors. Thus, it will be referred to as the early conventional dendritic cell committed progenitor (EDP) (see Figure 35).

4.3 *Irf8* is a tumor suppressor at the myeloid progenitor level

As a consequence of a myelo proliferative disorder that finally leads to a fatal myeloid leukemia observed in *Irf8*$^{-/-}$ mice, Holtschke et al. 1996 suggested a role for *Irf8* as a tumor suppressor and an active involvement in early haematopoietic differentiation. In haematopoietic development starting from stem cells throughout to committed effector cells each differentiation step is tightly controlled by a network of transcription factors (Gottgens et al. 1997; Cheng et al. 2010). Interference within this network, for example by dysregulation of certain transcription factors might favour the development of cancer. In human CML as well as in AML patients substantially reduced *Irf8* mRNA levels have been reported (Schmidt et al. 1998; Schmidt et al. 2001). Hence, *Irf8* seems to be a negative regulator to a key growth control program, as in the *Irf8* deficient system the myeloid compartment is drastically enlarged. This might be caused by impaired cytokine responses (Holtschke et al. 1996; Scheller et al. 1999; Ju et al. 2007). In the curent study this critical step was pinpointed at the transition from the MDP-like compartment, which was expanded, to the more committed CDP compartment, which in contrast was reduced in cell number. The total number of stem cells, however, was unchanged (our findings and (Wang et al. 2008)). Consequentially, cells were arrested at the MDP stage, thus blocking normal mononuclear phagocyte development. As an outcome of this differentiation block these mice show severely reduced numbers of monocytes/macrophages, an expansion of neutrophiles and were incapable of giving rise to CD8α^+ cDCs and migratory CD103$^+$ DCs (Aliberti et al. 2003; Ginhoux et al. 2009; la Sala et al. 2009).

Whole transcriptome analysis of the aberrant myeloid progenitor population provided evidence for a severely disturbed gene expression program within this progenitor population. Genes got classified into neutrophile, monocyte, DC, or combined monocyte/DC expression patterns. Here, the dominant overall monocyte and DC gene expression profile (93 % of up-regulated classified genes) in wildtype MDP like progenitors was fundamentally converted into a neutrophile gene profile (55 % up-regulated classified genes) in the IRF8 deficient system. These shifted expression patterns explain the increase of neutrophiles while

mononuclear phagocytes were reduced in numbers which manifests in myelo proliferative syndrome in *Irf8*$^{-/-}$ mice and CML in human (Holtschke et al. 1996; Schmidt et al. 1998; Schmidt et al. 2001).

IRF8 is a tumor suppressor and key player in myeloid development, and I here showed the lineage commitment stage at which the disease manifests.

4.4 The -50kb element directs *Irf8* expression in myeloid cells

A significant number of genes exhibit their respective function via regulatory non-coding DNA sequences. The latter provide motifs for transcription factors to bind, that way establishing specific expression patterns at well defined levels (Decker et al. 2009). Some genes even have multiple regulatory sequences each facilitating different, cell type specific, regulatory patterns as demonstrated for the PU.1 regulatory sequences (Rosenbauer et al. 2004; Rosenbauer et al. 2006; Leddin et al. 2011).

Irf8 shows dynamic expression patterns in haematopoiesis, playing an important role in lymphoid lineages where it is involved in B-cell maturation (Wang et al. 2009). Myelo-eryhroid lineages, on the other hand, show an even more dynamic pattern. Here *Irf8* was found to be a major player in the generation of mononuclear phagocytes, while it is not expressed in polymorphnuclear phagocytes (Scheller et al. 1999; Onai et al. 2007). This dynamic expression in different cell compartments has to be tightly regulated. Thus, it was likely that *Irf8* expression was controlled via regulatory DNA sequences.

4.4.1 Identification of potential *Irf8 cis*-regulatory elements

Prediction of putative regulatory elements is commonly done by *in silico* interspecies comparison of non-coding DNA sequence conservation e.g. (Leddin et al. 2011). This method became a valuable tool when genomes of multiple species were fully sequenced and made available for comparison. Conservation of DNA throughout evolution is given for sequences that were required for active regulation. In contrast, sequences that were not involved in any regulation would eventually acquire mutations that lead to fundamental changes of this sequence over time. Screening the *Irf8* locus for such putatively regulatory elements revealed multiple highly conserved DNA sequences. Following the *in silico* prediction, the chromatin signature of the *Irf8* locus was analyzed in detail. DNA elements that are actively involved in regulation were typically found to co-localize with unfolded chromatin structure. This can be visualized by hypersensitivity of this sequence for digestion with DNaseI. Since nucleosomes are removed from actively transcribed regions transcription factors can bind and DNA cutting

enzymes are more effective (Elgin 1988; Gross et al. 1988). Combination of this technique with state-of-the-art high-throughput sequencing technology allowed mapping of DNaseI hypersensitive sites throughout the genome. This technique became even more powerful when different cell compartments were compared for differences in DNA sequence accessibility e.g. (Leddin et al. 2011). In the current study DNaseI hypersensitivity of macrophages was compared to B-cells. This dataset was published recently (Leddin et al. 2011), and was here analyzed for the *Irf8* locus. Both cell types express *Irf8*, however, the chromatin structure revealed to be strikingly different. Particular sites that were accessible in macrophages were not accessible in B-cells. Probably multiple regulatory sequences orchestrate *Irf8* expression in a lineage restricted pattern. In fact, the overall DNaseI hypersensitive sequences exactly matched the *in silico* predictions of putatively regulatory elements. Furthermore supportive were ChIP-sequencing results of the acetyltransferase p300 binding in macrophages. P300 as a transcription cofactor is indicative for transcriptional activity as described (Ghisletti et al. 2010). This published dataset was reanalyzed for the *Irf8* locus. Strikingly, p300 binding was absolutely matching conservation data and DNaseI results from macrophages.
Another aspect of chromatin signature is the histone code (Bannister et al. 2011). Given that transcripionally active DNA is associated with acetylated histone lysine residues (H3K9) ChIP for histone acetylation at conserved DNA sequences was performed. In the *Irf8* expressing macrophage cell line RAW264.7 a distinct histone acetylation pattern was found. In contrast, NIH3T3 fibroblasts, that did not express *Irf8*, showed no acetylation throughout the locus.
Collectively, I found multiple conserved DNA elements for the *Irf8* locus, which were hypersensitive to DNaseI treatment, showed binding of p300 and conferred active histone marks. However, only functional assays can determine activity associated with such elements.

This was proven by reporter gene assays as described (Moreau et al. 1981). Since the *Irf8* promoter alone was not able to drive reporter gene expression in transient transfection assays (data not shown), stably transformed reporter cell lines in RAW264.7 macrophages and NIH3T3 fibroblasts were employed. Among the putative regulatory DNA elements two elements were able to stimulate the *Irf8* promoter for reporter expression, while the *Irf8* promoter alone did not suffice. The 50kb upstream of the *Irf8* TSS located sequence showed the highest enhancer capability, which matched the DNaseI, p300 and histone acetylation data. The 11kb upstream located element, however, showed enhancer capacity in macrophages but failed to be DNaseI hypersensitive in these cells. Instead, it had DNaseI hypersensitivity in B-cells. Since promoter and regulatory elements were artificially

constructed into the reporter vector, structural differences might account for expression of a B-cell regulatory element in a macrophage cell line.

Enhancer – promoter interaction involves physical proximity and linking of the two respective DNA sequences. This was called "looping" (Blackwood et al. 1998). Proof of direct interaction of the newly discovered -50kb enhancer with the *Irf8* promoter was achieved by chromosome conformation capture (3C) analysis (Dekker et al. 2002; Werth et al. 2010; Wicks et al. 2011). RAW264.7 macrophages showed extensive looping between the -50kb element and the *Irf8* promoter, while the -16kb located element also showed looping to some degree. It is important to note, that the resolution of the 3C assay close to the promoter of a gene is strictly dependent on a reasonable number of restriction sites. Thus, the looping between the -16kb element and the promoter has to be handled with care.

Once more comparing different cell compartments revealed distinct interaction of the -50kb enhancer and *Irf8* promoter in primary macrophages, but not in B-cells. That makes the -50kb element a macrophage specific element.

4.4.2 PU.1 and RUNX1 are indispensable for -50kb element governed *Irf8* expression

An important question at that point was which upstream transcription factors control *Irf8* expression via binding to the -50kb element.

Two overlapping motifs for the haematopoietic master regulator PU.1 and two binding motifs for the early haematopoietic transcription factor RUNX1 were found. Both factors play dominant roles in the orchestration of haematopoietic development (Rosenbauer et al. 2007).

PU.1 and IRF8 were long known interaction partners in innate immunity interferon response regulation. On protein level, they form heterodimers which are directing expression of IFN-γ response genes and can also induce IFN-ß production in mononuclear phagocytes (Marecki et al. 1999; Kubosaki et al. 2010; Li et al. 2011b). In the absence of PU.1, IRF8 can not bind certain DNA elements, e.g. the IFNγ activation site (GAS), or the IFN stimulated response element (ISRE), thus fails in regulating downstream targets (Kanno et al. 2005). Besides their cooperation on protein level, recent findings placed PU.1 upstream of *Irf8*, emphasized by genetic epistasis analysis in zebrafish (Li et al. 2011a), that I could confirm in cyclohexamide experiments on PU.1 inducible murine cells (data not shown).

In cell line experiments, I showed binding of PU.1 to the -50kb enhancer. sh-RNA mediated knock down of PU.1 resulted in a loss of activity of the enhancer in reporter studies, while mutation of the PU.1 binding motifs within the enhancer significantly reduced its activity to

10 % and 23 %, depending on the binding site. These findings demonstrated the dependency of proper *Irf8* expression in monocytes on the binding of PU.1 to the -50kb enhancer.
Even more striking, I showed in the PU.1 hypomorphic mouse model that *Irf8* is severely down-regulated at transcriptional level and is almost not detectable in mice which carry a deletion in a PU.1 regulatory element ($URE^{-/-}$), allowing for just 15 % of PU.1 levels in myeloid progenitor cells. Mice with this genotype display an expansion of the myeloid progenitor compartment and profoundly increased numbers of granulocytes and reduced numbers of monocytes. This preleukemic state progresses into acute myeloid leukaemia (AML) between 3 and 8 month. This phenotype partially resembles the expanded myeloid progenitor compartment and increased number of granulocytes that were found in $Irf8^{-/-}$ mice. It is conceivable that reduced *Irf8* levels in URE deficient mice contribute to the phenotype of these mice.
Taken together PU.1 and IRF8 regulate important mononuclear phagocyte functions and orchestrate myeloid cell fate decisions on transcriptional as well as on protein level.

The *Runx1* gene encodes for the Runt-related transcription factor 1 (RUNX1), also named acute myeloid leukaemia 1 (AML1) for its involvement in this disease (Schwieger et al. 2002; Putz et al. 2006). It is a key regulator of haematopoiesis and disruption of the *Runx1* gene is one of the most common aberrations in AML (Blyth et al. 2005; Friedman 2009). Highly frequent chromosomal translocations such as the t(8;21), known as AML/ETO, are resulting in the most common subset of AML (Durst et al. 2004). This places RUNX1 as a major regulator of myeloid development. Phenotypically, mice deficient for RUNX1 in a conditional mouse model display a myelo proliferative syndrome (MPS) that goes along with a spleenomegaly (Putz et al. 2006). It is characterized by an expansion of progenitor cells in the BM and an expanded granulocyte compartment. These mice can give rise to monocytes and macrophages, however, these were found to be impaired in their ability for phagocytosis. This phenotype clearly resembled the phenotype of IRF8 deficient mice, which was a correlative hint for a putative regulation of the *Irf8* gene by RUNX1. This is furthermore supported by AML1-ETO ectopic expression experiments in wildtype BM which led to similar defects as observed in IRF8 knockout mice (Schwieger et al. 2002). Investigation of RUNX1 deficient progenitor cells revealed significantly reduced *Irf8* levels. Thus, proper *Runx1* expression is required to regulate *Irf8* at progenitor cell level. However, there are further evidences, that RUNX1 regulates *Pu.1* during myelopoiesis and subsequently also controls *Irf8* (Huang et al. 2008).

In the current study I found RUNX1 binding two different binding motifs in the -50kb enhancer of IRF8. Knockdown of RUNX1 led to a loss of enhancer activity. Furthermore, mutation studies of the binding motifs demonstrated a significant reduction of the enhancer activity between 28 % and 6 %, depending on the binding site, in respect to a control sample. Clearly, binding of RUNX1 to the -50kb enhancer is a prerequisite for normal *Irf8* expression in monocytes/macrophages.

PU.1 and RUNX1 are key players in orchestration of haematopoietic development, starting already at earliest lineage commitment stages. Here, they act individually as well as together in a transcription factor network to facilitate chromatin remodelling and cell differentiation (Hoogenkamp et al. 2009). In the light of that, the regulatory function of both transcription factors at the -50kb enhancer, that way controlling *Irf8* expression, matched the published functions for these genes. This finding makes the -50kb element a key determinant of proper IRF8 function in mononuclear phagocytes. Although, it can not be excluded that other transcription factors also might bind the -50kb element and exert a lineage specific function.

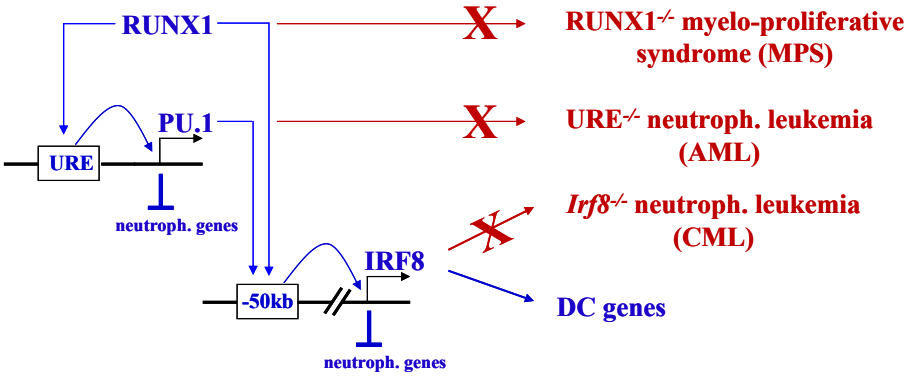

Figure 34: Model of transcription factor network controlling phagocyte differentiation. RUNX1 via the URE directly regulates PU.1, which in term via the -50kb element regulates *Irf8*. On top of that RUNX1 also binds the -50kb element, thus regulates *Irf8* in monocytes. A loss of RUNX1, PU.1 or IRF8 leads to abnormal haematopoiesis and eventually to leukaemia.

4.4.3 The -50kb element directs *Irf8* expression in myeloid cells *in vivo*

Cell line data revealed -50kb element enhancer function for *Irf8* in myeloid cells. *In vivo* relevance was proven employing the *Irf8*-VENUS PAC reporter mice. Here, deletion of the floxed -50kb element on the PAC resulted in a myeloid cell specific loss of reporter expression. The early stem cell compartment showed no difference in reporter activity, while the macrophage-dendritic cell fate committed progenitor MDP showed a reduction of reporter activity by more than 80 %. Apparently, the -50kb element exhibits its function starting on the earliest macrophage-dendritic primed progenitors, which have lost lymphoid lineage potential

but retain DC differentiation capacity. At CDP progenitor level which is purely DC committed, a similar loss of reporter activity was observed. Even though the lineage capacity of MDP and CDP is different, one can not discriminate between the different progenitors based on *Irf8* expression, probably because both progenitors are closely related and are only marginally different. Interestingly, among DC subpopulations CD8α^+ cDCs were controlled by the -50kb element, while pDCs seemed to be less affected. This emphasizes divergent regulatory mechanisms within DC lineages. However, differentiated monocytes and macrophages again showed 80 % reduced reporter expression, which is in line with the expression pattern within the MDP compartment. In the lymphoid compartment B-cell function also depends on *Irf8* expression, but not on the -50kb element, as the reporter activity in the -50kb deficient background remained almost unchanged.

Hence, the -50kb element is a monocyte/macrophage lineage restricted enhancer of *Irf8* expression *in vivo* which is in line with other reports about monocyte/macrophage specific enhancers in these highly specialized cells (Follows et al. 2003; Ghisletti et al. 2010; Sullivan et al. 2011).

4.5 Rescue of IRF8 deficiency

An important question remained to be answered. Can proper IRF8 function be conferred by introduction of the murine *Irf8*-PAC into the *Irf8*$^{-/-}$ background? Therefore, I crossed the *Irf8*-VENUS PAC and the -50kbΔ*Irf8*-VENUS PAC into the *Irf8*$^{-/-}$ background. That way all IRF8 protein originated from the PAC.

The monocyte/macrophage compartment could be re-established while granulocyte numbers were reduced to physiologic numbers, emphasizing that the PAC suffices to orchestrate myeloid specific developmental processes. Strikingly, the -50kb deficient PAC only partially rescued the myeloid progenitor cell compartment. This underlined the importance of the single regulatory element to confer proper myeloid cell development *in vivo*.

On the other hand, there still was an expansion of myeloid progenitor cells in the BM and a notably increased spleen in all *Irf8*-PAC rescued *Irf8*$^{-/-}$ animals. I conclude that the *Irf8*-PAC suffices in rescuing myeloid development but fails in fully rescuing IRF8 deficiency. Here I can only speculate that additional regulatory elements are missing on the PAC, making it incapable of acting like endogenous IRF8. It is conceivable that random introduction of the PAC construct into the chromosome puts it out of place, not allowing proper functionality of an otherwise adequate sequence. A reason for that could be sterically misfolded PAC construct. That hypothesis becomes less valid since it recently was shown for a PU.1-BAC

construct to overcome and to fully rescue the PU.1 deficiency (Leddin et al. 2011). However, in the current study the *Irf8* locus was altered on the one hand by addition of *lox*P sites around the regulatory element and on the other hand by the insertion of a reporter cassette in the untranslated region of the last exon of *Irf8*. The function of the untranslated part is not known and integration of the reporter cassette might have interfered with regulational processes exerted by that sequence. One could furthermore imagine that crosstalk between endogenous regulatory elements or cofactors and the PAC based IRF8 protein does not work outside of myeloid cell development, thus explaining increased spleen size and miss-expression in the progenitor compartment.

4.6 Conclusions and model

My data uncover an IRF8-dependent step-wise transcriptional program as the molecular mechanism driving early cDC development, while suppressing the formation of neutrophiles. Specifically the upstream located transcription factors RUNX1 and PU.1 orchestrate *Irf8* expression through binding to the novel -50kb enhancer from early macrophage/dendritic progenitors until differentiated macrophages. Furthermore, I could isolate a novel IRF8 labeled bone marrow-resident progenitor which selectively differentiates into CD8α$^+$ cDCs *in vivo*, underlining the importance for IRF8 in early cDC formation.

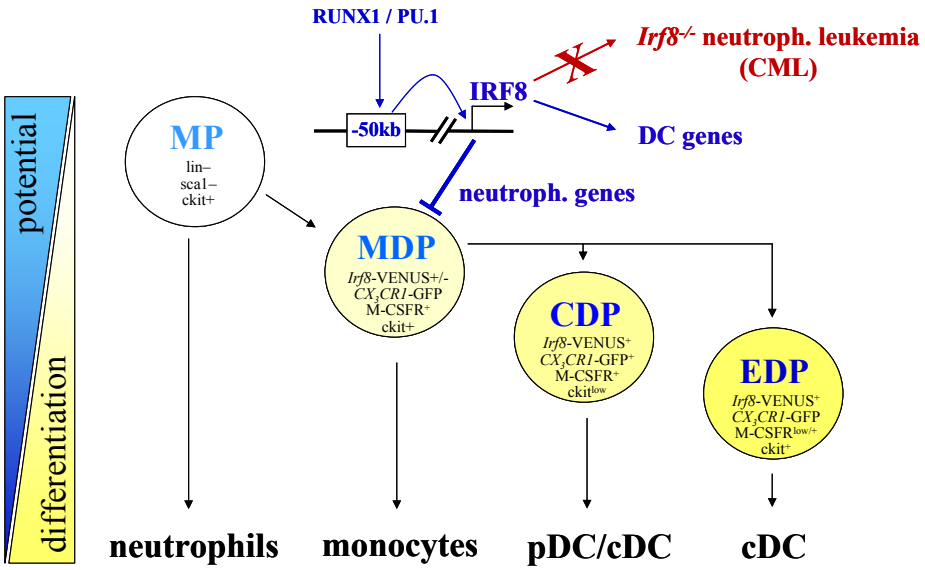

Figure 35: *Irf8*-VENUS$^+$ marked early DC committed progenitor (EDP) directs cDC development. Myeloid progenitors (MP) give rise to macrophage/dendritic cell progenitors (MDP) which have lost the potential to produce neutrophils. MDPs develop into common dendritic progenitors (CDP) which can produce all DC subsets but can no longer differentiate into macrophages. Based on the *Irf8* reporter system, we propose now the existence of a novel bone marrow-resident cDC-restricted progenitor which we term early cDC-committed progenitor (EDP). Our data further delineate that DC fate choice is initiated by a molecular pathway in which PU.1 and RUNX transcription factors bind the novel -50 kb enhancer to activate *Irf8* transcription. This step is required to construct a transcriptional DC program and inhibit expression of lineage-inappropriate neutrophile genes.

4.7 Perspective

Dendritic cells are highly specialized cells of the immune system. Their heterogeneous classification goes along with specific functions for the individual subsets. With the identification of the CDP, a joint progenitor was found that allows for the entire panel of DC subsets to develop. However, it was noted that this CDP gave preferentially rise to $CD8\alpha^-$ cDCs. With the identification of the EDP that differentiates dominantly into $CD8\alpha^+$ cDC, I here provide evidence that $CD8\alpha^-$ and $CD8\alpha^+$ cDC already diverge at the bone marrow, a process that was believed to occur at a later stage outside of the marrow. The identification of new branch points during cell differentiation that distinguishes individual subsets is the key in understanding cell fate decisions and evidently IRF8 is the discriminating factor at this level. Thus, the contribution of IRF8 in early DC commitment has to be much strengthened and with the help of the *Irf8*-Venus reporter mouse detailed mechanisms can be unraveled.

Strikingly, I identified a crucial regulatory element that acts in these early DC progenitors as well as in mature DCs and macrophages. The regulation of this element by the upstream transcription factors RUNX1 and PU.1 well supports their roles in haematopoietic development and was likewise found for other genes. Furthermore, there is evidence that there might be alternative regulatory mechanisms during B-cell development, since the -50kb element is not effecting *Irf8* expression in B-cells. However, $Irf8^{-/-}$ mice also show a strong phenotype in this lymphoid compartment and these cells confer a totally different DNaseI hypersensitivity pattern which calls for additional B-cell specific regulatory elements.

5 Bibliography

Accili, D., and K. C. Arden. "Foxos at the Crossroads of Cellular Metabolism, Differentiation, and Transformation." Cell 117.4 (2004): 421-6.

Akashi, K., D. Traver, T. Miyamoto, and I. L. Weissman. "A Clonogenic Common Myeloid Progenitor That Gives Rise to All Myeloid Lineages." Nature 404.6774 (2000): 193-7.

Aliberti, J., O. Schulz, D. J. Pennington, H. Tsujimura, C. Reis e Sousa, et al. "Essential Role for Icsbp in the in Vivo Development of Murine Cd8alpha + Dendritic Cells." Blood 101.1 (2003): 305-10.

Ardavin, C. "Origin, Precursors and Differentiation of Mouse Dendritic Cells." Nat Rev Immunol 3.7 (2003): 582-90.

Atchison, M. L. "Enhancers: Mechanisms of Action and Cell Specificity." Annu Rev Cell Biol 4 (1988): 127-53.

Auffray, C., D. K. Fogg, E. Narni-Mancinelli, B. Senechal, C. Trouillet, et al. "Cx3cr1+ Cd115+ Cd135+ Common Macrophage/Dc Precursors and the Role of Cx3cr1 in Their Response to Inflammation." J Exp Med 206.3 (2009): 595-606.

Bain, G., I. Engel, E. C. Robanus Maandag, H. P. te Riele, J. R. Voland, et al. "E2a Deficiency Leads to Abnormalities in Alphabeta T-Cell Development and to Rapid Development of T-Cell Lymphomas." Mol Cell Biol 17.8 (1997): 4782-91.

Bain, G., E. C. Maandag, D. J. Izon, D. Amsen, A. M. Kruisbeek, et al. "E2a Proteins Are Required for Proper B Cell Development and Initiation of Immunoglobulin Gene Rearrangements." Cell 79.5 (1994): 885-92.

Bannister, A. J., and T. Kouzarides. "Regulation of Chromatin by Histone Modifications." Cell Res 21.3 (2011): 381-95.

Bar-On, L., and S. Jung. "Defining Dendritic Cells by Conditional and Constitutive Cell Ablation." Immunol Rev 234.1 (2011): 76-89.

Battistini, A. "Interferon Regulatory Factors in Hematopoietic Cell Differentiation and Immune Regulation." J Interferon Cytokine Res 29.12 (2009): 765-80.

Bernstein, B. E., A. Meissner, and E. S. Lander. "The Mammalian Epigenome." Cell 128.4 (2007): 669-81.

Blackwood, E. M., and J. T. Kadonaga. "Going the Distance: A Current View of Enhancer Action." Science 281.5373 (1998): 60-3.

Blyth, K., E. R. Cameron, and J. C. Neil. "The Runx Genes: Gain or Loss of Function in Cancer." Nat Rev Cancer 5.5 (2005): 376-87.

Bonifer, C., and D. A. Hume. "The Transcriptional Regulation of the Colony-Stimulating Factor 1 Receptor (Csf1r) Gene During Hematopoiesis." Front Biosci 13 (2008): 549-60.

Brivanlou, A. H., and J. E. Darnell, Jr. "Signal Transduction and the Control of Gene Expression." Science 295.5556 (2002): 813-8.

Carbone, F. R., and M. J. Bevan. "Class I-Restricted Processing and Presentation of Exogenous Cell-Associated Antigen in Vivo." J Exp Med 171.2 (1990): 377-87.

Carotta, S., and S. L. Nutt. "Losing B Cell Identity." Bioessays 30.3 (2008): 203-7.

Chang, Z. L. "Recent Development of the Mononuclear Phagocyte System: In Memory of Metchnikoff and Ehrlich on the 100th Anniversary of the 1908 Nobel Prize in Physiology or Medicine." Biol Cell 101.12 (2009): 709-21.

Cheng, P., J. Zhou, and D. Gabrilovich. "Regulation of Dendritic Cell Differentiation and Function by Notch and Wnt Pathways." Immunol Rev 234.1 (2010): 105-19.

Cheshier, S. H., S. J. Morrison, X. Liao, and I. L. Weissman. "In Vivo Proliferation and Cell Cycle Kinetics of Long-Term Self-Renewing Hematopoietic Stem Cells." Proc Natl Acad Sci U S A 96.6 (1999): 3120-5.

Clayton, A. L., C. A. Hazzalin, and L. C. Mahadevan. "Enhanced Histone Acetylation and Transcription: A Dynamic Perspective." Mol Cell 23.3 (2006): 289-96.

de Wet, J. R., K. V. Wood, M. DeLuca, D. R. Helinski, and S. Subramani. "Firefly Luciferase Gene: Structure and Expression in Mammalian Cells." Mol Cell Biol 7.2 (1987): 725-37.

Decker, T., M. Pasca di Magliano, S. McManus, Q. Sun, C. Bonifer, et al. "Stepwise Activation of Enhancer and Promoter Regions of the B Cell Commitment Gene Pax5 in Early Lymphopoiesis." Immunity 30.4 (2009): 508-20.

Dekker, J. "The Three 'C' S of Chromosome Conformation Capture: Controls, Controls, Controls." Nat Methods 3.1 (2006): 17-21.

Dekker, J., K. Rippe, M. Dekker, and N. Kleckner. "Capturing Chromosome Conformation." Science 295.5558 (2002): 1306-11.

Delabesse, E., S. Ogilvy, M. A. Chapman, S. G. Piltz, B. Gottgens, et al. "Transcriptional Regulation of the Scl Locus: Identification of an Enhancer That Targets the Primitive Erythroid Lineage in Vivo." Mol Cell Biol 25.12 (2005): 5215-25.

Dexter, T. M., T. D. Allen, D. Scott, and N. M. Teich. "Isolation and Characterisation of a Bipotential Haematopoietic Cell Line." Nature 277.5696 (1979): 471-4.

Durst, K. L., and S. W. Hiebert. "Role of Runx Family Members in Transcriptional Repression and Gene Silencing." Oncogene 23.24 (2004): 4220-4.

Edelson, B. T., W. Kc, R. Juang, M. Kohyama, L. A. Benoit, et al. "Peripheral Cd103+ Dendritic Cells Form a Unified Subset Developmentally Related to Cd8alpha+ Conventional Dendritic Cells." J Exp Med 207.4 (2010): 823-36.

Elgin, S. C. "The Formation and Function of Dnase I Hypersensitive Sites in the Process of Gene Activation." J Biol Chem 263.36 (1988): 19259-62.

Esashi, E., Y. H. Wang, O. Perng, X. F. Qin, Y. J. Liu, et al. "The Signal Transducer Stat5 Inhibits Plasmacytoid Dendritic Cell Development by Suppressing Transcription Factor Irf8." Immunity 28.4 (2008): 509-20.

Feng, J., H. Wang, D. M. Shin, M. Masiuk, C. F. Qi, et al. "Ifn Regulatory Factor 8 Restricts the Size of the Marginal Zone and Follicular B Cell Pools." J Immunol 186.3 (2011): 1458-66.

Fogg, D. K., C. Sibon, C. Miled, S. Jung, P. Aucouturier, et al. "A Clonogenic Bone Marrow Progenitor Specific for Macrophages and Dendritic Cells." Science 311.5757 (2006): 83-7.

Follows, G. A., H. Tagoh, P. Lefevre, G. J. Morgan, and C. Bonifer. "Differential Transcription Factor Occupancy but Evolutionarily Conserved Chromatin Features at the Human and Mouse M-Csf (Csf-1) Receptor Loci." Nucleic Acids Res 31.20 (2003): 5805-16.

Forsberg, E. C., K. M. Downs, H. M. Christensen, H. Im, P. A. Nuzzi, et al. "Developmentally Dynamic Histone Acetylation Pattern of a Tissue-Specific Chromatin Domain." Proc Natl Acad Sci U S A 97.26 (2000): 14494-9.

Fourel, G., F. Magdinier, and E. Gilson. "Insulator Dynamics and the Setting of Chromatin Domains." Bioessays 26.5 (2004): 523-32.

Friedman, A. D. "Cell Cycle and Developmental Control of Hematopoiesis by Runx1." J Cell Physiol 219.3 (2009): 520-4.

Furney, S. J., D. G. Higgins, C. A. Ouzounis, and N. Lopez-Bigas. "Structural and Functional Properties of Genes Involved in Human Cancer." BMC Genomics 7 (2006): 3.

Gaszner, M., and G. Felsenfeld. "Insulators: Exploiting Transcriptional and Epigenetic Mechanisms." Nat Rev Genet 7.9 (2006): 703-13.

Geissmann, F., S. Gordon, D. A. Hume, A. M. Mowat, and G. J. Randolph. "Unravelling Mononuclear Phagocyte Heterogeneity." Nat Rev Immunol 10.6 (2010a): 453-60.

Geissmann, F., S. Jung, and D. R. Littman. "Blood Monocytes Consist of Two Principal Subsets with Distinct Migratory Properties." Immunity 19.1 (2003): 71-82.

Geissmann, F., M. G. Manz, S. Jung, M. H. Sieweke, M. Merad, et al. "Development of Monocytes, Macrophages, and Dendritic Cells." Science 327.5966 (2010b): 656-61.

Ghisletti, S., I. Barozzi, F. Mietton, S. Polletti, F. De Santa, et al. "Identification and Characterization of Enhancers Controlling the Inflammatory Gene Expression Program in Macrophages." Immunity 32.3 (2010): 317-28.

Giese, N. A., L. Gabriele, T. M. Doherty, D. M. Klinman, L. Tadesse-Heath, et al. "Interferon (Ifn) Consensus Sequence-Binding Protein, a Transcription Factor of the Ifn Regulatory Factor Family, Regulates Immune Responses in Vivo through Control of Interleukin 12 Expression." J Exp Med 186.9 (1997): 1535-46.

Ginhoux, F., K. Liu, J. Helft, M. Bogunovic, M. Greter, et al. "The Origin and Development of Nonlymphoid Tissue Cd103+ Dcs." J Exp Med 206.13 (2009): 3115-30.

Gordon, S., and P. R. Taylor. "Monocyte and Macrophage Heterogeneity." Nat Rev Immunol 5.12 (2005): 953-64.

Gottgens, B., F. McLaughlin, E. O. Bockamp, J. L. Fordham, C. G. Begley, et al. "Transcription of the Scl Gene in Erythroid and Cd34 Positive Primitive Myeloid Cells Is Controlled by a Complex Network of Lineage-Restricted Chromatin-Dependent and Chromatin-Independent Regulatory Elements." Oncogene 15.20 (1997): 2419-28.

Gross, D. S., and W. T. Garrard. "Nuclease Hypersensitive Sites in Chromatin." Annu Rev Biochem 57 (1988): 159-97.

Hacker, C., R. D. Kirsch, X. S. Ju, T. Hieronymus, T. C. Gust, et al. "Transcriptional Profiling Identifies Id2 Function in Dendritic Cell Development." Nat Immunol 4.4 (2003): 380-6.

Heinz, L. X., B. Platzer, P. M. Reisner, A. Jorgl, S. Taschner, et al. "Differential Involvement of Pu.1 and Id2 Downstream of Tgf-Beta1 During Langerhans-Cell Commitment." Blood 107.4 (2006): 1445-53.

Heinz, S., C. Benner, N. Spann, E. Bertolino, Y. C. Lin, et al. "Simple Combinations of Lineage-Determining Transcription Factors Prime Cis-Regulatory Elements Required for Macrophage and B Cell Identities." Mol Cell 38.4 (2010): 576-89.

Hershko, A., and A. Ciechanover. "The Ubiquitin System." Annu Rev Biochem 67 (1998): 425-79.

Higuchi, T., H. Kanzaki, M. Iwai, S. Narukawa, J. Fujita, et al. "Expression of Messenger Ribonucleic Acid for Gonadal Steroid Receptors in the Human Pelvic Peritoneum." Fertil Steril 63.1 (1995): 52-7.

Holtschke, T., J. Lohler, Y. Kanno, T. Fehr, N. Giese, et al. "Immunodeficiency and Chronic Myelogenous Leukemia-Like Syndrome in Mice with a Targeted Mutation of the Icsbp Gene." Cell 87.2 (1996): 307-17.

Hoogenkamp, M., M. Lichtinger, H. Krysinska, C. Lancrin, D. Clarke, et al. "Early Chromatin Unfolding by Runx1: A Molecular Explanation for Differential Requirements During Specification Versus Maintenance of the Hematopoietic Gene Expression Program." Blood 114.2 (2009): 299-309.

Huang, G., P. Zhang, H. Hirai, S. Elf, X. Yan, et al. "Pu.1 Is a Major Downstream Target of Aml1 (Runx1) in Adult Mouse Hematopoiesis." Nat Genet 40.1 (2008): 51-60.

Hume, D. A. "The Mononuclear Phagocyte System." Curr Opin Immunol 18.1 (2006): 49-53.

Hunter, A. J., N. Ottoson, N. Boerth, G. A. Koretzky, and Y. Shimizu. "Cutting Edge: A Novel Function for the Slap-130/Fyb Adapter Protein in Beta 1 Integrin Signaling and T Lymphocyte Migration." J Immunol 164.3 (2000): 1143-7.

Ju, X. S., D. Ruau, P. Jantti, K. Sere, C. Becker, et al. "Transforming Growth Factor Beta1 up-Regulates Interferon Regulatory Factor 8 During Dendritic Cell Development." Eur J Immunol 37.5 (2007): 1174-83.

Jung, S., J. Aliberti, P. Graemmel, M. J. Sunshine, G. W. Kreutzberg, et al. "Analysis of Fractalkine Receptor Cx(3)Cr1 Function by Targeted Deletion and Green Fluorescent Protein Reporter Gene Insertion." Mol Cell Biol 20.11 (2000): 4106-14.

Kaiho, S., and K. Mizuno. "Sensitive Assay Systems for Detection of Hemoglobin with 2,7-Diaminofluorene: Histochemistry and Colorimetry for Erythrodifferentiation." Anal Biochem 149.1 (1985): 117-20.

Kanno, Y., B. Z. Levi, T. Tamura, and K. Ozato. "Immune Cell-Specific Amplification of Interferon Signaling by the Irf-4/8-Pu.1 Complex." J Interferon Cytokine Res 25.12 (2005): 770-9.

Kaufmann, C., T. Yoshida, E. A. Perotti, E. Landhuis, P. Wu, et al. "A Complex Network of Regulatory Elements in Ikaros and Their Activity During Hemo-Lymphopoiesis." Embo J 22.9 (2003): 2211-23.

Krausgruber, T., K. Blazek, T. Smallie, S. Alzabin, H. Lockstone, et al. "Irf5 Promotes Inflammatory Macrophage Polarization and Th1-Th17 Responses." Nat Immunol 12.3 (2010): 231-8.

Kubosaki, A., G. Lindgren, M. Tagami, C. Simon, Y. Tomaru, et al. "The Combination of Gene Perturbation Assay and Chip-Chip Reveals Functional Direct Target Genes for Irf8 in Thp-1 Cells." Mol Immunol 47.14 (2010): 2295-302.

Kuhn, R., F. Schwenk, M. Aguet, and K. Rajewsky. "Inducible Gene Targeting in Mice." Science 269.5229 (1995): 1427-9.

la Sala, A., J. He, L. Laricchia-Robbio, S. Gorini, A. Iwasaki, et al. "Cholera Toxin Inhibits Il-12 Production and Cd8alpha+ Dendritic Cell Differentiation by Camp-Mediated Inhibition of Irf8 Function." J Exp Med 206.6 (2009): 1227-35.

Lausen, J., S. Liu, M. Fliegauf, M. Lubbert, and M. H. Werner. "Ela2 Is Regulated by Hematopoietic Transcription Factors, but Not Repressed by Aml1-Eto." Oncogene 25.9 (2006): 1349-57.

Leddin, M., C. Perrod, M. Hoogenkamp, S. Ghani, S. Assi, et al. "Two Distinct Auto-Regulatory Loops Operate at the Pu.1 Locus in B Cells and Myeloid Cells." Blood (2011). doi:10.1182/blood-2010-08-302976

Lee, J. S., E. Smith, and A. Shilatifard. "The Language of Histone Crosstalk." Cell 142.5 (2010): 682-5.

Lefevre, P., C. Lacroix, H. Tagoh, M. Hoogenkamp, S. Melnik, et al. "Differentiation-Dependent Alterations in Histone Methylation and Chromatin Architecture at the Inducible Chicken Lysozyme Gene." J Biol Chem 280.30 (2005): 27552-60.

Levine, M., and R. Tjian. "Transcription Regulation and Animal Diversity." Nature 424.6945 (2003): 147-51.

Li, L., H. Jin, J. Xu, Y. Shi, and Z. Wen. "Irf8 Regulates Macrophage Versus Neutrophil Fate During Zebrafish Primitive Myelopoiesis." Blood 117.4 (2011a): 1359-69.

Li, P., J. J. Wong, C. Sum, W. X. Sin, K. Q. Ng, et al. "Irf8 and Irf3 Co-Operatively Regulate Rapid Interferon-{Beta} Induction in Human Blood Monocytes." Blood (2011b).

Li, Y., Y. Okuno, P. Zhang, H. S. Radomska, H. Chen, et al. "Regulation of the Pu.1 Gene by Distal Elements." Blood 98.10 (2001): 2958-65.

Liu, K., G. D. Victora, T. A. Schwickert, P. Guermonprez, M. M. Meredith, et al. "In Vivo Analysis of Dendritic Cell Development and Homeostasis." Science 324.5925 (2009): 392-7.

Liu, P., N. A. Jenkins, and N. G. Copeland. "A Highly Efficient Recombineering-Based Method for Generating Conditional Knockout Mutations." Genome Res 13.3 (2003): 476-84.

Lohoff, M., and T. W. Mak. "Roles of Interferon-Regulatory Factors in T-Helper-Cell Differentiation." Nat Rev Immunol 5.2 (2005): 125-35.
Loose, M., G. Swiers, and R. Patient. "Transcriptional Networks Regulating Hematopoietic Cell Fate Decisions." Curr Opin Hematol 14.4 (2007): 307-14.
Lu, R., K. L. Medina, D. W. Lancki, and H. Singh. "Irf-4,8 Orchestrate the Pre-B-to-B Transition in Lymphocyte Development." Genes Dev 17.14 (2003): 1703-8.
Luscombe, N. M., M. M. Babu, H. Yu, M. Snyder, S. A. Teichmann, et al. "Genomic Analysis of Regulatory Network Dynamics Reveals Large Topological Changes." Nature 431.7006 (2004): 308-12.
Marecki, S., M. L. Atchison, and M. J. Fenton. "Differential Expression and Distinct Functions of Ifn Regulatory Factor 4 and Ifn Consensus Sequence Binding Protein in Macrophages." J Immunol 163.5 (1999): 2713-22.
Maston, G. A., S. K. Evans, and M. R. Green. "Transcriptional Regulatory Elements in the Human Genome." Annu Rev Genomics Hum Genet 7 (2006): 29-59.
Mattei, F., G. Schiavoni, P. Borghi, M. Venditti, I. Canini, et al. "Icsbp/Irf-8 Differentially Regulates Antigen Uptake During Dendritic-Cell Development and Affects Antigen Presentation to Cd4+ T Cells." Blood 108.2 (2006): 609-17.
Merad, M., and M. G. Manz. "Dendritic Cell Homeostasis." Blood 113.15 (2009): 3418-27.
Metcalf, D. "Stem Cells, Pre-Progenitor Cells and Lineage-Committed Cells: Are Our Dogmas Correct?" Ann N Y Acad Sci 872 (1999): 289-303; discussion 03-4.
Moreau, P., R. Hen, B. Wasylyk, R. Everett, M. P. Gaub, et al. "The Sv40 72 Base Repair Repeat Has a Striking Effect on Gene Expression Both in Sv40 and Other Chimeric Recombinants." Nucleic Acids Res 9.22 (1981): 6047-68.
Nagai, T., K. Ibata, E. S. Park, M. Kubota, K. Mikoshiba, et al. "A Variant of Yellow Fluorescent Protein with Fast and Efficient Maturation for Cell-Biological Applications." Nat Biotechnol 20.1 (2002): 87-90.
Nutt, S. L., D. Metcalf, A. D'Amico, M. Polli, and L. Wu. "Dynamic Regulation of Pu.1 Expression in Multipotent Hematopoietic Progenitors." J Exp Med 201.2 (2005): 221-31.
Ogawa, M. "Differentiation and Proliferation of Hematopoietic Stem Cells." Blood 81.11 (1993): 2844-53.
Ogbourne, S., and T. M. Antalis. "Transcriptional Control and the Role of Silencers in Transcriptional Regulation in Eukaryotes." Biochem J 331 (Pt 1) (1998): 1-14.
Ohlsson, R. "Gene Expression: The Coherent Mediator." Nature 467.7314 (2010): 406-7.
Okuno, Y., G. Huang, F. Rosenbauer, E. K. Evans, H. S. Radomska, et al. "Potential Autoregulation of Transcription Factor Pu.1 by an Upstream Regulatory Element." Mol Cell Biol 25.7 (2005): 2832-45.
Onai, N., A. Obata-Onai, M. A. Schmid, T. Ohteki, D. Jarrossay, et al. "Identification of Clonogenic Common Flt3+M-Csfr+ Plasmacytoid and Conventional Dendritic Cell Progenitors in Mouse Bone Marrow." Nat Immunol 8.11 (2007): 1207-16.
Orkin, S. H., and L. I. Zon. "Hematopoiesis and Stem Cells: Plasticity Versus Developmental Heterogeneity." Nat Immunol 3.4 (2002): 323-8.
Orkin, S. H., and L. I. Zon. "Hematopoiesis: An Evolving Paradigm for Stem Cell Biology." Cell 132.4 (2008): 631-44.
Orphanides, G., T. Lagrange, and D. Reinberg. "The General Transcription Factors of Rna Polymerase II." Genes Dev 10.21 (1996): 2657-83.
Putz, G., A. Rosner, I. Nuesslein, N. Schmitz, and F. Buchholz. "Aml1 Deletion in Adult Mice Causes Splenomegaly and Lymphomas." Oncogene 25.6 (2006): 929-39.
Radomska, H. S., A. B. Satterthwaite, T. C. Burn, I. A. Oliff, C. S. Huettner, et al. "Multiple Control Elements Are Required for Expression of the Human Cd34 Gene." Gene 222.2 (1998): 305-18.

Recillas-Targa, F., V. Valadez-Graham, and C. M. Farrell. "Prospects and Implications of Using Chromatin Insulators in Gene Therapy and Transgenesis." Bioessays 26.7 (2004): 796-807.

Riethoven, J. J. "Regulatory Regions in DNA: Promoters, Enhancers, Silencers, and Insulators." Methods Mol Biol 674 (2010): 33-42.

Rosenbauer, F., B. M. Owens, L. Yu, J. R. Tumang, U. Steidl, et al. "Lymphoid Cell Growth and Transformation Are Suppressed by a Key Regulatory Element of the Gene Encoding Pu.1." Nat Genet 38.1 (2006): 27-37.

Rosenbauer, F., and D. G. Tenen. "Transcription Factors in Myeloid Development: Balancing Differentiation with Transformation." Nat Rev Immunol 7.2 (2007): 105-17.

Rosenbauer, F., K. Wagner, J. L. Kutok, H. Iwasaki, M. M. Le Beau, et al. "Acute Myeloid Leukemia Induced by Graded Reduction of a Lineage-Specific Transcription Factor, Pu.1." Nat Genet 36.6 (2004): 624-30.

Sauer, B., and N. Henderson. "Cre-Stimulated Recombination at Loxp-Containing DNA Sequences Placed into the Mammalian Genome." Nucleic Acids Res 17.1 (1989): 147-61.

Sawado, T., K. Igarashi, and M. Groudine. "Activation of Beta-Major Globin Gene Transcription Is Associated with Recruitment of Nf-E2 to the Beta-Globin Lcr and Gene Promoter." Proc Natl Acad Sci U S A 98.18 (2001): 10226-31.

Scheller, M., J. Foerster, C. M. Heyworth, J. F. Waring, J. Lohler, et al. "Altered Development and Cytokine Responses of Myeloid Progenitors in the Absence of Transcription Factor, Interferon Consensus Sequence Binding Protein." Blood 94.11 (1999): 3764-71.

Schiavoni, G., F. Mattei, P. Borghi, P. Sestili, M. Venditti, et al. "Icsbp Is Critically Involved in the Normal Development and Trafficking of Langerhans Cells and Dermal Dendritic Cells." Blood 103.6 (2004): 2221-8.

Schiavoni, G., F. Mattei, P. Sestili, P. Borghi, M. Venditti, et al. "Icsbp Is Essential for the Development of Mouse Type I Interferon-Producing Cells and for the Generation and Activation of Cd8alpha(+) Dendritic Cells." J Exp Med 196.11 (2002): 1415-25.

Schmidt, M., A. Hochhaus, A. Nitsche, R. Hehlmann, and A. Neubauer. "Expression of Nuclear Transcription Factor Interferon Consensus Sequence Binding Protein in Chronic Myeloid Leukemia Correlates with Pretreatment Risk Features and Cytogenetic Response to Interferon-Alpha." Blood 97.11 (2001): 3648-50.

Schmidt, M., S. Nagel, J. Proba, C. Thiede, M. Ritter, et al. "Lack of Interferon Consensus Sequence Binding Protein (Icsbp) Transcripts in Human Myeloid Leukemias." Blood 91.1 (1998): 22-9.

Schwieger, M., J. Lohler, J. Friel, M. Scheller, I. Horak, et al. "Aml1-Eto Inhibits Maturation of Multiple Lymphohematopoietic Lineages and Induces Myeloblast Transformation in Synergy with Icsbp Deficiency." J Exp Med 196.9 (2002): 1227-40.

Sharrocks, A. D. "The Ets-Domain Transcription Factor Family." Nat Rev Mol Cell Biol 2.11 (2001): 827-37.

Shilatifard, A. "Chromatin Modifications by Methylation and Ubiquitination: Implications in the Regulation of Gene Expression." Annu Rev Biochem 75 (2006): 243-69.

Simon, I., J. Barnett, N. Hannett, C. T. Harbison, N. J. Rinaldi, et al. "Serial Regulation of Transcriptional Regulators in the Yeast Cell Cycle." Cell 106.6 (2001): 697-708.

Smale, S. T., and J. T. Kadonaga. "The Rna Polymerase II Core Promoter." Annu Rev Biochem 72 (2003): 449-79.

Spilianakis, C. G., and R. A. Flavell. "Long-Range Intrachromosomal Interactions in the T Helper Type 2 Cytokine Locus." Nat Immunol 5.10 (2004): 1017-27.

Steinman, R. M., and Z. A. Cohn. "Identification of a Novel Cell Type in Peripheral Lymphoid Organs of Mice. I. Morphology, Quantitation, Tissue Distribution." J Exp Med 137.5 (1973): 1142-62.

Steinman, R. M., and J. Idoyaga. "Features of the Dendritic Cell Lineage." Immunol Rev 234.1 (2010): 5-17.

Su, H., A. A. Mills, X. Wang, and A. Bradley. "A Targeted X-Linked Cmv-Cre Line." Genesis 32.2 (2002): 187-8.

Sullivan, A. L., C. Benner, S. Heinz, W. Huang, L. Xie, et al. "Serum Response Factor Utilizes Distinct Promoter- and Enhancer-Based Mechanisms to Regulate Cytoskeletal Gene Expression in Macrophages." Mol Cell Biol 31.4 (2011): 861-75.

Sunderkotter, C., T. Nikolic, M. J. Dillon, N. Van Rooijen, M. Stehling, et al. "Subpopulations of Mouse Blood Monocytes Differ in Maturation Stage and Inflammatory Response." J Immunol 172.7 (2004): 4410-7.

Swirski, F. K., M. Nahrendorf, M. Etzrodt, M. Wildgruber, V. Cortez-Retamozo, et al. "Identification of Splenic Reservoir Monocytes and Their Deployment to Inflammatory Sites." Science 325.5940 (2009): 612-6.

Tagoh, H., R. Himes, D. Clarke, P. J. Leenen, A. D. Riggs, et al. "Transcription Factor Complex Formation and Chromatin Fine Structure Alterations at the Murine C-Fms (Csf-1 Receptor) Locus During Maturation of Myeloid Precursor Cells." Genes Dev 16.13 (2002): 1721-37.

Tailor, P., T. Tamura, H. J. Kong, T. Kubota, M. Kubota, et al. "The Feedback Phase of Type I Interferon Induction in Dendritic Cells Requires Interferon Regulatory Factor 8." Immunity 27.2 (2007): 228-39.

Tamura, T., T. Nagamura-Inoue, Z. Shmeltzer, T. Kuwata, and K. Ozato. "Icsbp Directs Bipotential Myeloid Progenitor Cells to Differentiate into Mature Macrophages." Immunity 13.2 (2000): 155-65.

Tamura, T., P. Tailor, K. Yamaoka, H. J. Kong, H. Tsujimura, et al. "Ifn Regulatory Factor-4 and -8 Govern Dendritic Cell Subset Development and Their Functional Diversity." J Immunol 174.5 (2005): 2573-81.

Tolhuis, B., R. J. Palstra, E. Splinter, F. Grosveld, and W. de Laat. "Looping and Interaction between Hypersensitive Sites in the Active Beta-Globin Locus." Mol Cell 10.6 (2002): 1453-65.

Traver, D., and K. Akashi. "Lineage Commitment and Developmental Plasticity in Early Lymphoid Progenitor Subsets." Adv Immunol 83 (2004): 1-54.

Traver, D., K. Akashi, M. Manz, M. Merad, T. Miyamoto, et al. "Development of Cd8alpha-Positive Dendritic Cells from a Common Myeloid Progenitor." Science 290.5499 (2000): 2152-4.

Tsujimura, H., T. Nagamura-Inoue, T. Tamura, and K. Ozato. "Ifn Consensus Sequence Binding Protein/Ifn Regulatory Factor-8 Guides Bone Marrow Progenitor Cells toward the Macrophage Lineage." J Immunol 169.3 (2002): 1261-9.

Tsujimura, H., T. Tamura, C. Gongora, J. Aliberti, C. Reis e Sousa, et al. "Icsbp/Irf-8 Retrovirus Transduction Rescues Dendritic Cell Development in Vitro." Blood 101.3 (2003a): 961-9.

Tsujimura, H., T. Tamura, and K. Ozato. "Cutting Edge: Ifn Consensus Sequence Binding Protein/Ifn Regulatory Factor 8 Drives the Development of Type I Ifn-Producing Plasmacytoid Dendritic Cells." J Immunol 170.3 (2003b): 1131-5.

Turcotte, K., S. Gauthier, A. Tuite, A. Mullick, D. Malo, et al. "A Mutation in the Icsbp1 Gene Causes Susceptibility to Infection and a Chronic Myeloid Leukemia-Like Syndrome in Bxh-2 Mice." J Exp Med 201.6 (2005): 881-90.

van Furth, R. "The Mononuclear Phagocyte System." Verh Dtsch Ges Pathol 64 (1980): 1-11.

Vaquerizas, J. M., S. K. Kummerfeld, S. A. Teichmann, and N. M. Luscombe. "A Census of Human Transcription Factors: Function, Expression and Evolution." Nat Rev Genet 10.4 (2009): 252-63.

Varol, C., L. Landsman, D. K. Fogg, L. Greenshtein, B. Gildor, et al. "Monocytes Give Rise to Mucosal, but Not Splenic, Conventional Dendritic Cells." J Exp Med 204.1 (2007): 171-80.

Vilar, J. M., and L. Saiz. "DNA Looping in Gene Regulation: From the Assembly of Macromolecular Complexes to the Control of Transcriptional Noise." Curr Opin Genet Dev 15.2 (2005): 136-44.

Walter, K., C. Bonifer, and H. Tagoh. "Stem Cell-Specific Epigenetic Priming and B Cell-Specific Transcriptional Activation at the Mouse Cd19 Locus." Blood 112.5 (2008): 1673-82.

Wang, H., C. H. Lee, C. Qi, P. Tailor, J. Feng, et al. "Irf8 Regulates B-Cell Lineage Specification, Commitment, and Differentiation." Blood 112.10 (2008): 4028-38.

Wang, H., and H. C. Morse, 3rd. "Irf8 Regulates Myeloid and B Lymphoid Lineage Diversification." Immunol Res 43.1-3 (2009): 109-17.

Waskow, C., K. Liu, G. Darrasse-Jeze, P. Guermonprez, F. Ginhoux, et al. "The Receptor Tyrosine Kinase Flt3 Is Required for Dendritic Cell Development in Peripheral Lymphoid Tissues." Nat Immunol 9.6 (2008): 676-83.

Weisz, A., P. Marx, R. Sharf, E. Appella, P. H. Driggers, et al. "Human Interferon Consensus Sequence Binding Protein Is a Negative Regulator of Enhancer Elements Common to Interferon-Inducible Genes." J Biol Chem 267.35 (1992): 25589-96.

Werth, M., K. Walentin, A. Aue, J. Schonheit, A. Wuebken, et al. "The Transcription Factor Grainyhead-Like 2 Regulates the Molecular Composition of the Epithelial Apical Junctional Complex." Development 137.22 (2010): 3835-45.

Wicks, K., and J. C. Knight. "Transcriptional Repression and DNA Looping Associated with a Novel Regulatory Element in the Final Exon of the Lymphotoxin-Beta Gene." Genes Immun 12.2 (2011): 126-35.

Wilson, N. K., F. J. Calero-Nieto, R. Ferreira, and B. Gottgens. "Transcriptional Regulation of Haematopoietic Transcription Factors." Stem Cell Res Ther 2.1 (2011): 6.

Woollard, K. J., and F. Geissmann. "Monocytes in Atherosclerosis: Subsets and Functions." Nat Rev Cardiol 7.2 (2010): 77-86.

Yang, D., M. Thangaraju, D. D. Browning, Z. Dong, B. Korchin, et al. "Ifn Regulatory Factor 8 Mediates Apoptosis in Nonhemopoietic Tumor Cells Via Regulation of Fas Expression." J Immunol 179.7 (2007): 4775-82.

Yona, S., and S. Jung. "Monocytes: Subsets, Origins, Fates and Functions." Curr Opin Hematol 17.1 (2010): 53-9.

Yoshida, T., S. Y. Ng, J. C. Zuniga-Pflucker, and K. Georgopoulos. "Early Hematopoietic Lineage Restrictions Directed by Ikaros." Nat Immunol 7.4 (2006): 382-91.

Zhao, B., M. Takami, A. Yamada, X. Wang, T. Koga, et al. "Interferon Regulatory Factor-8 Regulates Bone Metabolism by Suppressing Osteoclastogenesis." Nat Med 15.9 (2009): 1066-71.

6 Abbreviations

%	percentage
°C	degree centigrade
3C	chromatin conformation capture
AB	antibody
AML	acute myeloid leukaemia
Amp	ampicilin
APC	allophycocyanin or antigen presenting cell
ATCC	american tissue culture collection
BM	bone marrow
BMM	bone marrow derived macrophages
bp	base pair
cDNA	complementary DNA
CDP	common dendritic progenitor
Chl	chloramphenicol
ChIP	chromatin immuno-precipitation
CLP	common lymphoid progenitor
CML	chronic myeloid leukaemia
CMP	common myeloid progenitor
CMV	cytomegalovirus
CO_2	carbon dioxide
cond.	conditional
Cre	cyclization recombination protein
DBD	DNA binding domain
DHS	DNaseI hypersensitivity assay
DMEM	Dulbeccos modified eagles medium
DMSO	dimethylsulfoxid
DNA	desoxyribonucleic acid
dNTP	deoxynucleotide triphosphate
ECL	enzymatic chemiluminescence
EDP	early dendritic cell progenitor
EDTA	ethylenediaminetetraacetate
e.g.	exempli gratia
EPO	erythropoietin
EMSA	electrophoretic mobility shift assay
EtOH	ethanol
FACS	fluorescent activated cell sorting
FCS	fetal calf serum
FITC	fluoresceinisothiocyanat
Flt3	Fms- related tyrosine kinase 3
Flt3L	Flt3 ligand
g	gravitational force
GAS	IFNγ activation site
GMP	granulocyte-macrophage precursor
G/M-CSF	granulocyte/macrophage stimulating factor
GFP	green-fluorescent protein
Gy	gray
h	hour
HCl	hydrochloric acid
HRP	horseradish peroxidase
HSC	hematopoietic stem cell
IAD	IFN association domain
ICSBP	interferon consensus sequence binding protein

IFN	interferon
IFNα	interferon alpha
IFNγ	interferon gamma
IgG	immune globulin gamma
IL	interleukin
iNOS	inducible nitric oxide synthase
IP	immunoprecipitation
IRES	internal ribosomal entry site
***Irf8* / IRF8**	interferon regulatory factor 8
ISRE	IFN stimulated response element
Kan	kanamycin
kb	kilobase
kDa	kilo Dalton
KCl	potassium chloride
kd	knock down
KH_2PO_4	potassium phosphate monobasic
ko	knock out
LB	lysogeny broth
LC	Langerhansche cells
lin	lineage
LP	lymphoid progenitors
LPS	lipo-poly-saccharide
LSK	lineage negative, sca1 positive, ckit positive stem- and early progenitor cells
M	molar
mA	milli ampere
MC	methylcellulose
M-CSF	macrophage colony stimulating factor
M-CSFR	macrophage colony stimulating factor receptor
MDS	myelodisplastic syndrome
MDSC	myeloid derived suppressor cells
MEP	megakaryocyte-erythrocyte precursor
MΦ	macrophage
MFI	mean fluorescent intensity
mg	milligram
$MgCl_2$	magnesium-cloride
min	minute/minutes
ml	millilitre
mM	milli-molar
M-MuLV	moloney murine leukemia virus
MPD	myelo proliferative disorder
MPP	multi potent progenitor
MPS	myelo proliferative syndrome
Mx1	myxovirus (influenza virus) resistance 1
mRNA	messenger ribonucleic acid
n	number
Na_2HPO_4	sodium phosphate dibasic
NaCl	sodium chloride
NaOH	sodium hydroxide
ng	nano gram
nm	nano meter
NDS/NGS	normal donkey/ normal goat serum
p	probability value
PAC	phage artificial chromosome
Pax5	paired box gene 5
PBS	phosphate buffered saline
PCR	polymerase-chain-reaction

pDNA	plasmid DNA
PE	phycoerythrin
PFGE	pulsed field gel electrophoresis
PFU	*Pyrococcus furiosus* derived polymerase
pH	potentia hydrogenii
PI	propidium iodide
p(I:C)	PolyIPolyC
Pol II	RNA polymerase II
Pu.1	transcription factor encoded by the *Spi-1* gene
PVDF	polyvenyldifluoride
P/S	penicillin/streptomycin
RNA	ribonucleic acid
RIN	RNA integrity number
RBC	red blood cells
rpm	revelations per minute
RT	reverse transcriptase / reverse transcription
RT	room temperature
SAP	shrimp alkaline phosphatise
SDS	sodiumdodecyle sulfate
s.d.	standard deviation
SCF	stem cell factor
SDS	sodiumdodecylsulfat
seq	sequencing
SSC	saline-sodium citrate buffer
TAE	Tris/acetate/EDTA buffer
Taq	*Thermus aquaticus* derived polymerase
TBE	Tris/borate/EDTA buffer
TBS	Tris buffered saline
TCA	1,1,1-trichloroethane
TCF	transgenic core facility
TE	Tris/EDTA
Tet	tetracyclin
TKN	Tris/KCl buffer
TNE	Tris/NaCl/EDTA buffer
TNF	tumor necrosis factor
TSS	transcription start site
U	units
URE	upstream open reading frame enhancer
UV	ultra-violet light
V	volt
v/v	volume per volume
VENUS	enhanced yellow fluorescent protein
w/v	weight per volume
wt	wildtype
YFP	yellow fluorescent protein
Zeo	Zeocin
[α-^{32}P]dCTP	deoxycytosine 5'-triphosphate [α-^{32}P]
[γ-^{32}P]dATP	deoxyadenosine 5'-triphosphate [γ-^{32}P]
µl	micro litre
µm	micrometer

Selbsständigkeitserklärung

Ich versichere hiermit, dass ich die von mir vorgelegte Dissertation eigenständig und ohne Benutzung anderer als der angegebenen Hilfsmittel angefertigt habe. Ich versichere, dass alle aus anderen Quellen oder indirekt übernommenen Daten und Konzepte, sowie Ergebnisse aus Kooperationsprojekten unter Angabe der Referenz gekennzeichnet sind. Für Abbildungen, die aus Publikationen entlehnt sind, wurden Copyright-Lizenzen erworben. Außerdem versichere ich, dass mir die aktuelle Promotionsordnung der Universität Potsdam bekannt ist und ich mich nicht anderweitig um einen Doktorgrad bewerbe, bzw. noch keinen entsprechenden Doktorgrad besitze.

Jörg Schönheit
Berlin, den 28.04.2011